IN VITRO VIABLE SKIN MODEL DEVELOPMENT TO ASSESS CUTANEOUS DELIVERY AND METABOLISM OF ESTER-TYPE COMPOUNDS

A Thesis Submitted to the
College of Graduate Studies and Research
in Partial Fulfillment of the Requirements
for the Degree of Doctor of Philosophy
in the Division of Pharmacy
College of Pharmacy and Nutrition
University of Saskatchewan
Saskatoon

by

Panida Asavapichayont

April 2000

In presenting this thesis in partial fulfillment of the requirements for a Postgraduate degree from the University of Saskatchewan, I agree that the Libraries of this University may make it freely available for inspection. I further agree that permission for copying of this thesis in any manner, in whole or in part, for scholarly purposes may be granted by the professor or professors who supervised my thesis work or, in their absence, by the Head of the Department or the Dean of the College in which my thesis work was done. It is understood that any copying or publication or use of this thesis or parts of thereof for financial gain shall not be allowed without my written permission. It is also understood that due recognition shall be given to me and to the University of Saskatchewan in any scholarly use which may be made of any material in my thesis.

Requests for permission to copy or to make any other use of material in this thesis in whole or in part should be addressed to:

Dean of the College of Pharmacy and Nutrition
University of Saskatchewan
Saskatoon, Saskatchewan S7N 5C9

ABSTRACT

A viable *in vitro* excised human skin model was developed to accurately assess cutaneous delivery and metabolism of two ester type compounds; tetracaine (TC) and methyl salicylate (MS). This model could maintain the viability of fresh skin in diffusion cells for 24 hours. Skin viability was assessed using two methods; oxygen consumption measurement and confocal laser scanning microscopy. Two fluorescent probes, calcein AM and ethidium homodimer-1, were used as live and dead markers, respectively. General morphology and localization of nonspecific esterase activity in the skin samples from diffusion cell were checked histologically. Cutaneous delivery and metabolism of MS was evaluated with this viable skin model and compared to human skin homogenate model.

A sensitive reversed phase ion-pairing high performance liquid chromatography (HPLC) assay was developed/refined to simultaneously analyze TC and its metabolite (4-BABA). Several factors affecting this HPLC system were identified. The limit of detection for TC and 4-BABA was 0.3 ng and 0.5 ng, respectively. The limit of quantitation for TC and 4-BABA was 10 ng and 5 ng, respectively. Linearity was in the range of 10 - 120 ng for TC and 5 - 60 ng for 4-BABA.

MS was hydrolyzed to salicylic acid (SA) during absorption through full thickness human breast skin in diffusion cells. The extent of MS hydrolysis was significantly higher in viable skin than in non-viable. The extent of absorption of SA through viable and non-viable skins was similar. In human skin homogenate, MS was hydrolyzed at the rate of 72.31 nmol/h/μg protein while the hydrolysis in phosphate buffered saline was very low. TC hydrolysis in human skin homogenate was not extensive due to substrate inhibition.

From the kinetic study of TC hydrolysis in human skin homogenate, K_m was in the 11-28 μM range and V_{max} was in the 2.0-2.8 μmol/h/μg protein range. Temperature over 60°C substantially reduced esterase activity in both models therefore caution must be taken during preparation and handling of tissue samples to preserve esterase activity. The viable *in vitro* excised skin model will provide more accurate quantitation of skin metabolism and absorption of xenobiotics.

ACKNOWLEDGEMENTS

I wish to express my sincere gratitude to my supervisor, Dr. Marianna Foldvari, for her advices, guidance and continual encouragement. Her contribution to the success of my program is highly appreciated.

I gratefully thank Dr. S.J. Whiting, the chair of my advisory committee, who assisted in every way for the completion of my study. I also appreciate the valuable suggestions, guidance and assistance from the other members of my advisory committee, Drs. J.O.K. Boison, D.K.J. Gorecki, E.M.Hawes, J. W. Hubbard, P.R. Hull, and H.A. Semple.

Many thanks to Drs. R. Naik and V. Gopal (Department of Pharmacology) for collaborating on the confocal laser scanning microscopy study; to Dr. J. Radhi (Department of Pathology) for the assistance and discussion of the histology part; to plastic surgeons and nurses at the Royal University Hospital and St. Paul's Hospital for providing human skin samples, to Dr. S. Sardari for helping with the illustrations and some general discussions.

I thank Pharmaderm Laboratories, Ltd. for the use of research equipments.

Major financial support throughout the program from the Canadian International Development Agency (CIDA) is gratefully acknowledged as well as some financial support from the College of Pharmacy and Nutrition, University of Saskatchewan.

I value the friendship, encouragement and support from my colleagues at the Faculty of Pharmacy, Silpakorn University, Thailand as well as staffs at the Drug Delivery Research group, fellow graduate students at the University of Saskatchewan and all my friends who in some ways have contributed to my survival and accomplishment.

To my family in Thailand for unconditional love, understanding and endless support.

TABLE OF CONTENTS

LIST OF TABLES

LIST OF FIGURES

LIST OF ABBREVIATIONS

ACN	acetonitrile
AHH	aryl hydrocarbon hydroxylase
ANOVA	analysis of variance
4-BABA	4-butylamino benzoic acid
BSA	bovine serum albumin
^{14}C	carbon fourteen radioactive label
°C	degrees Celsius
CAM	calcein AM
CE	capillary electrophoresis
CLSM	confocal laser scanning microscopy
CV	coefficient of variation (= relative standard deviation)
2D	two dimensional
3D	three dimensional
DBI	N-deschloro-benzoyl-indomethacin
DMSO	dimethylsulfoxide
EDTA	ethylene diamine tetraacetic acid
EN	ethyl nicotinate
EthD-1	ethidium homodimer-1
g	gram(s)
g	gravitational force
GC	gas chromatography
h	hour(s)
^{3}H	tritium radioisotope
H&E	hematoxylin and eosin
HHBSS	Hepes-buffered Hank's balanced salt solution
HPLC	high pressure liquid chromatography
HSA	hexane sulphonate
HSH	human skin homogenate
I.D.	inside diameter

IUB	the International Union of Biochemistry
K_m	Michaelis constant, substrate concentration at half V_{max}
kV	kilovolt(s)
LOD	limit of detection
LOQ	limit of quantitation
LPR	local power reference
M	molar
mg	milligram(s)
min	minute(s)
mL	milliliter(s)
mM	millimolar(s)
mOsm	milliosmolal(s)
MS	methyl salicylate
MTT	3-[4,5-dimethylthiazol-2-yl]-2,5-diphenyltetrazolium bromide (= tetrazolium salt)
NA	nicotinic acid
NAD^+	nicotinamide adenine dinucleotide (oxidized form)
nm	nanometer(s)
NSE	nonspecific esterase
O.D.	outside diameter
ODS	octadecylsilane
PABA	para-amino benzoic acid
PBS	phosphate buffered saline
PC	procaine
PCO_2	partial pressure of carbon dioxide
PCO_2-TC	transcutaneous carbon dioxide
pH	power of hydrogen, acidity where pH = log $(1/[H^+])$
pKa	dissociation constant
PO_2-TC	transcutaneous oxygen
ppm	parts per million

RP	reversed phase
rpm	revolutions per minute
RSD	relative standard deviation (= coefficient of variation)
[S]	substrate concentration(s)
SA	salicylic acid
SD	standard deviation
SEM	standard error of the means
SUA	salicyl uric acid
TC	tetracaine
[TC]	tetracaine concentration(s)
TFA	trifluoroacetic acid
UV	ultraviolet
V_0	initial velocity of enzyme reaction
V_{max}	maximum velocity of enzyme reaction
v/v	volume/volume ratio
w/v	weight/volume ratio
μg	microgram(s)
μL	microliter(s)
μM	micromolar(s)

CHAPTER ONE

RATIONALE AND OBJECTIVES

1.1 Rationale

In the evaluation of topical preparations, the general requirements of appearance, stability, microbial specification and bioavailability must be fulfilled. A percutaneous absorption study is also an essential criterion to ensure that adequate drug delivery is achieved. In addition, cutaneous metabolism during permeation is important. The ability of the skin to metabolize xenobiotics has been well demonstrated. This has significance in pharmacological and toxicological relevance. Active drugs may become inactivated after metabolism, e.g. nitroglycerin (Wester et al., 1983; Higo et al., 1992). This is normally considered a drawback, however, it is beneficial for the detoxification of compounds that are systemically toxic. On the other hand, inactive substances may be enzymatically transformed into the active form after penetration into or through the skin, which is the concept of prodrugs.

Since the drug preparations are developed for human use, the most reliable result is, of course, from a human *in vivo* study. However, there are many limitations that make this approach impractical, such as ethical and safety considerations, time, cost, etc. Although *in vitro* results may not exactly represent the real situation *in vivo*, some correlations or directions can be obtained. It may provide a predictive appraisal for human

skin absorption and metabolism, hence the bioavailability of topical xenobiotics. Considering that *in vivo* experiments are more difficult to conduct, time consuming and expensive, *in vitro* skin models are more practical and worth pursuing. Numerous experimental approaches have been developed to evaluate skin absorption. But there are still no commonly accepted methods that are entirely satisfactory (Kao, 1990). There are various important factors to be controlled and experimental designs are still being developed according to the modified and redefined rationales for a skin absorption study. Intact skin is the most similar *in vitro* sample to the real situation in living animals or human. Excised intact skin from humans and animals has been used in diffusion cell studies to evaluate penetration, metabolism and toxicity of xenobiotics. However, not so many studies paid attention to the viability maintenance of the skin during the experiment. This might lead to questionable values obtained from the metabolism studies. Skin homogenates are also popular in metabolism studies since this model is simple, not too difficult to prepare and can provide useful metabolism information. Skin from human source was used in both models, hence provided a closer approach to a human *in vivo* condition than models which use animal skins.

The most important aspect of the excised skin model is to maintain the viability of the skin during the experiment in order to validate the usefulness of the model in the study of metabolism during permeation. Although there are a number of viability assays available including morphological studies, metabolic assays (synthesis of proteins, lipids, nucleic acids, metabolites, tetrazolium salts reduction, etc.), few methods have been applied to evaluate the viability of the skin samples during permeation study. Some of the methods used are the detection of radioactive carbon dioxide generated from aerobic glucose

utilization and lactate formation from anaerobic glucose utilization (Collier et al., 1989). In this study, alternative non-radioactive approaches were developed using a relatively simple oxygen consumption measurement and a new methodology of confocal laser scanning microscopy (CLSM).

Live cells utilize oxygen under aerobic conditions. The extent of oxygen consumption depends on the number and activity of living cells. The detection of radioactive carbon dioxide generated from aerobic metabolism of glucose (May and DeClement, 1980; Collier et al., 1989) requires the use of radioactive material. An alternative method is to measure the oxygen concentration in the tissue itself using an oxygen electrode. However, this requires a special instrument and electrode. Zeiger et al. (1993) developed a simple system using a Clark-type polarographic oxygen electrode connected to a pH meter to measure the aerobic activity in small discs of split-thickness skin for viability assessment in the allograft skin banking. Their method was adapted and applied to assess the viability of full-thickness skin on diffusion cells in this study. An oxygen electrode was used to measure the oxygen concentration in the buffer above the skin surface on diffusion cells. The change in oxygen concentration in the buffer with time reflects the oxygen consumption by the skin sample and hence its viability.

For the viability assessment of skin samples using CLSM, Boderke et al. (1997) used propidium iodide to identify cell death in the study of aminopeptidase activity in freshly excised human skin. Imbert and Cullander (1997, 1999) reported the use of calcein AM (CAM) and ethidium homodimer-1 (EthD-1) to determine the viability of cornea and buccal mucosa, and compared to standard tetrazolium salt (MTT) assay. In this study, CAM and EthD-1 were employed to assess the viability of intact human skin in diffusion cells

during the permeation study. CAM which was virtually nonfluorescent, penetrated and was well retained within live cells. It was hydrolyzed by intracellular esterases to calcein which produced an intense uniform green fluorescence. EthD-1 did not penetrate live cells but passed through the membranes of dead cells. Upon binding to nucleic acids, it underwent a 40-fold enhancement of fluorescence and gave a bright red fluorescence (Molecular Probes, Inc., 1996). Quantitation of the viability of tissue was done by comparing the light intensities of the probes in the samples to those in the live and dead controls. The result was combined with the oxygen consumption result to indicate the viability of the skin on diffusion cells.

After the viability of the skin in diffusion cell was confirmed and maintained, the viable skin model was used in the assessment of metabolism and penetration of test compounds. Skin homogenate from human source was also used in this study as a parallel model to compare the metabolism of the model drugs.

Esterases are abundant hydrolytic enzymes in mammals and other living organisms (Long, 1961) with a broad range of substrate type, including esters, amides and peptides (Walker and Mackness, 1983; Deimling and Bocking, 1976). They play a significant role in the deactivation/detoxification of xenobiotics and endogenous compounds as well as the activation of prodrugs. Two ester-type drugs were selected as the model compounds in this study, tetracaine (TC) and methyl salicylate (MS).

TC, a potent local anesthetic with slow onset and long duration of action, has high systemic toxicity. Therefore, its use is limited to surface and spinal anesthesia. TC is an ester and is hydrolyzed by esterases in plasma and, to a lesser extent, in the liver (Reynolds, 1996). The expected enzymes that hydrolyze TC in the skin are esterases, specifically

carboxylesterase. However, other esterases in the skin may also contribute to the hydrolysis of TC. Since there are wide overlapping substrate specificity of these enzymes, it is difficult to specifically classify enzymes in this group. If TC is metabolized in the skin, the duration of anaesthesia and the potential systemic toxicity would be affected. It would be interesting to know where the drug distributes to, whether the drug is metabolized during percutaneous absorption and to what extent, after application to the skin. Hence, TC was chosen as a model compound for this investigation.

The rationale behind the selection of MS as another model compound in this study originated from the finding of substrate inhibition effect of TC on esterases in human skin homogenate model. Since TC had substrate inhibition effect at a clinical dose, another ester was needed to test the models. MS was selected because it is an ester drug which has been widely used topically. Preliminary experiments with MS, incubated with the skin homogenate, showed no substrate inhibition. Information on MS is available and includes its clinical uses, pharmacokinetics, metabolism, permeation, and toxicity. The use of MS as another model compound provided better characterization of the models used, especially the excised skin in the diffusion cell model, where the viability of the skin was maintained for 24 hours, hence making the model suitable for the investigation of metabolism during permeation study.

1.2 Objectives

The overall purpose of this study was to develop a viable *in vitro* skin model for evaluating the cutaneous delivery and metabolism of ester-type compounds. The main objectives of the study were:

1. To develop a viable excised human skin model that can be used in a diffusion cell system to simultaneously study drug absorption and cutaneous metabolism.
2. To identify and determine skin parameters that can reflect viability during the experimental period in diffusion cells.
3. To evaluate the viable skin model for metabolic activity using model ester type compounds; tetracaine and methyl salicylate.
4. To compare the viable excised human skin model with the human skin homogenate model regarding metabolism aspect.

These main objectives were carried out using the following steps:

1. The development/improvement of sensitive HPLC methods which can simultaneously analyze the model compounds, TC and MS, and their metabolites in order to determine the rate and extent of metabolism of the model compounds in the *in vitro* models.
2. The evaluation of the viability of the excised skin in diffusion cell model using two new alternative non-radioactive approaches, the oxygen consumption measurement and the CLSM methods.
3. The conductance of permeation and metabolism studies of the model ester compounds.

4. The comparison of metabolism results from the viable excised skin model with those from the skin homogenate model.

5. The identification of the important factors in the development of each model.

6. The localization of esterases in the skin. This was obtained from the morphology and the nonspecific esterase histology results. The information was combined with the available information in the literature to gain more insight about skin esterases.

CHAPTER TWO

LITERATURE REVIEW

2.1 Skin

The skin is the most external organ of the body. It forms a vast physical barrier between the body and its environment. Average adult human skin exceeds 2 m^2 in area and is the largest organ, in terms of mass, of the body (Odland, 1991).

2.1.1 Skin Structure

The skin is composed of a keratinized squamous stratified epithelium called the epidermis and an underlying dense connective tissue layer called the dermis or corium. Below the dermis is the subcutaneous tissue or hypodermis which contains variably thick layer of fat. Skin appendages such as the eccrine sweat glands, apocrine glands and pilosebaceous units (hair follicles and sebaceous glands) are interspersed in the dermis and the epidermis.

The epidermis is conventionally subdivided into five layers (strata) from inside out; stratum basale or stratum germinativum, stratum spinosum, stratum granulosum, stratum lucidum and stratum corneum. The keratinocytes in the stratum basale have a columna (elongated) shape in the vertical axis. Replication is restricted to the basal layer. Cells leaving the basal layer enter the stratum spinosum. The thickness of this layer depends largely on the anatomical site. In the stratum granulosum, cells become more flattened and

elongated in the direction parallel to the surface. Cells in this layer contain distinctive cytoplasmic inclusions called keratohyalin granules. The stratum lucidum is not a well defined layer. It is best seen in thick skin and stains poorly. The outer stratum corneum or horny layer consists of layers of flattened, fully keratinized dead cells which are eventually shed. The thickness of the epidermis varies relatively little over most of the body, between 75 and 150 μm, except on the palms and soles where the thickness may be between 400 and 600 μm, resulting from the very thick stratum corneum (Odland, 1991). The thickness of the stratum corneum varies regionally within a range of 15 to 20 cell layers over most of the body surface (Odland, 1991). The average transit time for stratum corneum cells is 14 days. If including the time for regeneration of the germinative cells, it may be estimated that normal human epidermis completely replaces itself in about 45 to 75 days (Odland, 1991). In addition to keratinocytes, which are the major cells in the epidermis, there are three other distinctive cell types; melanocytes, Langerhans cells and Merkel cells. Melanocytes produce melanin and are found in the basal layer. Langerhans cells are assumed to be specialized cells derived from the bone marrow and are involved in immunogenesis. Merkel cells are much more sparsely distributed than melanocytes and Langerhans cells and are believed to be a touch receptors (Leeson, 1985; Murphy, 1997).

The dermis constitutes the main mass of the skin. It consists mainly of moderately dense connective tissue with structural protein fibers; collagen and elastic fibers, embedded in an amorphous ground substance. The major cells of the dermis are fibroblasts which synthesize the main structural elements aforementioned. Other cells found ubiquitously are the perivascular mast cells which produce the ground substances and also linked to allergic responses of the skin, and variable numbers of tissue macrophages. The dermis may be

arbitrarily divided into two anatomical regions; the papillary dermis and the reticular dermis. The papillary dermis is the thin outermost part of the dermal tissue, which is molded against the epidermis in an undulated fashion. It encloses the vast microcirculatory blood and lymphatic plexuses. The reticular dermis lies beneath the papillary dermis. It is thicker, denser and relatively acellular and avascular when contrasted to the papillary dermis. The thickness of the dermis ranges from 1 to 5 mm (Flynn, 1996). The dermis supports extensive sensory nerve networks as well as the vasculature and lymphatics.

Skin appendages are epidermal derivatives but are embedded in the dermis. Eccrine sweat glands are present almost all over in the human skin but most abundant on the palms, the soles and the axillae. Their function is primarily temperature regulation. Apocrine glands represent scent glands and are found in only a few areas; the axillae and anogenital region. Sebaceous glands dispersed all over the skin except at the palms and soles. They are found together with hair structures on the skin. They produce sebum which moisturizes the skin (Murphy, 1997; Constantinides, 1974; Fawcett, 1981; Leeson, 1985; Montagna and Parakkal, 1974; Odland, 1991; Porter and Bonneville, 1972; Rhodin, 1963; Wheater et al., 1982).

2.1.2 Skin Functions

The primary functions of the skin include containment of body fluids and tissues, protection-barrier function, sensation of external stimuli, excretory, thermoregulation and synthesis and metabolic functions related to endogeneous and exogenous substrates (Flynn 1996; Wheater et al., 1982). The skin is also an important portal of entry of drugs and substances. The stratum corneum is often the major barrier to percutaneous absorption. Any substance that penetrates the stratum corneum is then subjected to metabolism in the viable

epidermis which is the major site of metabolism in the skin (Noonan and Wester, 1989).

2.1.3 Skin Metabolism

Skin is not only a barrier but also capable of metabolism. The capability of the skin to metabolize xenobiotics has been well documented. Among the different metabolizing organs in the body, the liver and the skin are the most important ones. Although the liver can still be considered the most important organ for metabolism of drugs in the body, but due to the broad surface area and the exposure to environment, the role of the skin cannot be overlooked.

Factors influencing skin metabolism include concentration/amount of substrate, level of enzymes-which is affected by age, sex, race, skin condition, enzyme inducers and inhibitors and duration of the exposure of substrate to the enzymes.

2.1.3.1 General Metabolism

Metabolism in skin includes phase I (oxidative, reductive, hydrolytic) and Phase II (conjugation) biotransformation reactions (Pannatier et al., 1978; Martin et al., 1987; Guy et al., 1987; Ademola et al., 1992; Boehnlein et al., 1994; Bickers et al., 1982; Tauber and Rost, 1987; Guzek et al., 1989; Potts et al., 1989).

Oxidation: Oxidation in skin has different forms. A bioactive compound can undergo a variety of reactions depending on the functionalities present in the molecule. There are alcohol dehydrogenases in the skin that are capable of oxidizing alcohol groups (Brimfield et al., 1998). Peroxidation of lipids can occur in the skin. Ascorbic acid and retinoids play a role in this reaction via induction or inhibition (Geesin et al., 1990). Epoxidation can take place by cytochrome P-450. One example is transformation of (7S,8S)-dihydroxy-7,8-dihydrobenzo[a]pyrene ((+)-BP-7,8-diol) to (7S,8R)-dihydroxy-

(9S,10R)-epoxy-7,8,9,10-tetrahydrobenzo[a]pyrene ((+)-syn-BPDE) via epoxidation by cytochrome P-450 isoenzymes and to (7S,8R)-dihydroxy-(9R,10S)-epoxy-7,8,9,10-tetrahydrobenzo[a]pyrene investigated in mouse skin (Ji and Marnett, 1992). There is evidence for metabolism via beta-oxidation in the skin (English et al., 1998). Alcohol groups can be modified to ketones in the skin. This is exemplified by the transformation of hydrocortisone to cortisone (Pannatier et al., 1978). In the pathway of melanin biosynthesis, oxidation of L-tyrosine by tyrosinase appears to be the rate limiting step. This can show the significance of oxidation in the physiology of the skin (Ramaiah, 1996). Another class of oxidation is deamination. Oxidation of carbon atom adjacent to the nitrogen can take place. Some examples are present in the literature, such as metabolism of norepinephrine by skin in rat and human (Hakanson and Moller, 1963). In addition to the enzyme catalyzed reactions, UV light from solar or other sources can induce production of free radicals and active oxygen species in the skin. This in turn can cause different oxidations to occur in this organ (Gonzalez and Pathak, 1996).

Reduction: Reduction reactions can occur in the skin. The most simple example is reduction of inorganic species. One example is reduction of chromate [Cr(VI)] in the skin of living rats. After application of aqueous solution of Cr(VI) on the skin of rats the transient species, Cr(V) was produced. Partial removal of the stratum corneum enhanced the rates of formation and disappearance of Cr(V). One of the implications of the reduction of Cr(VI) by the skin and subsequent generation of reactive Cr(V) species, could be in the mechanism of Cr(VI)-induced skin cancer (Liu et al., 1997). Carbonyl group can be reduced in the skin. One of the reported cases in this category is the transformation of various steroids. For example, the 20-oxo group of hydrocortisone can be reduced to alcohol

functionality (Hsia and Hao, 1966). In addition to carbonyl reduction, the carbon-carbon double bond may also be affected. An example for such a phenomenon is reduction of hydrocortisone to allodihydrocortisol (Hsia and Hao, 1966). There are non-enzymatic reactions leading to reduction of molecules in the skin. Nitric oxide (NO) is well-known to be generated from L-arginine by a series of NO synthase enzymes in mammalian cells. It is also indicated that NO is produced in human skin and suggest a different mechanism of production. Monomethyl L-arginine inhibits enzymatic NO synthesis. This compound has little effect on hand skin NO production. It has been proposed that NO generation from skin originates from sweat nitrite due to chemical reduction as a result of acidic nature of sweat (Weller et al., 1996).

Hydrolytic reactions: There are a number of examples indicating the hydrolytic reactions in the skin. The type of bonds that might be affected are amides and esters. Ester-type hydrolysis has been discussed in section 2.1.3.2. Amide hydrolysis of indomethacin was investigated in rabbit skin using the isolated perfused rabbit ear model. The hydrolytic product of indomethacin is N-deschloro-benzoyl-indomethacin (DBI). After 120 minutes of indomethacin application, a steady state was reached with both parent compound and DBI. In this experiment, formation of DBI was in the range of 0.65-2.01% (Behrendt and Korting, 1990). Although hydrolysis may inactivate the drugs, it has been used for pro-drug activation. This process has been studied in skin homogenate models (Lamb et al., 1994; Udata et al., 1999).

Conjugation reactions: It has been indicated that conjugation reactions happen in the skin. Within this group of reactions, glutathione, glucuronide, sulfate and glycine conjugations, and methylation can be mentioned. The glutathione S-transferase-dependent conjugation of reduced glutathione with leukotriene A4-methyl ester in rodent and human skin has been reported (Agarwal et al., 1992). Glucuronide formation has been observed in mouse skin. An example for this reaction is conjugation of glucuronic acid with the hydroxylation product of benzo[a]pyrene (Harper and Calcutt, 1960). The sulfation conjugation has been shown for a number of drugs. For example, cytosolic fraction of rat skin and liver is capable of transferring sulfate to minoxidil. The enzymic transfer of ^{35}S from sodium ^{35}sulphate to minoxidil was also shown suggesting that the rat skin is potentially able to synthesize 3'-phosphoadenosine-5'-phosphosulphate from inorganic sulphate and apply it for the biosynthesis of minoxidil sulphate, which is the active metabolite. In this context, it is understandable that the pharmacological action of minoxidil as an inducer of hair growth could be carried out by the cutaneous tissues without the contribution of liver or other extrahepatic organs (Wong et al., 1993). Glycine conjugation is an important route of metabolism and detoxication of carboxylic acids. Using freshly isolated keratinocytes and primary keratinocyte cultures, the *in vitro* cutaneous metabolism of [carboxyl-^{14}C]benzoic acid to its glycine conjugate hippuric acid in rat and human skin is studied. (Nasseri Sina et al., 1997). Methylation reaction in the skin can be exemplified as the formation of 3-O-methylated derivative of norepinephrine from this parent compound (Hakanson and Moller, 1963).

2.1.3.2 Ester Hydrolysis in the Skin

Esterases catalyze the hydrolysis of esters to acids and alcohols. They are abundant and widely distributed in mammals, insects, plants and fungi (Long, 1961). They are capable of hydrolyzing not only esters but also amides, peptides and halides (Walker and Mackness, 1983; Deimling and Bocking, 1976). They play an important role in the degradation of both endogenous and exogenous esters including drugs, pesticides and other chemicals. Clear classification of esterases is not easy due to the wide and overlapping substrate specificity. In the past, esterases were classified based on the substrates hydrolyzed, hence the trivial names such as aliesterases which hydrolyze aliphatic substrates; arylesterases which hydrolyze aromatic substrates; and cholinesterases which hydrolyze choline esters (Augustinsson, 1959, 1961; Walker and Mackness, 1983). Esterases were also classified according to the inhibition by organo-phosphorus compounds as A-esterases which are unaffected by, and even hydrolyze organophosphates while B-esterases are inhibited and C-esterases do not interact with them (Aldrige, 1953; Bergmann et al., 1957; Walker and Mackness, 1983). The Nomenclature Committee of the International Union of Biochemistry (IUB) classified esterases on the basis of substrate characteristics. According to this recommendation, hydrolases which act on ester bonds are in the 3.1.x.x group (Enzyme Nomenclature, 1984).

Serum cholinesterase (EC 3.1.1.8; acylcholine acyl-hydrolase; also known as pseudocholinesterase or butyrylcholinesterase) plays an important role in hydrolyzing xenobiotics in the body. There were reports about individual variation in the genotype of cholinesterase in the blood; "usual", "atypical" and the rare "silent" types. Patients who inherited the "atypical" cholinesterase, which has much lesser affinity for succinylcholine

than does the "usual" type, hydrolyzed the drug very slowly. As a consequence, they developed respiratory paralysis for several hours after the administration of normal doses of succinylcholine (Kalow and Genest, 1957). Atypical cholinesterase was also found to have lower binding affinity for heroin than did usual cholinesterase and the silent cholinesterase variant did not hydrolyze heroine at all (Lockridge et al., 1980). Kinetic parameters were determined for cholinesterase substrates and it was found that positively charged substrates (including tetracaine and procaine), as well as aspirin in the presence of calcium chloride, demonstrated lower affinity (K_m values) to atypical cholinesterase than to usual cholinesterase while neutral esters had similar K_m for both usual and atypical cholinesterase. The results implied that positively charged substrates and aspirin at therapeutic doses would be hydrolyzed at a lower rate in individuals with atypical cholinesterase, but neutral substrates would be hydrolyzed at regular rates (Valentino et al., 1981).

Topically applied ester prodrugs of an antiviral agent, ganciclovir, were developed to increase penetration through the stratum corneum and reduce systemic absorption and toxicity. Upon hydrolysis, active ganciclovir was produced in the skin (Powell et al., 1991). Various drugs have been investigated using the ester prodrug approach in topical drug delivery such as vidarabine (Yu et al., 1979, 1980), metronidazole (Bundgaard et al., 1983; Johansen et al., 1986), viprostol (prostaglandin E_2 analog) (Nicolau and Yacobi, 1989), zidovudine (Seki et al., 1990), buprenorphine (Imoto et al., 1996). Topical corticosteroid esters are additional examples of both important aspects of hydrolysis in the skin (inactivation of xenobiotics and activation of prodrugs). Being highly lipophilic, they partition readily into the skin and can be hydrolyzed to either active or inactive

corticosteroids. In most cases, the hydrolysis results in the activation because the free corticosteroids bind to the receptor stronger than their esters. However, inactivation has also been reported (Tauber and Rost, 1987). Stereospecific activity was reported for the hydrolysis of propranolol prodrugs in hairless mouse skin (Ahmed et al., 1995, 1997).

There are species differences in esterase activity. This has been described in detail for ethyl nicotinate (EN) in humans and several animal models (Rittirod et al., 1999). Simultaneous skin permeation and metabolism experiment of EN was carried out *in vitro* in side by side diffusion cells at 37^0 C, followed by an EN hydrolysis experiment was carried out using skin homogenate to estimate the kinetic parameters (V_{max} and K_m) by a computer program. Both EN and a metabolite, nicotinic acid (NA), were shown to be present in all receiver solutions in permeation studies but no significant chemical hydrolysis was found. Difference in total (EN + NA) flux, from EN-saturated solution, was found to be less than two folds among various species. The ratio of NA flux to total flux was highest for rat, followed by hairless rat, mouse, human and hairless mouse; this, therefore, indicated a great species difference in skin esterase activity. Total flux increased in a linear manner with increase in donor concentration in all species. For hairless rat, mouse and hairless mouse, NA fluxes increased with increase in EN donor concentration and reached a plateau, indicating that metabolic saturation can occur in skin. Kinetic parameters for EN hydrolysis using skin homogenate were significantly higher in rats compared to those in mice. In order to predict skin permeability in humans using an animal model, the species difference in skin metabolism has to be taken into consideration.

2.1.3.3 Distribution of Enzymes in the Skin

The study of skin metabolism is of great importance not only in the field of drug delivery via transdermal routes, but also for the safe and efficient local skin treatment with topically applied compounds. Since it has become clear that even peptides may be delivered across the permeation barrier of the stratum corneum, e.g. by means of iontophoresis, sonophoresis or electroporation, the enzymatic barrier of the epidermis deserves more attention as another important limiting factor for the dermal delivery of drugs. Since the epidermis is only a thin layer and constitutes only a small percentage of the body weight, its activity might be underestimated.

The viable epidermis is the major site of metabolism in the skin. Examples of differences in enzyme activity at various anatomical sites are reported in the literature, but the exact localization in the distinct layers of the skin and the anatomical distribution of the enzyme system mostly remain uncertain (Steinstrasser and Merkle, 1995). Hydrocortisone 5α-reductase activity was detected in the human foreskin, while in the skin preparations from other body sites activity of this enzyme could not be shown (Hsia and Hao, 1966). The anatomical site of skin sampling may have a considerable influence on the enzymatic activity measured and therefore, should be chosen carefully. The estimated enzyme activities in epidermis and dermis separated by different techniques may vary significantly due to the presence or absence of cell layers, like basal keratinocytes (Thompson and Slaga, 1976). Therefore, studies on the localization of enzyme activities in the skin are only as reliable as the separation technique employed (Finnen, 1987).

In order to study the distribution and localization of enzymes in the tissues, histochemical and immunohistochemical techniques can be used. The histochemical

procedure involves the incubation of fixed tissue with a compound and a coupling substance. After the compound (substrate) is metabolized by the enzyme in the tissue, the resulting metabolite reacts with the coupling substance and form a highly colored derivative, which is readily detected by a light microscope. Lojda et al. (1976) have described the use of histochemical methods in the study of distribution and localization of aminopeptidases in various tissues using amino acid naphthylamides as substrates and fast blue B as coupling agent. The preparation and fixation of the tissue can considerably influence the activity of the enzymes, and the coupling substance may block enzyme activity (Lojda et al.,1976). Accordingly, histochemical methods have to be carefully applied to localize specific enzymes in skin tissue. Examples of the immunohistochemical detection methods are the immunoperoxidase and the indirect immunofluorescence staining techniques. The skin is fixed and cut into 4-7 mm thick sections, then incubated with the antibody against the enzyme of interest. The antibody can be tagged with fluorescence label or another enzyme such as peroxidase which is capable of producing colored product and then can be observed at the light microscopic level. Cytochrome P-450 isoenzymes can be visualized in cultured human epidermal cells (van Pelt et al., 1990), and in rat skin (Baron et al., 1986) by using the immunohistochemical technique. The antibodies against the enzymes of interest have to be specifically prepared. Information on the catalytic function and the metabolic capacity of the enzymes is not provided by either of these methods.

2.2 Experimental Models in Dermal Drug Delivery and Metabolism

Percutaneous absorption of topically applied drugs can significantly be influenced by skin metabolism. The advantages of transcutaneous drug delivery are numerous and usually include avoidance of biotransformation and metabolism in the gastrointestinal tract and liver, better control of absorption, availability of several skin sites to avoid local irritation and toxicity, and improved patient compliance. The disadvantages may include the potential for localized irritation and allergic cutaneous reactions, systemic toxicity, and difficulties associated with the time necessary for a drug to penetrate through the skin (Berti and Lipsky, 1995). The extent and kinetics of drug diffusion and skin metabolism are difficult to assess. However, several methods using different techniques have been used, and are explained here.

2.2.1 *In Vivo* Models

Human, animal or skin flap models may be used as *in vivo* models. An example of human *in vivo* model is cutaneous microdialysis. This method allows continuous monitoring of compounds in the interstitial fluid of dermal or subcutaneous tissue. Microdialysis probes with a certain molecular weight cut off are introduced through a guide into the dermis or subcutaneous tissue at a given depth in an intradermally anesthetized area. The probes are fastened then perfused with normal saline. The ends of probes contain a small dialysis membrane window where the compounds can exchange from the interstitial fluid. After equilibration, topical formulations are applied to the area over the probe tips but not at the insertion points. Dialysate samples are collected at various time intervals and the samples assayed (Cross et al., 1997, 1998). This technique was used to study the endogenous cutaneous release of antihistamine in reaction to topical stimuli (Anderson et

al., 1992) and the penetration of topically applied organic solvents (Anderson et al., 1991, 1996). It also had an application in the characterization of transdermal transport (Muller et al., 1995; Hegemann et al., 1995).

An *in vivo* human model would be the most accurate for the evaluation of dermal drug delivery and metabolism. However, in general, it is not easy to design and conduct experiments with human beings since the drug level is usually very low and radiotracer technique may be required. This imposes ethical considerations. Moreover, the sampling may be difficult or impossible in very deep areas. It is expensive as well.

Animal models are widely used to assess dermal delivery and metabolism due to various considerations. Animal models are very useful for toxicological studies. Metabolism studies require vital tissue for examination. Readily available laboratory animals, such as rats and mice, allow the acquisition of large amounts of tissue. In addition, breeding specific laboratory strains can provide genetically uniform subjects that are accessible in large numbers (Mershon and Callahan, 1975). Minimizing inter-individual variations of the test results can be achieved by the use of genetically uniform skin samples. However, the interpretation and extrapolation of the results must be carefully done since enzyme activity and enzyme distribution may be completely different from those in human skin (Martin et al., 1987). The existing differences in the metabolic properties of the skin from different species may contribute to species variations in the absorption and cutaneous fate of topically applied substances.

Human skin sandwich flap model consists of a skin sandwich, which is generated as a flap by grafting a split-thickness skin graft from donor source to the subcutaneous surface of the abdominal skin of a congenital athymic nude rat. The flap is an "island skin

flap" type, i.e. a piece of living skin isolated and maintained by an independent and defined vasculature (Petry and Wortham, 1984). So the grafted skin is viable with an isolated and functioning, yet accessible, vasculature on the nude rat. The donor skin can be from human, pig or rat. The congenital athymic nude rats are used because of their depressed immune system and partial to complete hairlessness (Pershing and Krueger, 1989). The model was used to quantitate absorption, metabolism, and residual compound within and across the skin and was reusable (up to 3 to 4 experiments on a single skin flap). However, this model requires considerable skill and it is costly.

For the isolated perfused porcine skin flap model, an island-tubed skin flap was created in weanling pigs then transferred 2 or 6 days later to a perfusion chamber for further study. The viability was maintained for 10 to 16 hours. The maintenance of the physical permeation barrier of the stratum corneum and of the metabolic barrier of the viable part of the epidermis, together with perfusion of the underlying vascularized tissue simulating the natural blood flow are among the advantages of this system. This method has been indicated as a humane alternative animal model for investigations in cutaneous toxicology, physiology, oncology, percutaneous absorption and drug metabolism (Riviere et al., 1986, 1987). Similar to the previous model, the drawbacks of this model are the need for considerable expertise and the high cost.

2.2.2 *In Vitro* Models

Previous *in vitro* skin metabolism studies included intact excised skin (Collier et al., 1989; Nathan et al., 1990; Guzek et al., 1989; Boehnlein et al., 1994; Higo et al., 1992; Tauber and Rost, 1987), skin homogenates (Woolfson et al., 1990; Johansen et al., 1986; Powell et al., 1991; Ademola et al., 1992; Bickers et al., 1982; Guzek et al., 1989; Higo et

al., 1992; Tauber and Rost, 1987), isolated microsomes (Pohl et al., 1976), epidermal cells in culture (Parkinson and Newbold, 1980; Bickers et al., 1982; Kao et al., 1983), isolated skin cells (Coomes et al., 1983), reconstituted epidermis derived from the outer root sheath cells of hair follicles (Pham et al., 1990) and living skin equivalent (Kubota et al., 1994; Roy et al., 1993; Steinstrasser and Merkle, 1995). In the following section, various types of *in vitro* models are discussed.

Isolated cells: The techniques involving the incubation of trypsin or other enzymes with skin were developed for separating epidermis from dermis and splitting cell contacts in the epidermis (Laerum, 1969). By applying this method, isolated epidermal cells may be obtained for primary cell cultures. Moreover, these isolated cells have been used to study skin metabolism (Laerum, 1969; Finnen and Shuster, 1985). To prepare a cell suspension, skin samples are cut into pieces and floated in a trypsin solution. It is noted that performing the enzymatic treatment under gentle conditions is important in order to obtain a high number of viable cells. It was indicated that incubation at 2^0-4^0C for 18 h resulted in 86% viable epidermal cells while trypsinization at 37^0C yielded less than 20% viable cells (Finnen and Shuster, 1985). Another mild method using pronase in place of trypsin was introduced by Pohl et al. (1984). The epidermis is peeled off the dermis after incubation with pronase and put in a solution containing DNAse. The separated epidermal cells are harvested by centrifugation, then the isolated cells may be subfractionated into sebaceous cells, basal keratinocytes and differentiated keratinocytes by centrifugation in a discontinuous metrizamide gradient (Pohl et al., 1984). Coomes et al. (1983) demonstrated that different cell fractions show differences in their capability to metabolize foreign substances and the sebaceous cells being the most active of the three cell types isolated with

respect to the enzymes tested. An advantage of the freshly isolated cells is that they can reflect the enzymatic activity occurring in cells *in vivo* (Coomes et al., 1983) without the danger of dedifferentiation, which may occur in cell culture. However, the cells stay viable for only short periods due to separation from their original tissue organization and, therefore, their use is limited to short-term experiments.

Primary cell cultures of human epidermal cells: After a successful method to establish primary cell cultures of human keratinocytes was introduced by Rheinwald and Green (1975), this technique has been widely applied and modified. Epidermal cells are separated from the skin samples by overnight incubation with trypsin at 4^0C. Trypsin is blocked by the addition of the growth medium containing serum. The cell suspension obtained, is plated on a feeder layer of lethally irradiated 3T3 cells (Swiss mouse fibroblasts). The feeder layer permits attachment and growth of keratinocytes but inhibits the growth of fibroblasts. Fibroblasts, which may contaminate keratinocyte cell suspensions, would overgrow the slower proliferating keratinocytes, without the feeder layer. Under these growth conditions the keratinocytes make large colonies of a basal cell layer of multiplying cells and upper layers of differentiating cells. Less complicated and more defined systems allowing keratinocyte culture with serum-free media and without the need of feeder layers was the result of improvements to this method (Boyce and Ham, 1985). Pooled keratinocytes from different skin sources for primary cell cultures are available commercially. This is to minimize possible dissimilarities in cell growth and proliferation between different donors. In a similar fashion, human hair follicle keratinocytes can be cultured as described by Weterings et al. (1981). Bovine eye lens capsules, act as a natural basement membrane-like matrix, for the cells to grown on. By

comparing benzo(a)pyrene metabolism in cultured hair follicle keratinocytes and in freshly isolated hair follicles, it was shown that the systems formed the same range of organic solvent-soluble metabolites. Hair follicle keratinocytes cultured for 2-3 weeks, therefore, maintain the activity and function of benzo(a)pyrene-metabolizing enzymes of freshly isolated hair follicles.

Transformed cell lines: Transformed cell lines have the important advantages of unlimited growth and high reproducibility, contrary to primary cell cultures. To gain the potential immortality of a cell, different techniques like virus infection or transfection with isolated DNA were applied. Only a few transformed epidermal cell lines were described and used for skin metabolism studies (Ree et al., 1981). The advantages of epidermal cell lines for metabolism studies are remarkable. They are easily available, simple to culture and allow unlimited access to cells by passaging and cryopreservation. In addition, the application of cell lines can provide structural and biochemical reproducibility, which is usually not available with skin organ cultures or skin homogenates. However, it has to be noted that the cells are transformed and the expression of full enzyme patterns has not yet been completely proven. Hence, in regard to the metabolic activities and cellular functions, cell line models have to be well characterized, before general use as a universal model system for metabolism is going to take place.

Cultured 3D skin: Three-dimensional (3D) cell cultures with significant differentiation similar to normal skin were developed with more sophisticated techniques using collagen-containing matrices as substrates for keratinocytes, and by lifting the cultures to the air-liquid interface (Asselineau et al., 1987; Cumpstone et al., 1989; Pham et al., 1990). This cell culture model has been used for metabolism studies by Slivka (1992)

and Slivka et al. (1993). A very similar pattern of testosterone metabolites was found to be established in the 3D skin model as compared to neonatal foreskin. Steffens et al. (1992) compared metabolism of glyceryl trinitrate in a commercially available skin model with that in normal skin. It became clear that the metabolism in the normal human skin *in vitro* and in the cultured skin corresponded well both in the preference for a specific metabolite and in the extent of metabolism. Normal differentiation of human skin can be mimicked to a considerable extent in such complex cell cultures. Therefore, similar metabolite patterns and similar kinetics of the metabolism of topically applied substances can be expected, although, the preparation of the cell sheets is quite complex, costly and time consuming.

Full thickness skin in organ culture: The penetration of the topically applied substances in mouse skin is affected by the viability and the metabolic status of the skin (Holland et al., 1984). Kao et al. (1984) reported that viability maintenance of the tissue can be obtained by full-thickness mammalian skin in organ culture. Skin disks, freshly excised, and supported by sterile filter paper, are placed epidermal side up in an organ culture dish. Culture medium that contains foetal calf serum is then added so that the surface of the skin stays above the level of the medium. Viability, assessed by glucose utilization, can be maintained for about 24 hours. This technique is quite cost effective and economical since the size of one sample is small (usually about 5 cm^2) and the skin samples may be obtained from surgery or from laboratory animals.

Isolated perfused rabbit ear: A perfused skin organ model, according to what described by Behrendt and Kampffmeyer (1989), is the isolated perfused rabbit ear. In this technique, after removal of the ear the visible main artery is cannulated and perfused with a buffer solution. The marginal vein, which would be visualized by the effluent, is also

cannulated and the ear is transferred to a perfusion apparatus. Ester cleavage of methyl salicylate, after dermal application was investigated by applying this technique. It was shown that ester cleavage is a main metabolic reaction in the skin. The disadvantage of this technique is the requirement of considerable technical expertise for preparation of an also costly model (Behrendt and Kampffmeyer, 1989).

Contrary to the above-mentioned invasive techniques, an easy and simple technique to obtain samples from skin has been used by Merk et al.(1984, 1987). In this method, freshly plucked human hair follicles were applied, for example, to investigate the activity and inducibility of aryl hydrocarbon hydroxylase (AHH), an enzyme activating particular polycyclic hydrocarbons to carcinogenic forms. About twenty hair follicles were incubated at 37^{0}C with the precarcinogenic compound benzo(a)pyrene for 90 minutes. Then the metabolites were extracted from the incubation mixture and subjected to analysis. Because the hair follicles share their ectodermal origin with the epidermis it was assumed that metabolism in hair follicles may imitate that in the epidermis. A useful method of examining enzyme activity could be developed, if this could be proven systematically, as the hair follicles are readily accessible without significant discomfort.

2.2.3 Skin Homogenate Metabolism Studies

Homogenates were used for most of the studies on enzyme activities in the skin. Skin preparations or whole skin can be homogenized by different instruments, e.g., a Polytron tissue homogenizer or a Dounce homogenizer. Homogenates of whole animal or human skin were used for experiments on the proteolytic enzymes present in the skin as reported by Seppa et al. (1971) and Hopsu-Havu et al. (1977). Ghosh and Mitra (1990) applied homogenates of whole athymic nude mouse skin to examine hydrolase activity. The

metabolites of propranolol formed in the skin during percutaneous absorption have been studied after homogenizing the skin samples (Ademola et al., 1993). Since the homogenate of whole skin is made of different cell types and extracellular structures, the source of the individual enzymes is unknown. Applying the homogenates of more defined skin sections, e.g. isolated epidermis or dermis, the site and distribution of enzymatic activity may be determined with more accuracy. By using this technique, Bickers et al. (1985) indicated that the conversion of premutagens into mutagenic metabolites takes place both in the dermis and the epidermis. The location of AHH in mouse skin was studied by Wiebel et al. (1975), Wiebel (1980), Norred and Akin (1976), and Thompson and Slaga (1976). Highest enzyme activities were reported in the epidermis and in the superficial layer of the dermis containing the sebaceous glands, based to the applied separation technique. Skin is very resistant to homogenization, thus the harsh techniques necessary to disrupt the cells often result in the destruction of enzyme activities (Norred and Akin, 1976).

Subcellular fractions: To determine the subcellular localization of enzymes in the skin, cell homogenate fractions have to be prepared. Isolation of microsomal from cytosolic fractions is achieved by differential ultracentrifugation of the homogenate. The supernatant contains the soluble enzymes. The pellet, which contains the microsomes, is then resuspended in buffer. These fractions, properly diluted, are used to assay the activity of the enzymes of interest. By using the subcellular fractions of epidermal homogenates, AHH activity was found to be maximum in the microsomal fraction (Finnen and Shuster, 1985; Das et al., 1986a,b). In subcellular fractions of epidermis, both membrane bound and soluble amino acid 2-naphthylamidases were identified (Gray et al., 1977; Gray and Dana, 1979).

Isolated enzymes and purified enzyme fractions: Purification steps may be carried out to obtain enzyme fractions or isolated enzymes. Katagata and Aso (1986, 1988) showed that keratin polypeptides interact with a proteolytic enzyme fraction made from human epidermis. This might indicate an important step during differentiation in the human epidermis. Different peptidases, which metabolize peptides and peptide derivatives have been isolated from rat epidermis, eg., an aminoendopeptidase (Ito et al., 1984) a soluble dipeptidyl peptidase IV (Kikuchi et al., 1988) or a dipeptide naphthylamidase (Hopsu-Havu and Tuohimaa, 1970). The above-mentioned peptidases may be involved in postsynthetic changes of epidermal proteins although their natural substrates are often unknown. Cytochrome P-450 was purified from skin microsomes that was obtained from mouse skin after induction of mouse skin with benzo(a)anthracene (Ichikawa et al., 1989a,b). The studied enzyme, that is related to cytochrome P-450 isolated from rat liver, catalyzes benzo(a)pyrene hydroxylation and 7-ethoxycoumarin 0-deethylation and may play a role in the metabolic activation of chemical pre-carcinogens like polycyclic aromatic hydrocarbons.

Isolated and purified enzyme fractions and separated enzymes from defined skin structures usually have significance in the study of their substrate specificity, inducibility or of ways to control their activity. However, often isolated enzymes or enzyme fractions are only valuable *in vitro* models if several activators or coenzymes are added which are required for the enzyme to function.

2.2.4 Excised Skin Model

Excised full-thickness skin and skin preparations such as split-thickness (dermatomed) skin or isolated epidermis can be mounted in diffusion cells for permeation and metabolism studies. Diffusion cells consist of donor and receiver compartments, separated by the skin sample or other membranes. The skin exposes a defined area to both compartments. Temperature of the skin can be maintained by a thermostated water jacket at 32 or 37^{0}C. There are two main types of diffusion cells; flow-through and static types. In the flow-through type diffusion cells, the dermal side of the skin is exposed to the receiver medium which is continuously perfused through the cell at a defined flow rate mimicking the blood stream and may support skin viability. The receiver fluid is collected for analysis. In static diffusion cells the receiver medium is constantly stirred but it is not exchanged during the experiment. After samples are withdrawn from the receiver cell at various time intervals, the same volume is replaced by fresh medium. The use of diffusion cells for skin metabolism studies provides a defined area of the skin or of a skin preparation exposed to the drug preparation. The compartments can be steadily stirred so that best mixing conditions are achieved. In addition, the sampling ports allow regular removal of samples during the experiment (Collier et al., 1989). The use of full-thickness skin may be disadvantageous because the contribution of the relatively thick dermis is inconsistent with the skin under natural conditions, where substances are taken up into the capillary system shortly below the epidermal-dermal junction which cannot take place with excised skin (Steinstrasser and Merkle, 1995). However, for the evaluation of the permeability or partition of lipophilic drugs into the skin, full-thickness skin provides closer simulation of the real situation.

2.3 The Model Compounds

2.3.1 Tetracaine

2.3.1.1 Physicochemical Properties of Tetracaine

Tetracaine (TC, or amethocaine) is a p-aminobenzoic acid (PABA) derivative. Its molecular weight is 264.4, dissociation constant (pKa) 8.39. TC occurs as a white or light yellow waxy solid, melting point 41° to 46°. It is very slightly soluble in water, 1 part is soluble in 5 parts of alcohol and 2 parts of chloroform and ether (Windholz et al., 1983). Its hydrochloride salt, which is very soluble in water, is generally used in aqueous solutions, eye drops, injections and creams while the base is used in ointments and lozenges (Reynolds, 1996). It should be stored in air tight container and protected from light.

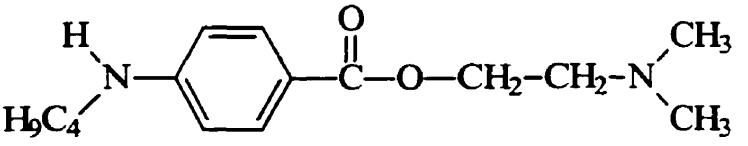

2-dimethylaminoethyl 4-butylaminobenzoate

Figure 2.1 Chemical structure of tetracaine

2.3.1.2 Pharmacological Uses of Tetracaine

Tetracaine is a potent local anesthetic with slow onset and long duration of action. However, its high systemic toxicity limits its use to surface and spinal anesthesia. Its absorption from mucous membranes is rapid and closely simulates intravenous injection. The nonpolar n-butyl group on the aromatic nitrogen atom might account for its higher lipid solubility (Darling, 1991) than procaine (the prototype of the aminobenzoic derivative local

anesthetics), hence the greater potency.

2.3.1.3 Metabolism and Degradation of Tetracaine

In aqueous solution, TC hydrolyzes to 4-(butylamino)benzoic acid (4-BABA) and dimethylaminoethanol (Figure 2.2). 4-BABA undergoes decarboxylation to butylaniline which oxidizes to form various purple-colored products. TC hydrolysis is catalyzed by both hydrogen and hydroxyl ions but it is more sensitive to base catalysis (Chalardsunthornvatee and Thomas, 1961). Aqueous solutions of TC are most stable at about pH 3.5 at 25 °C (The Pharmaceutical Codex, 1979). In the body, TC is hydrolyzed by both plasma esterases and liver esterases (Swinyard, 1990; Reynolds, 1996). In man, plasma hydrolysis is the highly

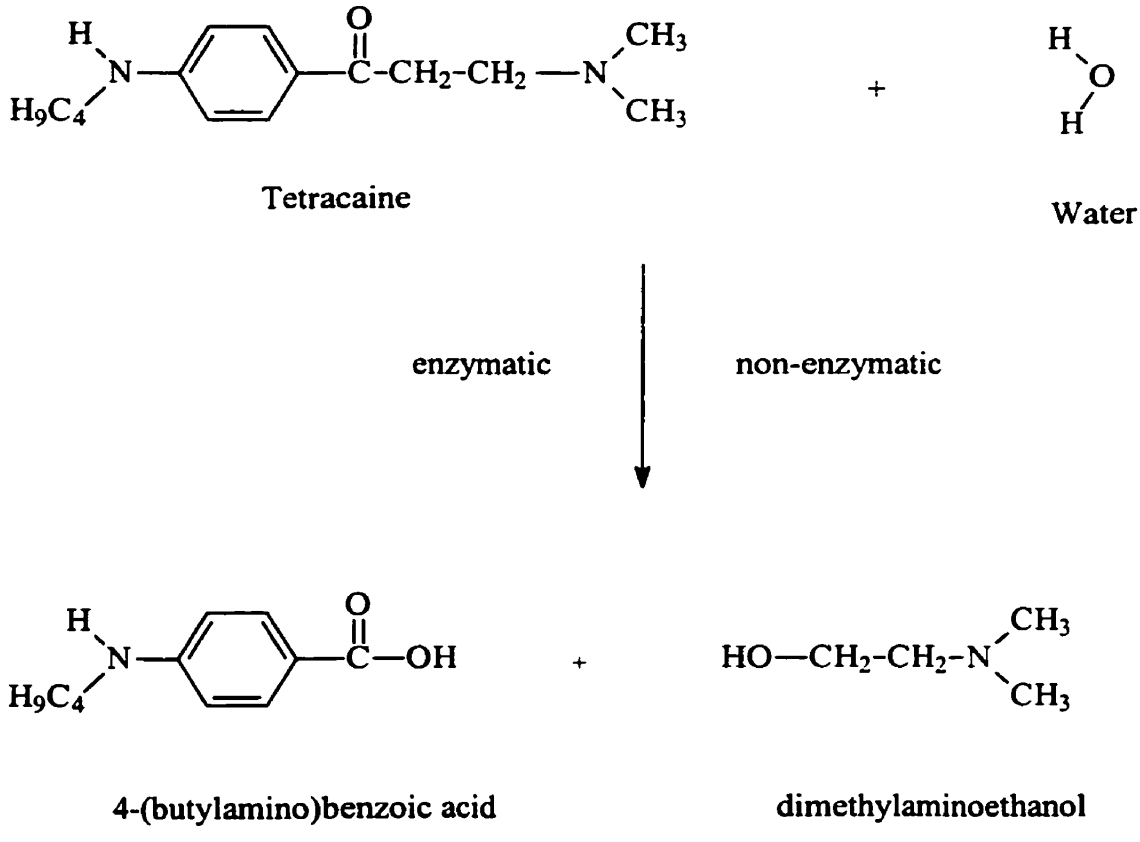

Figure 2.2 Metabolism of tetracaine

important metabolism route for ester-type local anesthetics. The hydrolysis rate in plasma is 4-20 times faster in human than in various animals. Thus, very little amount of the drug is available to be hydrolyzed by liver esterases. Spinal fluid has little or no esterases, accordingly, anesthesia caused by intrathecal injection of TC will persist until the drug is absorbed into the blood circulation. In contrast to the amide type local anesthetics, there is less pharmacokinetic data available on the ester type local anesthetics. Due to rapid metabolism, determination of drug concentrations in the blood is not easy (Swinyard, 1990).

The produced metabolites of TC are mainly excreted by the kidney, however, biliary excretion of TC also occurs in animals (Drug Information, 1988). Oxidation of TC in rats, mice, rabbits and horses after subcutaneous injection was reported and the urinary metabolite was identified as tetracaine N-oxide (Momose and Fukuda, 1976).

4-BABA has weaker pharmacological effect due to lower partition coefficient (2.61 as compared to 4.32 for TC, n-octanol and water system). It has a pKa of 2.52 and water solubility of approximately 140 mg/L (Grouls et al., 1997).

2.3.1.4 Analysis of Tetracaine

TC assays may be performed using the following methods; ultraviolet spectrophotometry (UV), gas chromatography (GC), high pressure liquid chromatography (HPLC), mass spectrometry and capillary electrophoresis (CE). Some methods are used for the analysis of TC, others for mixture of TC and other drugs or metabolites/degradation compounds in preparations (Venkateshwaran and Stewart, 1995; Wang et al., 1988; Larson et al., 1996; Bauer et al., 1984). Assays in blood samples have been conducted as well and no (Terndrup et al., 1992) or very little amount of TC was found after topical application

(Mazumdar et al., 1991) or intravenous or transtracheal administration (Porush et al., 1965).

Simultaneous determination of tetracaine HCl and its degradation product (4-BABA) in tetracaine HCl injection using a simple ion pair HPLC method was described by Menon and Norris (1981). The linear range was 0.4-2.0 mg/mL for tetracaine HCl and 0.003-0.02 mg/mL for 4-BABA at the UV response of 305 nm. The lowest amount measured by HPLC analysis was 2 μg for TC and 150 ng for 4-BABA. Woolfson et al. (1990) reported simultaneous analysis of TC and 4-BABA in skin homogenate samples from human and porcine sources using ion pair HPLC analysis. The linear range was 5.14-46.30 μg/mL for TC and 2.62-13.05 μg/mL for 4-BABA. From the calculation inferring to the lowest amounts measured, 128 ng was found for TC and 65 ng was found for 4-BABA.

2.3.2 Methyl Salicylate

Methyl salicylate (MS) is a topical analgesic and anti-inflammatory agent which is widely used in liniments, creams or ointments. Its molecular weight is 152.14, pKa 9.9. MS occurs as colorless, yellowish or reddish, oily liquid, with an odor and taste of gualtheria, melting point -8.6°, boiling point 220-224°. It is slightly soluble in water (1 g in about 1500 mL water), soluble in chloroform and ether, miscible with alcohol and glacial acetic acid (Windholz et al., 1983).

MS, an ester, is hydrolyzed in blood, liver and skin to salicylic acid (SA) which also has the analgesic and anti-inflammatory effect. SA is metabolized in the body by conjugation with glycine to produce salicyluric acid (SUA, major metabolite, 75%), or with glucuronic acid to form glucuronide ether and ester (15%). A small fraction of SA is oxidized to gentisic acid (2,5-dihydroxybenzoic acid) and to 2,3-dihydroxybenzoic acid and 2,3,5-trihydroxybenzoic acid. The rest of SA (10%) is excreted unchanged in the urine

(Foye et al., 1995; Hardman and Limbird, 1996). Metabolism of MS and SA are shown in Figures 2.3 and 2.4 respectively.

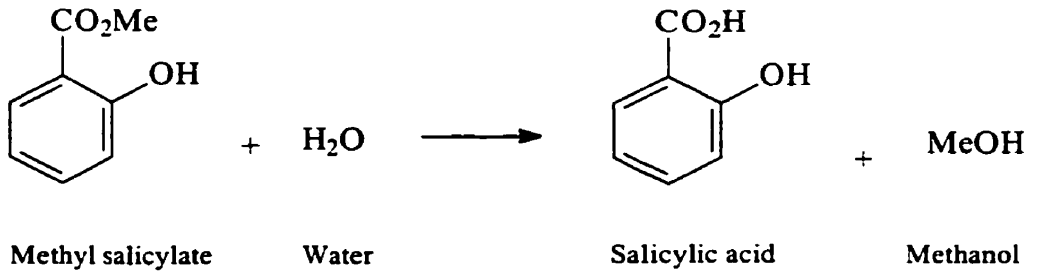

Figure 2.3 Metabolism of methyl salicylate

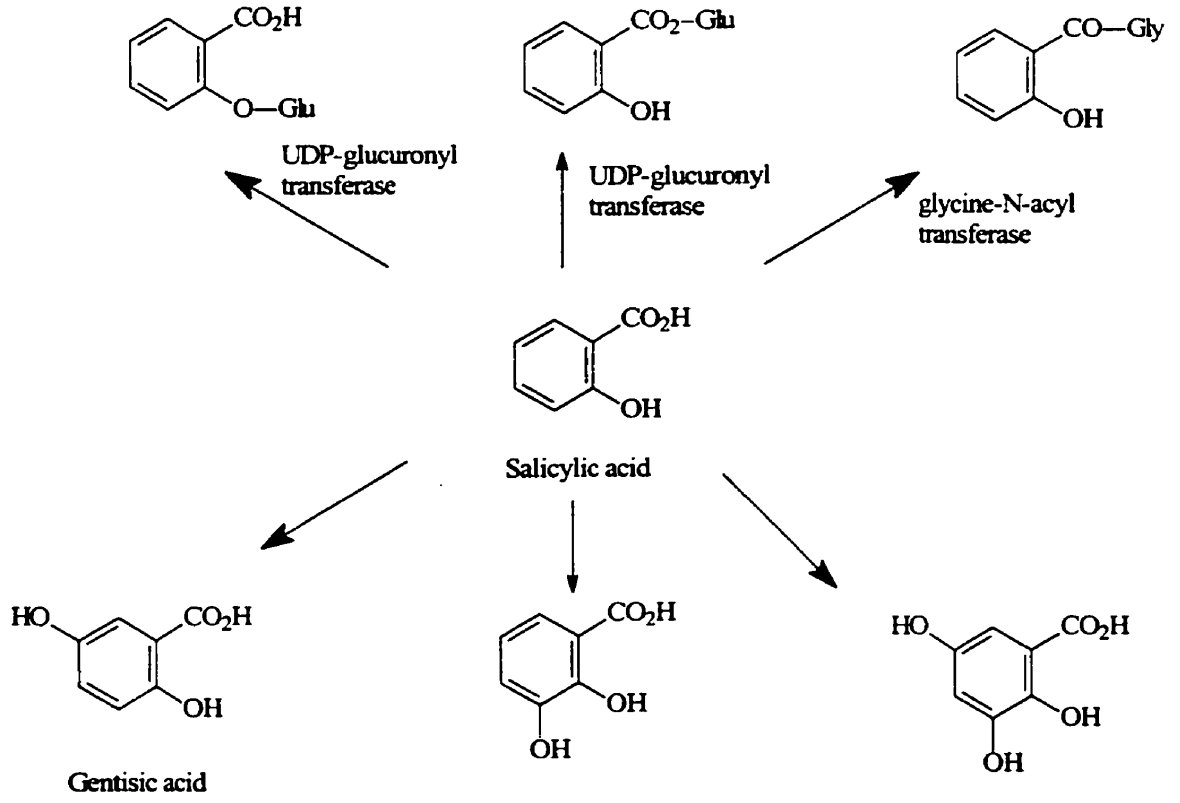

Figure 2.4 Metabolism of salicylic acid

SA has a molecular weight of 138.12, pKa 2.5 (Wilson and Gisvold, 1990). It appears as acicular crystals or crystalline powder, melting point 157-159°, boiling point 211°. One gram dissolves in 460 mL water, 15 mL boiling water, 2.7 mL alcohol. It is also soluble in acetone, chloroform and ether. It should be stored protected from light (Windholz et al., 1983). SA is used topically as keratolytic agent in form of ointments and solutions.

MS metabolism in skin homogenate was studied with hairless mouse skin by Yano et al. (1991). They showed that MS was hydrolyzed by hairless mice skin as well as by liver and blood. The hydrolytic activity of the skin homogenate was found similar to that of the serum but much lower than that of the liver. Moreover, it was found that *l*-menthol and *dl*-camphor inhibited MS hydrolysis.

MS metabolism during permeation study was examined with hairless guinea pig skin and was dependent on skin viability and the sex of the animal (Boehnlein et al., 1994). In their study MS, SA and SUA were found in the receptor fluid from viable skin while only SA and MS were found in non-viable skin. MS was hydrolyzed to a greater extent in viable skin than in non-viable skin. MS hydrolysis was greater in male than in female hairless guinea pig skin. However, percutaneous absorption values for MS through viable and non-viable skin were not significantly different.

In vitro percutaneous penetration and metabolism of MS and other SA derivatives across hairless mouse skin in a flow-through type diffusion cells was investigated (Higo et al., 1995). The percutaneous absorption of salicylates displayed a parabolic dependence on their n-octanol/water partition coefficient. Application of MS at lower concentration resulted in lower flux through the skin, and therefore a higher percentage of hydrolysis. Treatment of the skin with *l*-menthol prior to the application of salicylates inhibited

cutaneous hydrolysis of these compounds. However, in this investigation, the receptor chamber was perfused with phosphate buffered saline (PBS) pH 7.4 which would not maintain the skin viability during the 10 hours experimental period as demonstrated by Collier et al. (1989).

For *in vivo* studies, Overman and White (1983) demonstrated that MS was absorbed through skin of hamsters in teratogenic amounts. Roberts et al. (1982) calculated skin permeability coefficients, fraction of salicylate absorbed, and steady-state salicylate concentration for MS from urinary data after continuous topical absorption from a single application of commercial MS products to human. It was found that only 12 to 20% of the applied amount was absorbed into systemic circulation after 10 hours of application. Good agreement in urinary salicylate recovery in the first 24 hours from MS ointment application in healthy human volunteers was reported (Morra et al., 1996). This group also investigated the rate and extent of systemic salicylate absorption after single and multiple applications of MS ointment and pharmacokinetic parameters were calculated from serum and urine data. Using cutaneous microdialysis technique, Cross et al. (1997) demonstrated that MS was extensively metabolized to SA in the dermal and subcutaneous tissue of human volunteers after topical application. It was shown that commercial formulations containing MS allowed direct penetration, not recirculation in the blood, of salicylate into the underlying dermal and subcutaneous tissues. Subsequently, the same group also used cutaneous microdialysis technique to determine the difference in the extent of direct penetration of salicylates from commercial ester and salt formulations into dermal and subcutaneous tissue of human volunteers. They also compared the extent of MS hydrolysis *in vivo* to *in vitro* skin diffusion cells. However, non-viable skin (previously stored at

-20°C) was used in their experiment and the receptor fluid was 20% ethanol and 80% distilled water which would not maintain the viability of fresh skin during the permeation study (Cross et al., 1998).

2.4 Enzyme Kinetic Study

Enzyme kinetics is saturation kinetics because the enzyme concentration is limited in the reaction. Study of enzyme kinetics is useful in understanding the mechanism of action and control of isolated enzymes. It also helps us to appreciate the role of enzymes under the conditions which exist in the cell as well as the response of an enzyme to changes in the concentration of the substrate and metabolites. It may help to demonstrate how the activity of an enzyme can be controlled which may provide a valuable pointer to the mechanisms of regulation under physiological conditions (Price and Steven, 1993).

Enzyme kinetic data can be obtained by varying substrate concentrations ([S]) and determining the initial rate of the reaction (V_0) by either measuring the rate of product formation or the rate of substrate disappearance. Plot of [S] and V_0 obeys the Michaelis-Menten equation (Eq. 2.1)

$$V_0 = \frac{V_{max}[S]}{K_m + [S]} \qquad (2.1)$$

where V_0 = initial velocity of the reaction

V_{max} = maximum attainable velocity of the reaction

[S] = substrate concentration

K_m = substrate concentration at half V_{max}

The initial velocity of the reaction is the velocity at a time where [S] does not

change and no product is produced yet hence there is no influence from reverse reaction, substrate depletion or product inhibition. K_m, also known as Michaelis constant, describes the affinity of the enzyme for the substrate. A low K_m indicates strong interaction between the substrate and the enzyme. [S] used in the experiment is normally in the range of 4-5 K_m to ensure that the reaction is not limited by [S]. For enzyme kinetic studies, however, [S] range should lie inside the K_m.

2.4.1 Calculation of Enzyme Kinetic Parameters

Plot of [S] and V_0 results in a nonlinear graph due to the saturation kinetics (Fig 2.5). It is not easy to calculate the V_{max}, and subsequently the K_m, because very high [S] is needed to reach the steady state and practically it may not be possible due to solubility problem and the high cost. The Michaelis-Menten equation was derived in 4 ways in order to better calculate the V_{max} and K_m. The plots from the derivatives of Michaelis-Menten equation are Lineweaver-Burk plot, Eadie-Hofstee plot, Hanes plot and direct linear plot (Cornish-Bowden, A., 1995; Price and Steven, 1993).

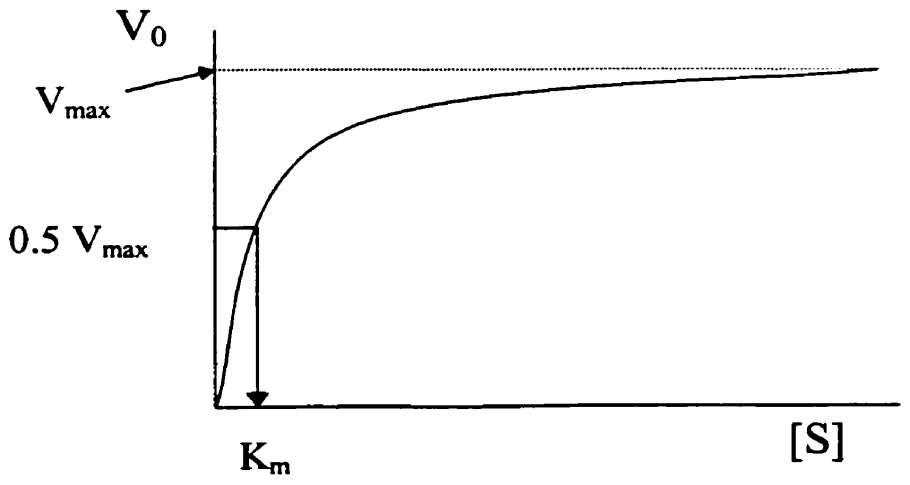

Figure 2.5 Plot of [S] and V_0

The Lineweaver-Burk plot or double reciprocal plot (Fig. 2.6) is the plot between $1/V_0$ and $1/[S]$. The equation (Eq. 2.2) is obtained by inversing the Michaelis-Menten equation;

$$\frac{1}{V_0} = \frac{K_m}{V_{max}} \cdot \frac{1}{[S]} + \frac{1}{V_{max}} \qquad (2.2)$$

V_{max} and K_m can be calculated from the y-intercept and the x-intercept respectively. This method is the most commonly used because of its simplicity. However, there is a non-uniform distribution of error in the values of $1/[S]$ and $1/V_0$ especially at very low [S].

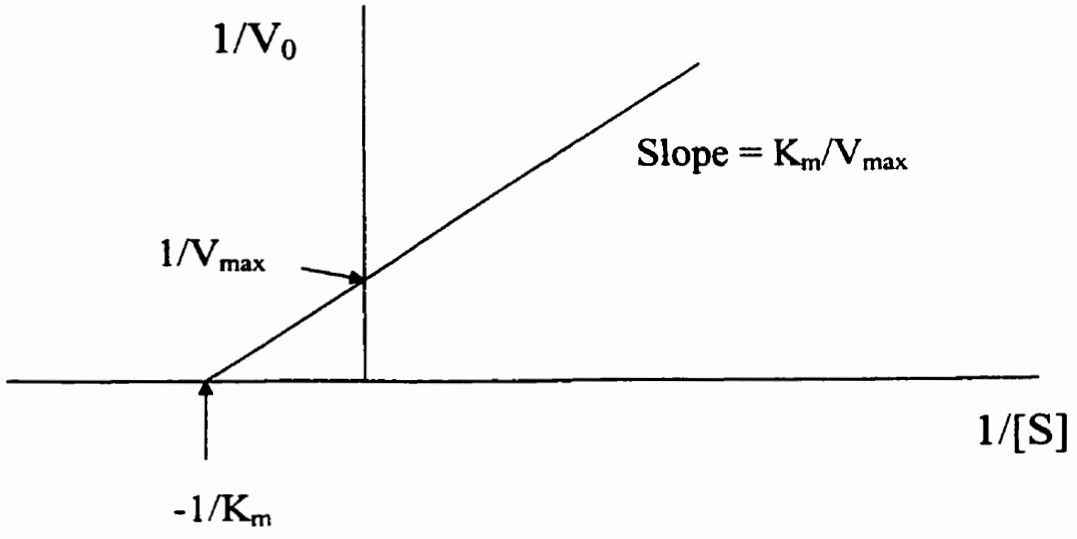

Figure 2.6 Lineweaver-Burk plot

The Eadie-Hofstee plot (Fig. 2.7) is the plot between V_0 and $V_0/[S]$. The equation (Eq. 2.3) is as follows;

$$V_0 = -K_m \cdot \frac{V_0}{[S]} + V_{max} \qquad (2.3)$$

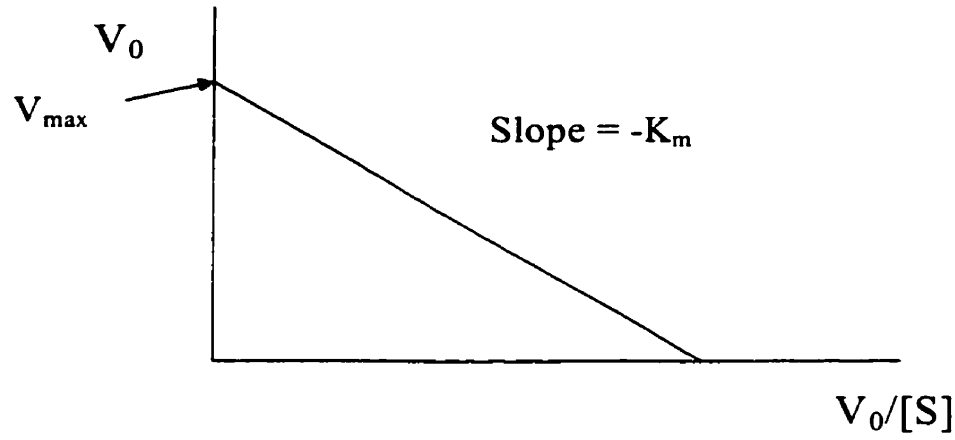

Figure 2.7 Eadie-Hofstee plot

V_{max} can be obtained directly from the y-intercept and K_m can be calculated from the slope. Although more manipulation of the data is required, this method provides much more uniform distribution of the [S] and V_0 as compared to the Lineweaver-Burk plot, hence more accurate values of K_m and V_{max}.

The Hanes plot (Fig. 2.8) is the plot between $[S]/V_0$ and [S]. The equation (Eq. 2.4) is as follows;

$$\frac{[S]}{V_0} = \frac{1}{V_{max}} \cdot [S] + \frac{K_m}{V_{max}} \qquad (2.4)$$

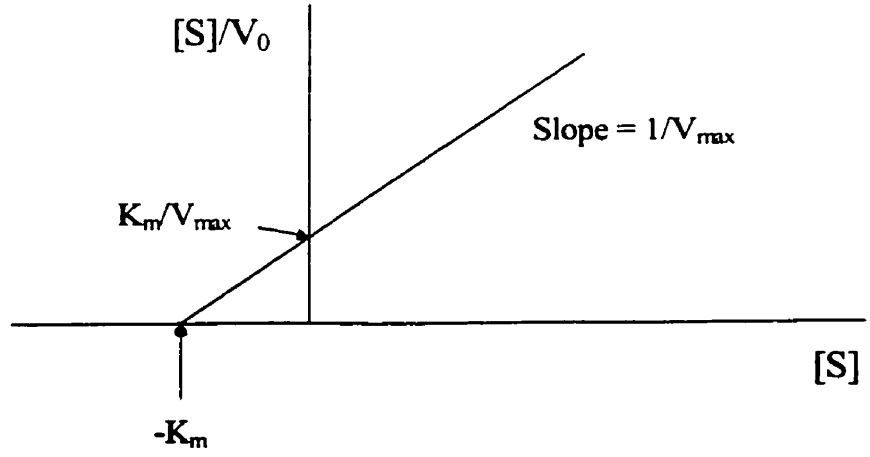

Figure 2.8 Hanes plot

K_m can be obtained directly from the x-intercept and V_{max} can be calculated from the slope. Similar to the Eadie-Hofstee plot, this method requires more manipulation of the data but it provides more uniform distribution of the [S] and V_0 as compared to the Lineweaver-Burk plot, hence more accurate values of K_m and V_{max}.

The direct linear plot (Fig. 2.9) is the plot between V_{max} and K_m. The equation (Eq. 2.5) is as follows;

$$V_{max} = \frac{V_0}{[S]} \cdot K_m + V_0 \qquad (2.5)$$

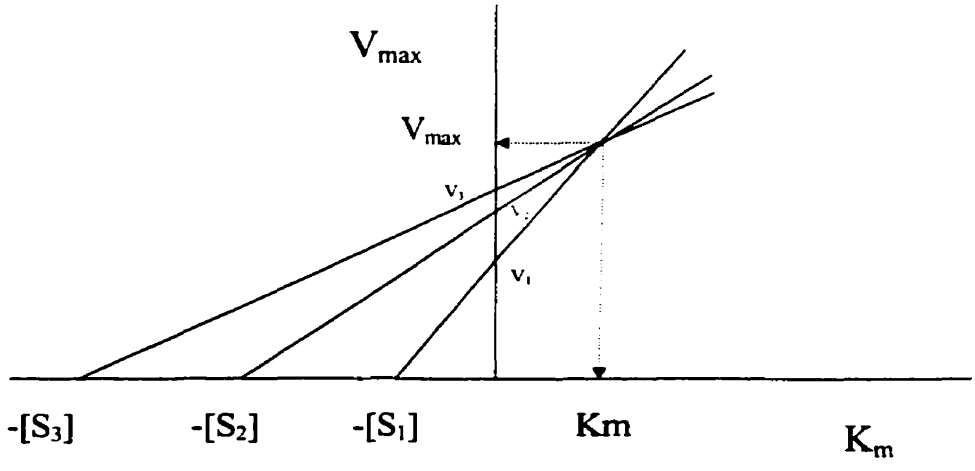

Figure 2.9 Direct linear plot

At each [S], V_0 is measured, namely V_1, V_2, V_3, etc. Then each V_0 is plotted against each -[S] and a line is drawn. If there is no error at all, the lines will intersect at one point. The extrapolation to the y-axis is the V_{max} and the extrapolation to the x-axis is the K_m. In real situations, however, there will be some errors and there will be several intersection points. In this case, the V_{max} and K_m are determined from the median values.

Inhibition of enzyme activity might be irreversible or reversible. Inhibitors can be classified as competitive, noncompetitive, uncompetitive and mixed type. Substrate inhibition and product inhibition occur as well.

2.5 Viability Assessment of Skin in *in Vitro* Models

2.5.1 General

Methods to assess viability include determination of protein synthesis, histological appearance and morphological changes, physiological indicators such as perfusate flow and pH, pressure and vascular resistance (in isolated perfused skin flap models), biochemical indicators which can be dye exclusion (trypan blue), skin surface fluorescence, glucose utilization (aerobic and anaerobic) or enzyme function.

Viability assessment was extensively evaluated in cryopreservation of tissues. There were only few evaluations of skin viability during permeation studies. Some of which were the measurement of anaerobic glucose utilization by determining lactate formation (Collier et al., 1989) and aerobic glucose utilization by measuring $^{14}CO_2$ formation.(May and DeClement, 1980; Collier et al., 1989).

The viability of fresh native human skin and cryopreserved human skin was evaluated using the tetrazolium salt, MTT (3-[4,5-dimethylthiazol-2-yl]-2,5-diphenyltetrazolium bromide), under a wide variety of conditions (Klein et al., 1996). The MTT assay has been claimed to provide a precise and reproducible index of viability for both fresh and cryopreserved skin. The simplicity, precision, and cost effectiveness of the MTT assay are among the advantages of this method that makes it a candidate for routine assessment of skin viability in skin banks, burn centers, and skin biology research units.

A rather complex method for skin viability estimation is using skin microcirculation. Nutritional circulation is the factor that skin viability depends upon. The conventional macrocirculatory methods that evaluate total blood supply cannot assess nutritional circulation. The major advantage of the microcirculatory methods is to provide information directly in the affected and diseased skin areas and assess the effectiveness of vasoactive agents where they are supposed to act. Among the techniques that are available today to evaluate the skin microcirculation, are capillaroscopy and transcutaneous measurement of the partial oxygen pressure. These methods are of special interest because they provide information that is directly useful in clinical practice (Bongard and Bounameaux, 1993).

2.5.2 Oxygen Consumption Assessment

Transcutaneous oxygen tension (PO_2-TC) measurement was extensively used to monitor blood oxygen tension in newborn and perioperative patient management, evaluation of lower limb ischemia, and also in viability assessments of skin flaps. This technique was developed in the early 1970s. Oxygen was measured with polarographic electrode which has a special sensor attached tightly to the skin. It is a noninvasive method. PO_2-TC depends on systemic oxygen tension in the arterial blood, the local perfusion pressure, the capillary density and local metabolic rate. Therefore, the information provided needs to be carefully interpreted (Fuch and Thiele, 1998). Invasive techniques such as insertion of needle electrodes and a microelectrode into the skin to measure intracutaneous oxygen pressure were used as well. These methods introduced bleeding, edema and vasoconstriction which might alter the level of oxygen in the skin as well as caused discomfort and damage to the skin.

Although transcutaneous oxygen monitoring has been commonly used in humans to assess the skin viability, few studies paid attention to the use of transcutaneous carbon dioxide (PCO_2-TC) monitoring for the same purpose. The application of PCO_2-TC monitoring for evaluating skin viability in dogs, for example, has been investigated (Rochat et al., 1993). Transcutaneous PCO_2 and local power reference (LPR) values were recorded for skin flap. Analysis of the arterial blood gas was taken to compare central partial pressure of carbon dioxide (PCO_2) values with peripheral skin PCO_2 values. Significant differences were detected between the PCO_2-TC values for apices and bases of the flaps, while a significant difference was not found between the LPR values for bases and apices.

Detection of radioactive carbon dioxide generated from aerobic metabolism of glucose was used by Collier et al. (1989) and Cornwell et al. (1997) to assess viability of skin in diffusion cells during permeation studies.

Zeiger et al. (1993) developed a simple system to measure the aerobic activity in small discs of split-thickness skin for viability assessment in the allograft skin banking using a Clark-type polarographic oxygen electrode connecting to a pH meter.

2.5.3 Confocal Laser Scanning Microscopic Method

Confocal laser scanning microscopy (CLSM) was first commercialized in 1988. It offers advantages over conventional optical microscopy as a non-destructive and rapid method for imaging complex structure matrices. It is capable of optically sectioning the specimens without the need of fixing and embedding (although many studies on fixed tissues were also applied), hence it requires little or no pretreatment of tissue before imaging. The images have better contrast and resolution due to the elimination of the scattered, reflected or fluorescent light from out-of-focus planes, especially in thick

samples. Figure 2.10 shows the diagram of the principle of CLSM.

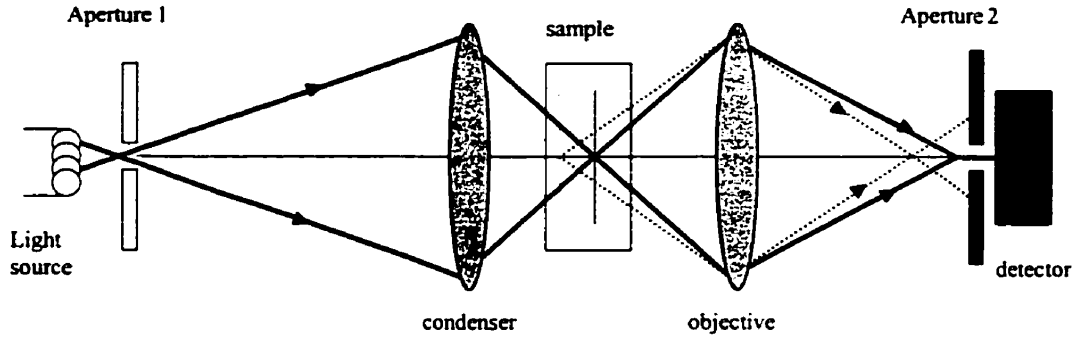

Figure 2.10 Principle of CLSM. Solid lines are illumination light while dotted lines display the directions of scattered light which form defocused spot and are mostly excluded from the detector by the second aperture. (Modified from Cullander, 1996.)

Three-dimensional (3D) images can be reconstructed from 2D optical sections. Video-rate confocal microscopy allows successful *in vivo* confocal imaging (reflected-light mode). In fluorescent mode, samples, which are auto-fluorescent or stained with fluorescent probes can be detected with an epi-fluorescent microscope. Simultaneous quantitation of up to 3-4 fluorescent markers at different wavelengths is possible. The applications to skin include morphology studies of human and animal skins (de Carvalho and Taboga, 1996; Vardaxis et al., 1997; Veiro and Cummins, 1994), keratinocyte culture (Hanthamrongwit et al., 1996), fibroblast culture (Braber et al., 1996) and reconstructed epidermis (Simonetti et al., 1995), *in situ* hybridization on fixed and embedded skin specimens (Mahoney et al., 1994; Thompson et al., 1994; Yokota et al., 1996), quantitative and morphological studies

of Langerhans' cells (Scheynius and Lundahl, 1990; Emilson et al., 1993, 1998; Yu et al., 1994; Emilson and Scheynius, 1995), enzyme aminopeptidase activity study (Boderke et al., 1997), and video-rate CLSM morphology studies of human skin *in vivo* (Corcuff and Leveque, 1993; Rajadhyaksha et al., 1995; Corcuff and Pierard, 1998). Additional applications in pathology and dermatology were reviewed by Fink-Puches et al. (1995). Fluorescence probes used were acridine orange for the study of nuclei and nucleoli (Veiro and Cummins, 1994), nile red for lipid material of epidermis (Veiro and Cummins, 1994; Simonetti et al., 1995), acriflavin and ethidium bromide (Hanthamrongwit et al., 1996), Pontamine Sky Blueleosin (Vardaxis et al., 1997) and many immunostains (Scheynius and Lundahl, 1990; Emilson et al., 1993; Yu et al., 1994; Emilson and Scheynius, 1995; Vardaxis et al., 1997).

The interaction of phospholipid liposomes with skin and stratum corneum lipid liposomes and the influence of phospholipid liposomes on the skin permeability of model drugs have been evaluated using confocal microscopy (Kirjavainen et al., 1999). Confocal microscopy studies showed that egg phosphatidyl cholesterol (EPC) (egg yolk lecithin), did not penetrate into the skin from water solutions, while from ethanol solutions, EPC penetrated deeply into the stratum corneum.

Computers can bring powerful applications to confocal techniques. Among these benefits are the use of segmentation of confocal microscope images of cell nuclei in thick tissue sections (Ortiz de Solorzano et al., 1999). Segmentation of intact cell nuclei from 3D images of thick tissue sections is a major basic capability necessary for many biological research studies.

Regarding viability assessment, Jones and Senft (1985) used fluorescein diacetate and propidium iodide double-staining procedure to determine cell viability in cell suspensions from mice spleen and compared this method to trypan blue dye exclusion. For skin samples, propidium iodide was used to identify cell death in the study of aminopeptidase activity in freshly excised human skin (Boderke et al., 1997). Calcein AM (CAM) and ethidium homodimer-1 (EthD-1) were used to determine the relative viability of the cornea and buccal mucosa (Imbert and Cullander, 1997, 1999).

CHAPTER THREE

EXPERIMENTAL

3.1 HPLC Analytical Methods

Reagents and Chemicals. Tetracaine, 4-BABA and 1-hexanesulfonic acid, sodium salt were purchased from Aldrich Chemical Company, Inc. (Milwaukee, WI, USA). Procaine HCl and salicyluric acid were from Sigma Chemical Company (St. Louis, MO, USA). All the solvents were of HPLC or ACS grade; acetonitrile, methanol and dimethylsulfoxide were obtained from EM Science (Gibbstown, NJ, USA). Salicylic acid, methyl salicylate (NF grade), propyl paraben (BP grade) and glacial acetic acid (ACS grade) were from BDH Inc. (Toronto, ON, Canada).

3.1.1 HPLC Methods for Tetracaine and its Metabolite

3.1.1.1 HPLC Method 1

From a previous metabolism study of topical TC preparations in rabbits in our lab, an unknown peak was found in rabbit blood samples stored at -20°C. The same peak was found in solutions of TC and 4-BABA in methanol after storage or after incubation in PBS at 37°C for 4 hours. This unknown peak was neither 4-BABA nor PABA. In order to analyze TC and 4-BABA and to identify the unknown peak, the HPLC method was further modified systemically from that described by Woolfson et al. (1990), using procaine HCl (PC) as the internal standard. The analysis conditions started from the following:

The HPLC system consisted of a Beckman System Gold programable solvent module 126, a Rheodyne injector, a Beckman System Gold diode array detector module 168 (Beckman Instruments Inc.) and a Dell Ultrascan 486P microcomputer to control the conditions and manipulate the data. The column was the Ultrasphere™ 4.6 x 150 mm, 5 μm ODS column with a 45 mm guard column (Beckman Instruments Inc., Fullerton, CA, USA). The mobile phase was acetonitrile (ACN): 5 mM hexanesulfonic acid (HSA) in water (75:25) at the flow rate of 1 mL/min. The peaks were detected as the UV absorbance at wavelength 310 nm.

The following manipulations were used to optimize the HPLC procedure:

1. Changing the composition of the mobile phase and using a premixed mobile phase instead of using 2 pumps to mix the mobile phase. The composition of the mobile phase were ACN: 5 mM HSA = 75:25, 80:20, 85:15 and 90:10.

2. Adjusting the pH of the mobile phase; 0.1 M acetic acid was used to adjust the pH of the mobile phase. The pH was varied from about 5.50 to 6.50 with 0.25 unit increments. The optimum pH was 6.00 where the 4 major peaks were separated, although not completely for 4-BABA, PC and the unknown. The mobile phase pH from then was adjusted to about 6.00.

3. Using a new guard column.

4. Changing the injection volume; injection volumes of 15 and 25 μL were used.

5. Changing the flow rate; the flow rate was reduced from 1 to 0.75 mL/min, and later, the flow rate was varied from 1 to 1.5 and 2 mL/min.

6. Modifying the concentration of the ion-pairing reagent; various concentrations of HSA were used: 0, 1.25, 2.5, 5, 7.5 and 10 mM, in the ratio of ACN:HSA = 75:25, pH

about 6.00.

7. Changing the composition of the mobile phase; the percentage of ACN was varied from ACN:2.5 mM HSA = 75:25 to 80:20 and 70:30. Subsequently, methanol (MeOH) was added in the mobile phase. The percentage of MeOH was varied from 4 to 40, by substituting ACN percentage and keeping the 2.5 mM HSA constant at 25%.

8. Using buffer; phosphate buffer was used at various concentrations. The concentration of the buffer was limited to 1-10 mM range due to the limited solubility of the buffer components in the mobile phase.

9. Temperature control; in one experiment the temperature of the column was varied from 25 to 75°C.

3.1.1.2 HPLC Method 2

This method was developed for the enzyme kinetic study of TC in human skin homogenate as HPLC method 1 could not be further modified to achieve better sensitivity. The HPLC system used was Waters 2690 Separations Module, with 996 diode array detector module and Millennium® system control and data acquisition software (Waters Corporation). The following approaches were used to optimize the HPLC procedure:

1. Changing the column; the columns used were Luna™ 4.6 x 150 mm, 5 µm ODS column with a 4.6 x 30 mm, 5 µm guard column (Phenomenex, Torrance, CA, USA) or SymmetryShield™ RP18, 3.9 x 150 mm, 5 µm with a 3.9 x 20 mm, 5 µm guard column (Waters Corporation) or Symmetry™ RP8, 3.9 x 250 mm, 5 µm (Waters Corporation).

2. Changing the composition and the pH of the mobile phase; gradient and isocratic runs of ACN and 10 mM phosphate buffer were performed. The pH of phosphate buffer were 3, 5, 7 and 10.

3. Changing the type and concentration of the buffer used in mobile phase; phosphate buffer concentrations of 10 and 25 mM were tried as well as 0.1% trifluoroacetic acid (TFA) or triethyl ammonium acetate as a composition in the mobile phase with ACN or ACN and MeOH mixture.

4. Varying the concentration of the ion-pairing agent; 1.25 and 2.5 mM HSA were used.

The flow rate was 1 mL/min.

3.1.1.3 Method Validation

Limit of detection (LOD) was determined by comparing the absorbance of known concentrations of the analyte with that of the baseline (the signal-to-noise ratio). The minimum concentration which resulted in a signal-to-noise ratio of 2:1 or 3:1 was considered as the LOD. Validation of the LOD was done by analysis of 6 samples prepared at the LOD. Limit of quantitation (LOQ) was assessed by analyzing the progressively lower concentrations of the standard solutions of the analyte. The best estimate of the lowest concentration that gives a coefficient of variation (CV) of approximately 10% on six injections was accepted as the LOQ. For accuracy determination, six assays of the analyte were performed. For the determination of intra-day precision, six assays of the analyte mixture were performed on a single day and for the determination of inter-day precision, six assays of the analyte were performed on three different days. For the linearity, calibration curves were determined from 6 concentrations of TC and 4-BABA (from 50 to 750 ng), excluding blank values. The range was estimated from the linearity and was verified by confirming that the method provides acceptable precision and accuracy when applied to samples containing analyte at the extremes of the range as well as within the

range.

3.1.1.4 Selection of Appropriate Solvents for Metabolism Study

Several solvents beside methanol and ethanol were tried for TC and 4-BABA; glycerol, propylene glycol, polyethylene glycol 300, ACN, dimethylsulfoxide (DMSO), mobile phase without methanol (ACN:2.5 mM HSA = 75:25), phosphate buffer saline (PBS) pH 7.2, and water. The parameters to be considered were the solubility, suitability as the solvent for analysis, and suitability as vehicle for the drug preparation.

3.1.1.5 Sample Preparation

For stock solutions; accurately weighed 20 mg of TC base was dissolved in DMSO and adjusted to 1 mL in a volumetric tube. The solution was then diluted with ACN to the required concentration. 4-BABA stock solutions were prepared the same way as TC solutions. PC was dissolved in water. All stock solutions were stored at -20°C.

For solutions; mixture of TC, 4-BABA and PC solutions were made at required concentrations from each stock solution using ACN as the solvent.

For human skin homogenate samples; human skin homogenate was incubated with TC solution in DMSO. At time intervals, an aliquot was taken and placed in ice-cold ACN, and mixed. Internal standard solution (if used) was added at this time and mixed. The solution was centrifuged at 16,000 x *g*, 4°C for 10 minutes or passed through 0.45 μm Millipore membrane filter before being analyzed by HPLC.

3.1.2 HPLC Method for the Analysis of Methyl Salicylate and its Metabolites

An HPLC assay method was used for the analysis of methyl salicylate (MS) and its metabolites, salicylic acid (SA) and salicyluric acid (SUA). The method was modified from that of Cham et al. (1979). The assay condition is as follows:

The HPLC system consisted of a Waters 2690 Separations Module, with a 996 diode array detector module and a Millennium® system control and data acquisition software (Waters Corporation). The column was the Ultrasphere™ 4.6 x 250 mm, 5 μm ODS column (Beckman Instruments Inc., Fullerton, CA, USA). The mobile phase was ACN : MeOH: 5% acetic acid in water (30:25:45) with the flow rate of 1 mL/min. Detection was by UV absorbance at wavelength 240 nm. Propylparaben was used as the internal standard.

3.2 Human Skin Homogenate Model

3.2.1 Preparation of Skin Homogenate

Technique for the preparation of the skin homogenate was developed by modifying the technique described by Woolfson et al. (1990).

Protocol for the preparation of skin homogenate.

Flow diagram

skin → trim, wash → weigh → mince → freeze in liquid nitrogen → grind → weigh → add PBS → homogenize → centrifuge → separate supernatant → freeze at -70°C

Fresh skin from breast reduction surgery was placed in sterile PBS and kept in an ice box during transportation to the laboratory. The following steps were performed under sterile conditions in a biological safety cabinet (Forma Scientific, Ohio, USA).

1) Fat and dead tissue were trimmed off under sterile PBS, on ice. The skin was cut into small pieces and washed with sterile PBS.

2) The skin was weighed then minced with scissors and frozen in liquid nitrogen.

3) The Analytical Mill® (IKA-Labortechnik, Germany) was cooled with liquid nitrogen. The frozen skin chunks were placed in the mill, then ground until being

powder. Liquid nitrogen was added from time to time to keep the frozen status.

4) The skin powder was transferred into a sterile, pre-weighed centrifuge tube. Sterile PBS was added in the ratio of skin weight:PBS volume = 1:5

5) The skin suspension was homogenized with Polytron® homogenizer (Brinkmann Instruments Inc., Rexdale, ON, Canada) at speed setting of 5 for 30 seconds, 4 times with 5 minute interval. During the interval, the chunks formed from collagen and elastic fibers were cut with scissors into small pieces. The temperature was kept cool at all times by surrounding the skin suspension with ice and by cooling the homogenizer head with liquid nitrogen before each homogenization.

6) The skin homogenate was centrifuged at 2300 x *g*, 4°C for 20 minutes (Accuspin FR Centrifuge, Beckman Instruments, Inc.). The supernatant was separated, pooled and divided into small portions, then kept at -70°C until required.

7) One-half of the supernatant was heated in boiling water for 2 hours and cooled before being divided into small portions and kept at -70°C. This was used as negative control in the metabolism study.

3.2.2 Protein Determinations

The protein content in the skin homogenates was determined by a modified micro-Lowry method (Lowry et al. 1951). Lowry reagent was prepared by mixing 1 mL of 1% w/v copper sulfate (Wiler Fine Chemicals Ltd., London, ON) and 1 mL of 2% w/v sodium potassium tartrate (BDH) and then adding 100 mL of 2% w/v sodium carbonate (Sigma) in 0.1 N sodium hydroxide (BDH). For each assay, 1 mL of diluted skin homogenate sample or working protein standard solution of bovine serum albumin (BSA, Sigma Diagnostics) was mixed with 1 mL Lowry reagent. After 10 minutes 0.1 mL of Folin &

Ciocalteu's Phenol reagent (BDH) was added and mixed. The solutions were left to allow color development for 1 hour then the absorbance was read at 750 nm (Novaspec II, Pharmacia LKB,). The protein concentration was determined from a calibration curve with the concentration range of 30 to 150 μg protein. The protein contents determined were used in the expression of the enzyme activity.

3.2.3 Metabolism Experiments

3.2.3.1 Tetracaine as Substrate

3.2.3.1.1 Pilot Study

Skin homogenate 960 μL was warmed at 37°C in a gently shaking water bath for 10 minutes (Gyrotory water bath shaker model G76, New Brunswick Scientific Co., Inc., New Brunswick, NJ, USA). At time 0, 40 μL of TC solution in DMSO (2% w/v) was added to the skin homogenate yielding the initial TC concentration of 303 μM in the incubation mixture. The mixture was mixed, then 25 μL aliquot was immediately taken. The aliquot was placed in 975 μL of ice-cold ACN and mixed in order to precipitate proteins hence stop the reaction. Internal standard solution (PC) was added and mixed. The solution was filtered through 0.45-μm Millipore membrane filter or centrifuged at 16,000 x *g*, 4°C for 10 minutes (Eppendorf Micro Centrifuge 5415C, Brinkmann Instruments, Inc., Rexdale, ON, Canada) then 25 μL of the filtrate or the supernatant was analyzed for TC and 4-BABA amounts by HPLC method 1. Additional aliquots are taken at time intervals up to 72 hours and analyzed in the same way. All samples were stored at -20°C if not immediately analyzed.

Negative controls (the same skin homogenate which was heated in boiling water for 2 hours and cooled) were incubated at the same time as the skin homogenates and were

processed in the same way as the skin homogenates.

3.2.3.1.2 Enzyme Kinetic Study of Tetracaine

Since it was found in the pilot study that TC had substrate inhibition at the initial TC concentrations used (303 μM) and there was no report about kinetic parameters of TC hydrolysis in human skin homogenate, enzyme kinetic study of TC in human skin homogenate was conducted.

3.2.3.1.2.1 Experimental Design

The experiment was conducted by varying TC concentration ([TC]), starting from a very broad range of initial [TC]. Series of TC solutions in DMSO were prepared so that the same volume was added to each skin homogenate, thus keeping the amount of added DMSO constant. TC solutions at specified concentrations were added to skin homogenates and the experiments were carried out following the protocol in section 3.2.3.1.1. The original incubation volume was 1 mL. Except for the first experiment, an appropriate standard curve was made according to the concentration range analyzed in each experiment.

1) Initial [TC] were 1, 10, 100, 1000, and 7500 μM; analyzed at time 0 and 1 hour.

2) Initial [TC] were 10, 50, 100, and 500 μM; analyzed at time 0 to 20 hours. Double sampling volume was performed at initial [TC] of 10 and 50 μM to enable the analysis at these low concentrations.

3) Initial [TC] were 50, 100, 250, 500, 750 and 1000 μM, analyzed at time 0 to 24 hours (6 time points).

4) Initial [TC] at 50, 75, 100, 150, 200, 250, 300, 400, and 500 μM, analyzed at time 0 to 24 hours (9 time points). Since the LOQ of TC was 5 ng, the lowest initial [TC] which still be accurately analyzed at time 0 would be 25 μM. However, once incubated, TC

amount will be depleted and the assay would not be accurate anymore. So the lowest [TC] was kept at 50 μM but [TC] were gradually increased to 500 μM.

5) Initial [TC] at 20, 40, 60, 80, 100, 120, 140, 160, 180 and 200 μM, analyzed at time 0 to 6 hours (7 time points). Human skin homogenate from full thickness skin of 3 sources were used. However, due to the limited amount of the skin source, the experiment with the third skin homogenate was conducted at initial [TC] of 40, 60, 80, 100, 120, and 140 μM. The skin homogenate was prepared by using the skin to PBS ratio of 1:2 which was 2 times more concentrated than previous skin homogenates. The incubation protocol was adjusted to be as follows:

Human skin homogenate 950 μL was warmed at 37°C in a gently shaking water bath for 10 minutes (Gyrotory water bath shaker model G76, New Brunswick Scientific Co., Inc., New Brunswick, NJ, USA). At time 0, 50 μL of TC solution in DMSO was added and mixed. A 100-μL aliquot was taken at time intervals (0, 1, 2, 3, 4, 5 and 6 hours). The aliquot was placed in 900 μL of ice-cold ACN, mixed to stop the reaction and precipitate the proteins, then centrifuged at 16,000 x *g*, 4°C for 10 minutes (Eppendorf Micro Centrifuge 5415C, Brinkmann Instruments, Inc., Rexdale, ON, Canada). The supernatant was analyzed by HPLC method 2. Negative controls were incubated at the same time as the skin homogenates and were processed in the same way as the skin homogenates. Positive control was Pseudocholinesterase enzyme (13 units). All samples were stored at -20°C if not immediately analyzed.

3.2.3.1.2.2 Determination of Enzyme Kinetic Parameters

The rate of 4-BABA formation was determined from the slope of the plot of 4-BABA concentration versus time at each initial [TC]. Then the rate of the reaction was

plotted with the initial [TC]. The slope of the linear regression at the initial part of the curve was calculated. The Lineweaver-Burk plot, the Eadie-Hofstee plot and the Hanes plot were drawn then the K_m and V_{max} values were determined from each method. The values from each method were compared.

3.2.3.2 Methyl Salicylate as Substrate

Human skin homogenate from full thickness skin of 3 subjects were used. Each experiment was run with 3 replicates for each sample. Positive control was Pseudocholinesterase enzyme (13 units) and negative controls were PBS and the skin homogenate from the same source which was heated in boiling water for 2 hours and then cooled. The incubation protocol was as follows:

Human skin homogenate 950 μL was warmed at 37°C in a gently shaking water bath for 10 minutes (Gyrotory water bath shaker model G76, New Brunswick Scientific Co., Inc., New Brunswick, NJ, USA). At time 0, 50 μL of MS solution in DMSO (100 mM) was added and mixed to make a total concentration of 5 mM MS in the incubation mixture. A 20-μL aliquot was taken at time intervals (0, 1, 2, 3, 4 hours). The aliquot was placed in 980 μL of ice-cold methanol, mixed to stop the reaction and precipitate the proteins, then centrifuged at 16,000 x *g*, 4°C for 10 minutes (Eppendorf Micro Centrifuge 5415C, Brinkmann Instruments, Inc., Rexdale, ON, Canada). The supernatant was analyzed by HPLC. All samples were stored at -20°C or 4°C if not immediately analyzed.

3.2.3.3 Effect of Heat on Esterase Activity in Human Skin Homogenate.

Skin homogenates were exposed to 60°C temperature (water bath) for 2 minutes or 2 hours prior to the incubation with MS solution. The experiment was then carried out in the same way as that described in section 3.2.3.2.

3.3 Excised Human Skin Model (*In Vitro* Flow-Through Diffusion Cell Study)

3.3.1 Viability Assessment of the Skin During Diffusion Cell Study

3.3.1.1 Diffusion Cell Setup

Fresh skin from breast reduction surgery was placed in sterile Hepes-buffered Hank's balanced salt solution (HHBSS), pH 7.4, and kept in an ice box during transportation to the laboratory. The full-thickness skin was cleaned, trimmed off the fat, cut into pieces then mounted, epidermis side up, on Flow-Thru-type diffusion cells (Amie System, USA) with a receptor volume of 400 μL and exposed surface area of 0.32 cm^2 (Figure 3.1). The bore of the top of the diffusion cell was enlarged to accommodate the oxygen probe. The diffusion cells were placed on a Posiblock heater which was maintained at 37°C by circulating water bath, yielding a skin surface temperature of 32°C. Sterile HHBSS which was proven to maintain the viability of the skin for 24 hours during permeation study (Collier et al., 1989) was gassed with oxygen and maintained at 37°C. It was perfused through the receiver chambers of the diffusion cells at 3.5 mL/hour by a peristaltic pump (Sarah standard cassette pump, Manostat Corporation, New York, NY, USA). Fresh skin samples from surgery were used as live tissue and skin samples which were stored at -20°C for 5-16 months were used as dead controls (shams).

The experiment was run for 24 hours. Oxygen consumption measurement was performed at times 0, 4, 10 and 22 hours. At 24 hours, the skin samples were taken out from the diffusion cells and processed for the confocal laser scanning microscopic study.

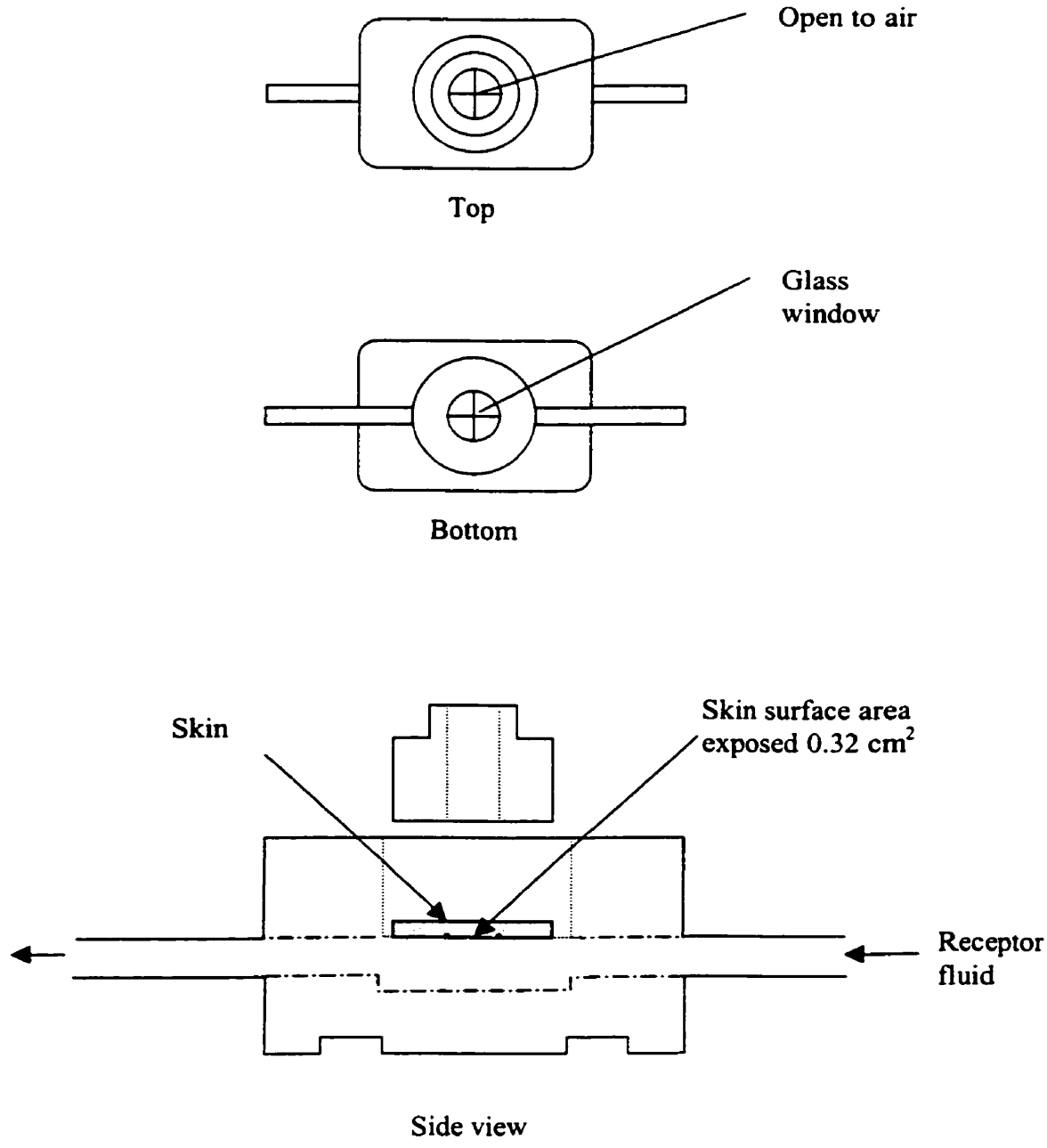

Figure 3.1 Diagram of the Flow-Thru-type diffusion cell used in the permeation study.

3.3.1.2 Oxygen Consumption Measurement

An oxygen electrode was used to measure the oxygen concentration in the buffer above the skin surface on diffusion cells. The change in oxygen concentration in the buffer with time reflects the oxygen consumption by the skin sample and hence its viability.

At time of measurement, 300 - 400 μL of HHBSS was pipetted into the bore on top of the diffusion cell, covered with parafilm and was equilibrated for 5 minutes. An oxygen electrode (Orion Research, USA) connected to a pH/ion meter (Accumet 25, Fisher Scientific, USA) was calibrated in the water-saturated air and then was used to measure the oxygen concentration in the buffer continuously for 10 minutes then the buffer was pipetted out. The pH meter was linked to a computer to collect data on file. The collected data were processed in a spreadsheet program (Microsoft Excel 97, Microsoft Corporation, USA). Figure 3.2 depicts the oxygen concentration measurement in the diffusion cell and how the system was set up. Two parameters were derived; the slope of the linear regression using data from 100 to 600 seconds (process 1) and the difference between the oxygen concentrations at peak of the graph and at the 600th second (process 2). These parameters for live and sham samples were compared. Statistical significance was determined using ANOVA and means comparisons (SuperANOVA, Abacus Concepts, Inc., CA, USA).

3.3.1.3 Confocal Laser Scanning Microscopy Study

This part was conducted in collaboration with Dr. Radha Naik, Department of Pharmacology.

3.3.1.3.1 Sample Preparation

Thick samples: The skin sample from the diffusion area or control was mechanically cut in the cross-section plane into pieces of approximately 1 mm x 1 mm and 200 - 400 μm

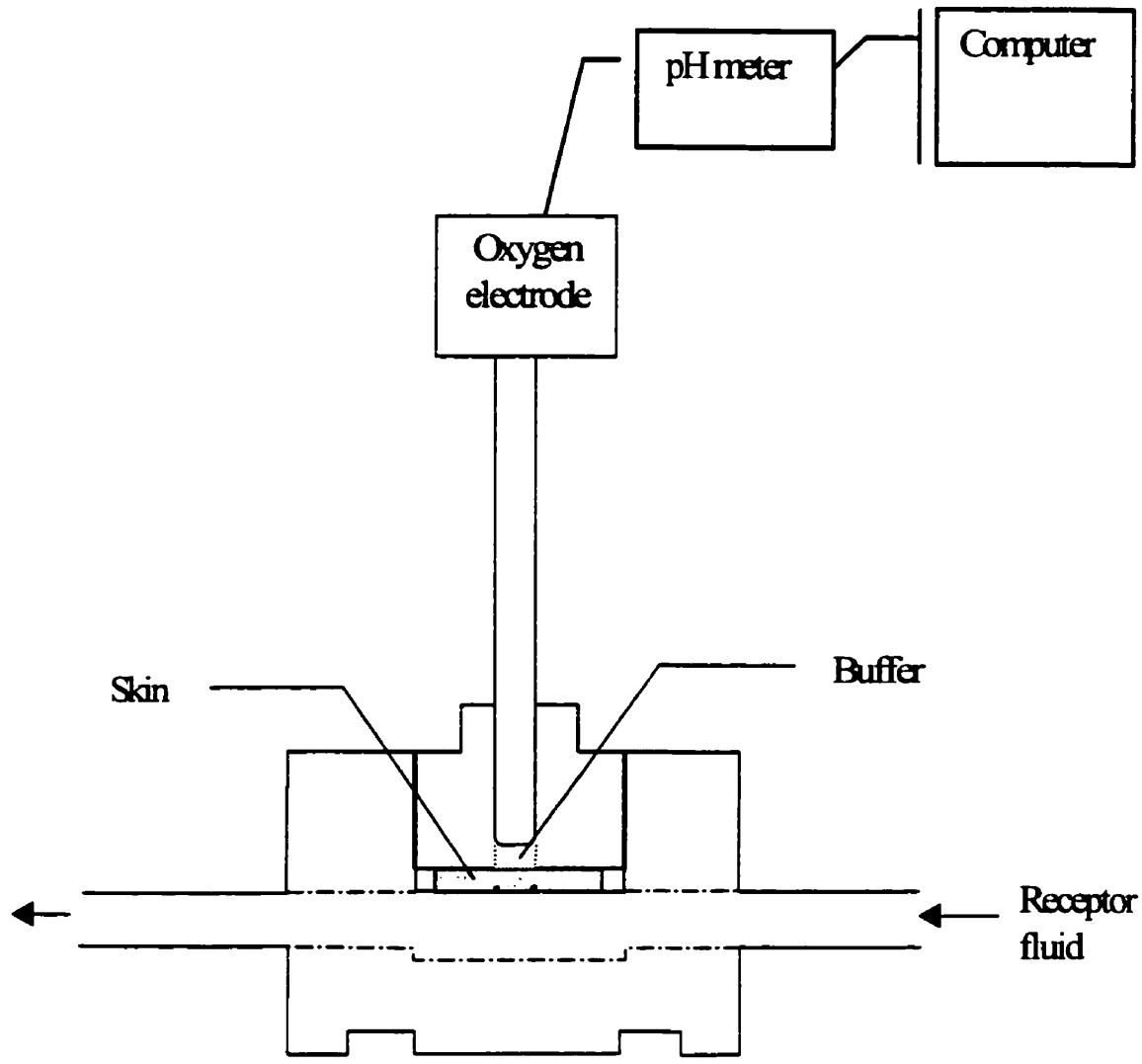

Figure 3.2 Oxygen concentration measurement in diffusion cell. The oxygen electrode was inserted into the bore in the top part of the diffusion cell. It measured oxygen concentration in the buffer above the epidermis side of skin in the diffusion cell. The electrode was connected to a pH meter which was linked to a computer to collect data during measurements.

thickness with a razor blade then stained with solutions of EthD-1 and CAM according to the proper staining protocol before examining with CLSM.

Samples of 100 μm thickness: The skin sample from the diffusion area or control was cut (cross-sectioned) into pieces of approximately 2 mm x 3 mm, then encased between thin sheets of dental wax and mounted on a glass slide with an aid of low heat from a hot plate. The slide was cooled in refrigerator for at least 10 minutes to harden the wax then it was mounted on the specimen holder of the Vibroslice™ microtome (Campden Instruments, UK). The encased skin sample was cross-sectioned in the cool buffer bath into 100 μm thickness sections. The skin slices were taken off the wax and stained with solutions of EthD-1 and CAM according to the proper staining protocol then hydrolyzed in normal saline solution before examined with CLSM.

3.3.1.3.2 Staining Protocols

Fluorescent probes (CAM and EthD-1) were purchased as the Live/Dead® Viability/Cytotoxicity Kit for animal cells (Molecular Probes, Eugene, OR, USA) and were stored at -20°C. Working solutions were prepared fresh and used within the same day. The concentration of the probes and the staining time and temperature were varied to obtain an optimal condition:

Thick samples: The concentration of CAM and EthD-1 were 4 μM and 10 μM respectively. The staining time of CAM was varied from 45 to 90 minutes while that of EthD-1 was varied from 10 to 20 minutes. The staining temperatures were 4°C and 37°C.

Samples of 100 μm thickness: The concentration of CAM was 4 μM, EthD-1 concentration was varied from 4 to 15 μM. The staining time of CAM and EthD-1 was varied from 30 to 45 minutes and from 10 to 90 minutes respectively. The staining

temperatures were 4°C, room temperature and 37°C.

3.3.1.3.3 Effect of Scan Depth and Tissue Thickness on the Light Intensities of Probes In the Skin Samples

In order to know whether tissue thickness and scan depth would give any difference in the light intensities of probes in the skin samples, both thick (200- to 400-μm) and the 100-μm skin slices were scanned at the depth of 5, 10, 20, 40, 80, and 100 μm from the cutting surface using 2.5x objective. The relative intensities for both probes were analyzed as described in the CLSM observation section (3.3.1.3.4).

3.3.1.3.4 Confocal Laser Scanning Microscopy Observation

Skin samples were placed, with a small amount of normal saline solution to prevent drying out, in a glass chamber containing a #0 coverslip (Carolina Biological Supply Company, Burlington, NC, USA) and scanned with a Multiprobe 2001 (Molecular Dynamics, USA) argon/krypton CLSM, equipped with a Nikon Diaphot epifluorescence inverted microscope. Figure 3.3 shows how the skin sample was cut and the orientation of the skin in the glass chamber during the observation with the CLSM. A 488 nm argon laser line (30 mV) directed through a 510 primary dichroic filter and attenuated with a 10% neutral density filter was used. The pinhole size was set at 100 μm. The primary and secondary beam splitters were set at 510 and 565 respectively. Detector filters of 640 df 20 and 510 were used. The image size was 512 x 512 pixels with a pixel size of 20.31 μm and 1.27 μm for the 2.5x and 20x objectives respectively. All settings, including the photomultiplier tube and photometric gain were kept constant once the appropriate settings were determined.

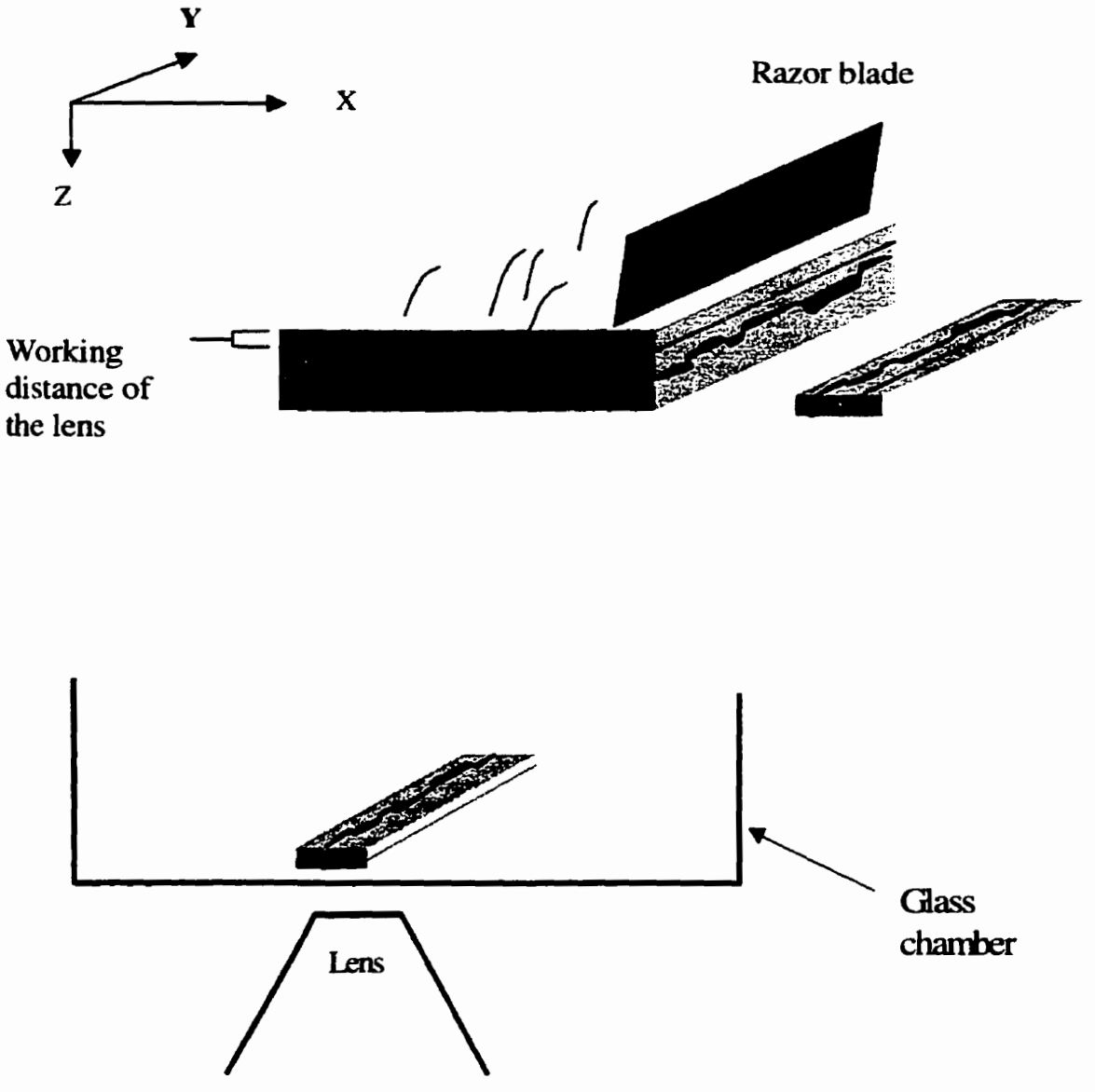

Figure 3.3 The cutting plane of the skin for the CLSM experiment. The skin sample was cut with a razor blade in the cross-section plane. During the observation with the CLSM, the skin section was placed on its side in a glass chamber so that both the epidermis and the dermis could be scanned at the same depth.

3.3.1.3.5 Data Analysis

Analysis of relative intensities for both probes were performed on a Silicon Graphics Indy computer with the Image Space software. This software was used both for data acquistion and analysis. Background fluoresence was determined to be below 15, so a cut off for intensities below 15 was used. The results are expressed as a ratio of the intensity value obtained in channel two (calceine) over that in channel one (EthD-1). Statistical significance of the ratios was determined using ANOVA and means comparisons where appropriate (SuperANOVA, Abacus Concepts, Inc., CA, USA).

3.3.2 Metabolism of Methyl Salicylate During Permeation Study in Diffusion Cells

Absorption and metabolism experiments were conducted using flow-through diffusion cells (Crown Glass Corporation, USA). Fresh human breast skin was obtained immediately after plastic surgery. The skin sample was cleaned, subcutaneous fat trimmed off, cut into pieces then mounted, epidermis side up, in the diffusion cell. The skin viability was maintained during handling, transportation and in the diffusion cells by using HHBSS as medium and the receptor fluid. The receptor fluid was gassed with oxygen during the experiment. The flow rate was 1 mL/hour.

One hundred mg of 20% w/w MS cream in Glaxal base (Glaxo Canada) was applied on the skin, then the opening of the top part of the diffusion cell was covered with Parafilm to prevent the evaporation of MS. The eluates were collected at 2, 4, 6, 12, 18, and 24 hours. After 24 hours, the cells were dismantled, MS cream recovered and the surface of the skin was washed with copious amount of sterile deionized distilled water. The wash was collected, combined with the recovered cream, sonicated, filtered through 0.45 μm membrane then analyzed by HPLC. The diffusion area of the skin was cut out, stripped

once with Scotch tape™ (3M, St. Paul, MN, USA), weighed then homogenized in methanol by a tissue homogenizer (Cyclone Virtishear, Canberra Packard Canada). The tissue homogenate was centrifuged at 2300 x *g*, 4°C for 10 minutes (Accuspin FR Centrifuge, Beckman Instruments, Inc.). The supernatant was further centrifuged at 16,000 x *g*, 4°C for 10 minutes (Eppendorf Micro Centrifuge 5415C, Brinkmann Instruments, Inc., Rexdale, ON, Canada) and the supernatant was analyzed by HPLC. Aliquot of all receptor fractions were diluted with methanol at a ratio of fraction:methanol = 1:2, then centrifuged at 16,000 x *g*, 4°C for 10 minutes and the supernatant was analyzed by HPLC. All samples were stored at -20°C or 4°C if not immediately analyzed.

The skin was obtained from 3 different subjects, aged 30-35 years. Each experiment was run with 4 replicates. Negative control was the skin from the same source, stored at -20°C and heated in deionized distilled water at 60°C for 2 hours, then cooled in HHBSS on ice prior to being mounted in the diffusion cells. Two tailed, paired t-test was used as the statistical tool (Microsoft Excel 97, Microsoft Corporation, USA).

3.4 Localization of Esterases in the Skin

Skin samples, fixed in formalin solution, from the viability studies on diffusion cells were submitted to the Department of Pathology for morphology and staining for esterases. The skin samples were processed for morphology study using paraffin sections stained with hematoxylin and eosin (H&E).

α-Naphthyl acetate esterase assay kit (procedure no. 90, Sigma Diagnostics) was used to demonstrate nonspecific esterase (NSE) activity. Paraffin sections of the skin sample (cross-sections) were strippped off the wax and incubated with α-naphthyl acetate in the presence of a stable diazonium salt. Enzymatic hydrolysis of the ester linkages

liberates free naphthol compounds which couple with the diazonium salt, form black deposits at the sites of enzyme activity.

CHAPTER FOUR

RESULTS AND DISCUSSION

4.1 HPLC Analytical Methods

4.1.1 Optimal HPLC Analytical Method for Tetracaine and its Metabolite

4.1.1.1 HPLC Method 1

Several approaches were used to optimize the HPLC method 1.

By changing the composition of the mobile phase and using a premixed mobile phase instead of using 2 pumps to mix the mobile phase (the composition of the mobile phase were ACN: 5 mM HSA = 75:25, 80:20, 85:15 and 90:10); none of these systems could resolve all the analyte peaks.

The mechanism of separation in this system is reverse-phase ion-pair chromatography, using HSA as the ion-pairing reagent. pH plays a significant role in the ionization of the analytes, hence the separation. The pH of the mobile phase was varied from about 5.50 to 6.50 with 0.25 unit increments. TC, PC and 4-BABA were all sensitive to pH change and the retention times of these compounds changed with the changing pH. The unknown peak was relatively stable to pH change and the retention time was 3.5 minutes. The optimum pH was 6.00 where the 4 major peaks were separated, although not completely for 4-BABA, PC and the unknown (Figure 4.1). The mobile phase pH from then was adjusted to about 6.00.

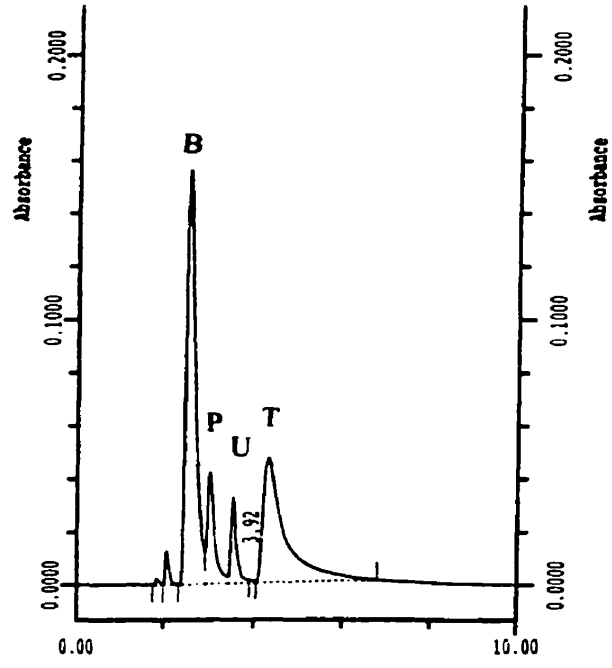

Figure 4.1 HPLC chromatogram of 4-BABA (B), procaine (P), the unknown (U) and tetracaine (T). The column was Ultrasphere™ 4.6 x 150 mm with 45 mm guard column, the mobile phase was ACN : 5 mM HSA = 75:25, pH 5.98, flow rate 1 mL/min.

After changing to a new guard column, TC peak shifted to longer retention time than with the old guard column. However, the separation of the other 3 peaks was not improved.

Because there was tailing of TC and 4-BABA peaks, injection volume was reduced from 25 μL to 15 μL. However, this neither overcame the tailing problem nor helped the separation. Moreover, other peaks looked broader and had more tailing. So the injection volume was kept at 25 μL.

The flow rate was reduced from 1 to 0.75 mL/min in an attempt to separate the 3 overlapping peaks. But the peaks were still overlapped and looked broader. Thus the flow rate of 1 mL/min was used for the analysis. However, after several months the retention times of the analytes shifted from 3.6 to 4.4 min for PC and 6.3 to 7.4 min for TC. Although all peaks were still resolved, there was a concern about analysis time, especially when high concentration of TC was analyzed. Since TC peak had a long tail, a longer analysis time was needed (e.g. from 10 to 15 min) in order to correctly integrate the peak area and let the system return to the baseline before introducing the next sample. Flow rate was adjusted from 1 to 2 mL/min (Fig. 4.2), the retention times decreased from 2.89 to 1.45 min for 4-BABA, from 4.36 to 2.19 min for PC and from 7.49 to 3.70 min for TC. Although the peak areas decreased, the peak shape of TC was improved and the analysis time could be reduced to 7 minutes per assay.

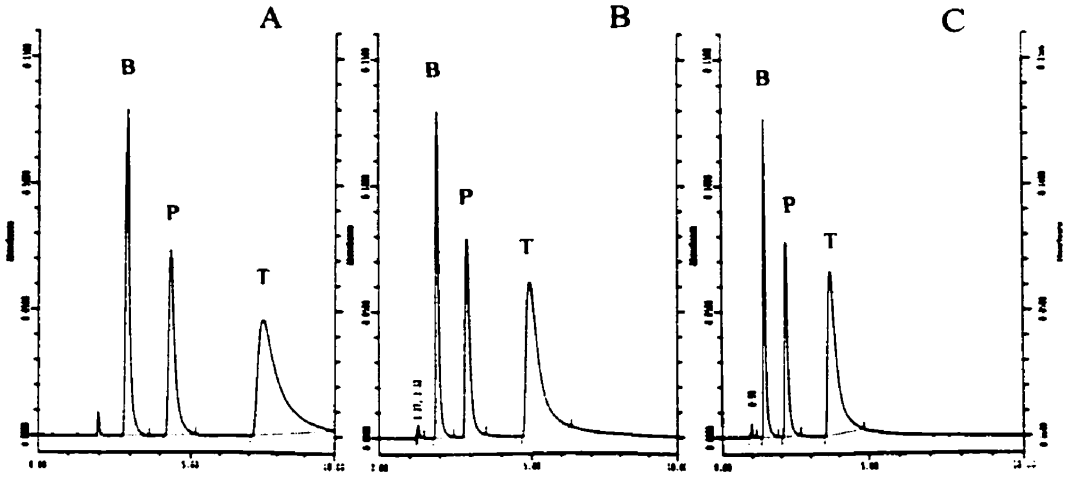

Figure 4.2 Effect of flow rate on the retention times and peak shapes of 4-BABA (B), procaine (P) and tetracaine (T). The column was Ultrasphere™ 4.6 x 150 mm with 45 mm guard column, the mobile phase was MeOH:ACN:2.5 mM HSA = 40:35:25, pH 6.00. Flow rates ; (A) 1 mL/min, (B) 1.5 mL/min, (C) 2 mL/min.

Since the organic phase constitutes at least 70% of the mobile phase, concentration of the ion-pairing reagent might be an important factor in the separation of the analytes. Various concentrations of HSA were used: 0, 1.25, 2.5, 5, 7.5 and 10 mM, in the ratio of ACN:HSA = 75:25, pH ~ 6.00. At 0% HSA, PC and TC peaks had very short retention times, about 1.4 min, and could not be separated. With samples which were kept for 2 months, the PC and TC peaks were hardly detectable. At higher than 5mM HSA, the peaks were overlapped. The best available results were from 2.5 and 1.25 mM HSA where there was slightly overlapping of 4-BABA and the unknown peaks. The concentration of 2.5 mM HSA was selected for further experiments because it provided better peak shapes and peak areas of the analytes and all peaks could be analysed within 10 minutes as compared to 15 minutes for the 1.25 mM concentration (Figure 4.3).

By changing the ratio of ACN to 2.5mM HSA from 75:25 to 80:20 and 70:30, all analytes still could not be resolved. MeOH was added to the mobile phase and it improved the peak shapes of TC, PC, and especially, 4-BABA. Percentage of MeOH was varied from 4 to 40, by substituting ACN percentage and keeping the 2.5 mM HSA constant at 25%. The compositions which all major analytes could be resolved were at the ratio of MeOH:ACN:2.5mM HSA of 4:71:25, 5:70:25, 30:45:25 and 40:35:25 (Figure 4.4). The 40:35:25 composition was chosen to be the optimum mobile phase because it provided better peak shape for 4-BABA while TC and PC peaks in other systems with low percentage of MeOH were quite similar. The 40:35:25 ratio provided better peak positions of the analytes than the 30:45:25 system.

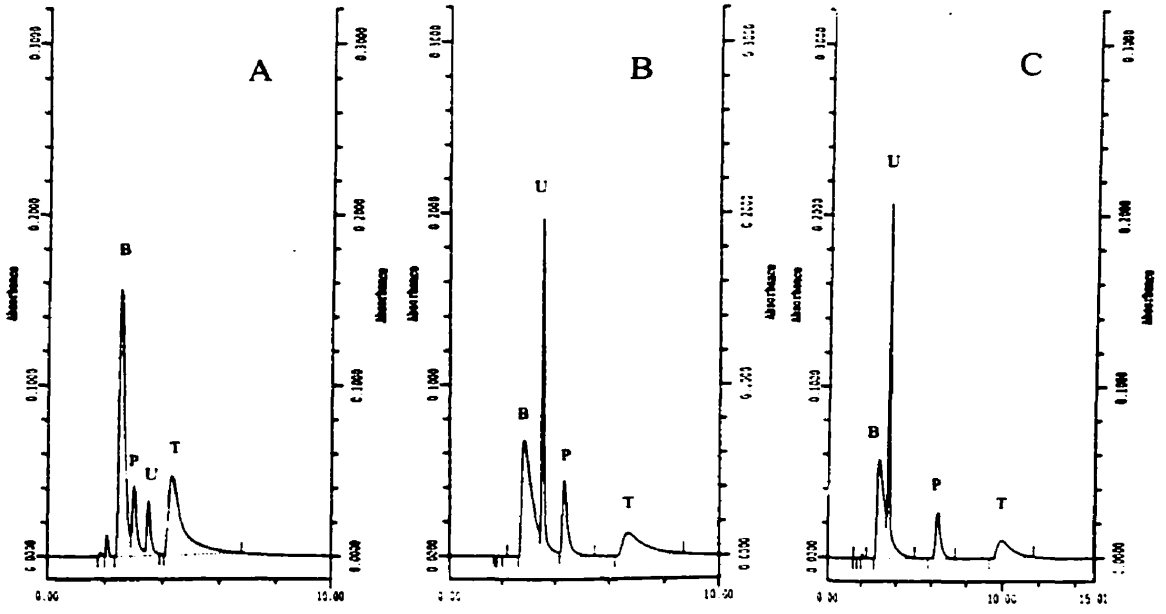

Figure 4.3 Effect of the concentration of the ion-pairing reagent on HPLC chromatogram of 4-BABA (B), procaine (P), the unknown (U) and tetracaine (T). The column was Ultrasphere™ 4.6 x 150 mm with 45 mm guard column, the mobile phase (pH 6) were (A) ACN : 5 mM HSA = 75:25, (B) ACN : 2.5 mM HSA = 75:25, (C) ACN : 1.25 mM HSA = 75:25, flow rate 1 mL/min.

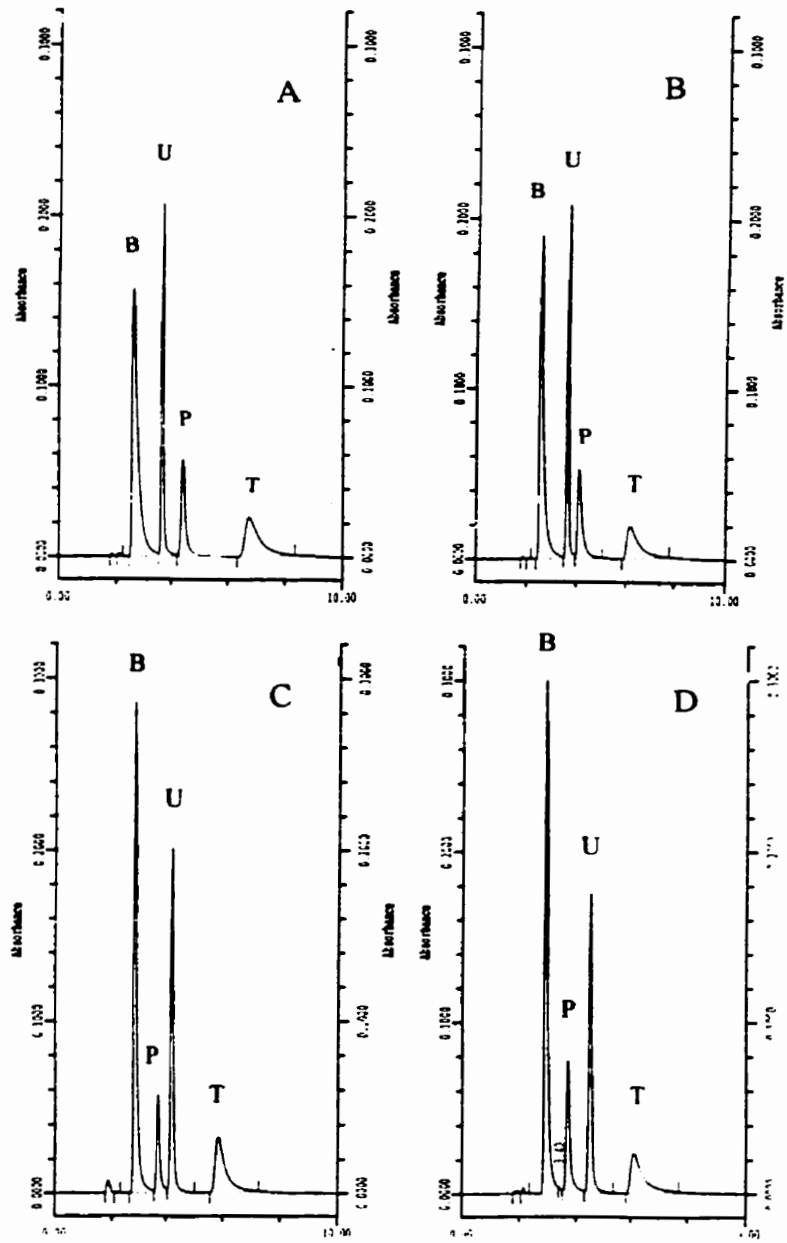

Figure 4.4 Effect of MeOH percentage on HPLC chromatogram of 4-BABA (B), procaine (P), the unknown (U) and tetracaine (T). The column was Ultrasphere™ 4.6 x 150 mm with 45 mm guard column, the mobile phase (pH 6) was MeOH:ACN:2.5mM HSA in the ratio of (A) 4:71:25, (B) 5:70:25, (C) 30:45:25, (D) 40:35:25, flow rate 1 mL/min.

Because the pH of the mobile phase changed after sitting in the reservoir, buffer was tried. Phosphate buffer was used at various concentrations. The concentration of the buffer was limited to 1-10 mM range due to the limited solubility of the buffer components in the mobile phase. Peak shapes of 4-BABA and PC were improved but not all peaks were resolved. With this concentration range, the buffer capacity of the system was very low. In addition, more time would be needed to optimize the buffer concentration and composition of the mobile phase. Considering these reasons and the fact that there were some other acceptable systems available, the buffer approach was not further developed.

In one experiment the temperature of the column was varied from 25 to 75 °C. The result (Figure 4.5) showed that temperature change affected the retention times of all analytes: the higher the temperature, the shorter the retention time. However, there was no significant change in the peak area and peak height. Since it was not practical to apply high temperature to the column and a few degree change in temperature would not affect the retention times too much, the temperature was controlled at the ambient temperature (22-25°C) by wrapping a silicone tubing around the column and connecting the tubing to a circulating water bath (HPLC method 1) or by housing the columns in a column chamber (HPLC method 2).

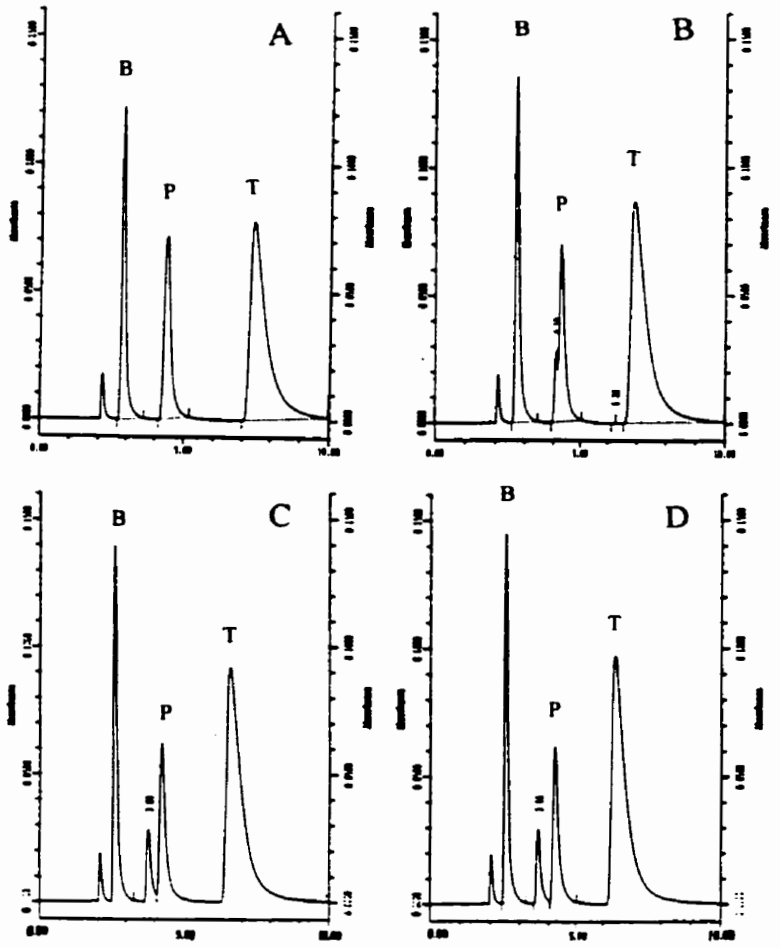

Figure 4.5 Effect of temperature on HPLC chromatogram of 4-BABA (B), procaine (P) and tetracaine (T); (A) 25°C, (B) 37°C, (C) 50°C, (D) 75°C. The column was Ultrasphere™ 4.6 x 150 mm with 45 mm guard column, the mobile phase was MeOH : ACN : 2.5mM HSA = 40:35:25, pH 6, flow rate 2 mL/min.

In conclusion, the optimal HPLC method 1 for the analysis of TC and its degradation products was as follows:

HPLC system: Beckman System Gold programable solvent module 126, Rheodyne injector, Beckman System Gold diode array detector module 168 and a Dell Ultrascan 486P microcomputer to control the conditions and manipulate the data.

Column : Beckman Ultrasphere™ 4.6 x 150 mm, 5 μm ODS column with a 45 mm guard column.

Column temperature : controlled at the ambient temperature.

Mobile phase : MeOH :ACN: 2.5 mM HSA in water = 40:35:25, pH 6.

Flow rate : 2 mL/min.

Detection : UV absorbance at wavelength 310 nm.

Internal standard : procaine HCl solution in water.

The mechanism of the separation might be explained as reversed phase ion pair HPLC. Anionic counter ions (Y^-) react with organic bases (X^+) to form non-dissociated ion pairs (X^+Y). HSA (Figure 6) in the mobile phase was a strong ion pairing reagent bearing a negative charge. At pH 6, TC which had a pKa of 8.39 was ionized with positive charge on the amine group. This functional group interacted with the negatively charged SO_3 of HSA and form ion pair. The C6 chain of HSA interacted with the C18 part of the column via hydrophobic bond, thus TC ion pair was retained longer in the column (retention time about 5-6 minutes at the flow rate of 2 mL/min). 4-BABA, which had a pKa about 2.5, was also ionized at pH 6, bearing a negative charge at the carboxylic group. This functional group repelled by the negatively charged SO_3 hence shortly retained in the column

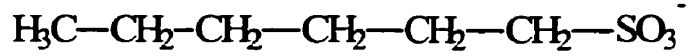

Hexanesulfonate

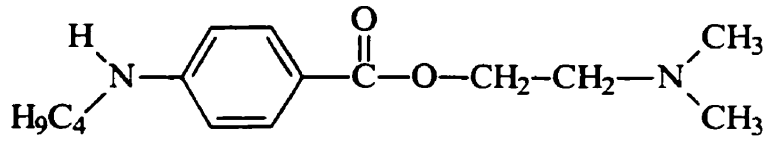

Tetracaine

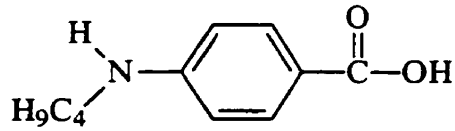

4-(butylamino)benzoic acid

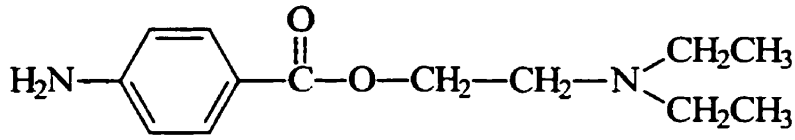

Procaine

Figure 4.6 Chemical structures of hexanesulfonate, tetracaine, 4-BABA and procaine.

(retention time about 1.5 minutes at the flow rate of 2 mL/min). PC had a pKa of 8.9 but had a retention time of about 4 minutes at the flow rate of 2 mL/min instead of longer retention time than that of TC. This might be from the steric hindrance effect of the butyl group on TC molecule as compared to the hydrogen group on PC molecule. The butyl group made TC more hydrophobic and interacted with the hydrophobic part of the stationary phase, hence retained longer than PC.

There were many factors affecting HPLC analysis in this system. The pH of the mobile phase affected the ionization of all species in the system, hence the interaction between the species and the separation. The composition of the mobile phase and the concentration of the ion-pairing reagent had to be optimized. Salts/buffer components were important as both positively and negatively charged groups interfered with the interaction between the ion-pairing reagent and the analytes. Basic compounds (TC and PC) were more sensitive to temperature change than the acidic compound (4-BABA). The temperature should be controlled in this system in order to achieve less variation in the retention time of the basic compounds. Flow rate affected the peak shape of the analytes, especially TC peak which had long tailing. The tailing was the result of the interaction of basic compound with the free hydroxyl group of the silica which was the base of the column packing. Incomplete interaction of C18 with the silica due to steric hindrance caused exposure of free hydroxyl groups. This problem occurred with older generation of HPLC columns such as the Ultrasphere™ column used in this system.

Method validation parameters for the HPLC method 1 is summarized in Table 4.1.

Table 4.1 Method validation parameters for the HPLC analysis, method 1.

Parameter	Tetracaine	4-BABA
Selectivity	Yes	Yes
Limit of detection	0.8 ng	0.2 ng
Limit of quantitation	5 ng	5 ng
Linear regression equation*	Y = 119.362 X + 1.80306 (n = 3)	Y = 105.084 X + 2.8686 (n = 3)
r^2	0.99985	0.99986
Range	5 - 100 ng	5 - 100 ng
Accuracy, RSD	102.45%, 1.24% (n = 6)	100%, 1.03 % (n = 6)
Precision		
Intra-day, RSD	7.08 % (n = 6)	4.83 % (n = 6)
Inter-day, RSD	9.96 % (n = 13)	7.33 % (n = 12)

* X = amount of the analyte, Y = detector response

Note: the RSD of the internal standard recovery was 1.37%, n = 30.

This method was used in the study of TC metabolism in human skin homogenate. However, it was not sensitive enough for the kinetic study which required analysis at very low concentrations of 4-BABA and TC. Several approaches were tried to improve the sensitivity of the analysis.

By increasing the sampling volume from the incubation mixture from 25 µL up to 50 µL, PC (internal standard) peak was affected, e.g. flattened or had shoulder. The cause might be from the salt component in the skin homogenate. With the effect on the internal standard peak, accurate concentrations of 4-BABA and TC might not be achieved. The maximum sampling volume was 35 µL.

By increasing the HPLC injection volume from 25 μL up to 100 μL, 4-BABA peak was affected. Originally, 4-BABA peak was very close to the solvent peak. When increasing the injection volume, the solvent peak and the 4-BABA peak itself became larger and interfered with each other. The maximum injection volume was 30 μL.

Combination of both previous approaches was tried using an injection volume of 30 μL and varying the sampling volume from 25 μL to 50 μL. But 4-BABA peak was still affected. So the sampling volume should be kept at 25 μL at this injection volume.

New internal standards (benzocaine and dibucaine) were tested. Benzocaine eluted with the solvent front. The dibucaine peak partially overlapped with TC peak. More adjustment with the analytical condition would be needed if either of these substances would be used as the internal standard.

Capillary Electrophoresis (CE) assay was also used for the analysis of TC and 4-BABA. This part was done in collaboration with Dr. Jiaping Hu. The CE system consisted of a Beckman P/ACE system 5500 fully automated capillary electropherograph with a P/ACE diode Array detector, P/ACE Station system control and data acquisition software. The capillary was the eCAP capillary 100-μm I.D., 375-μm O.D., 37-cm total length, 7-cm detection length. The system was conditioned for 2 minutes with the running buffer (25 mM H_3PO_4) at the capillary temperature of 23 °C. Injection was done by pressure injection for 10 seconds. The separation voltage was 10 kV, detection by UV at 227 nm. The capillary was washed for 1 minute with 0.1 M HCl after each run. TC and 4-BABA solutions were prepared from stock solutions but further diluted with deionized distilled water to the required concentration. Procaine HCl aqueous solution was used as the internal standard. Although the minimum amount per sample vial required for CE analysis was smaller than

that of HPLC, the sensitivity of CE was not necessarily better than that of HPLC. At the same concentrations as the LOQs of TC and 4-BABA from HPLC method, the present CE system did not give a better sensitivity (RSD= 13.71% and 15.54% for TC and 4-BABA respectively). Moreover, CE took longer time for the simultaneous analysis of the analytes. It was not easy to find a suitable sample preparation method for simultaneous analysis of TC and 4-BABA due to the very different pKa of the analytes. Skin homogenate samples require more steps for sample preparation for CE analysis;i.e. after stopping the reaction with ACN (which also extracted TC and 4-BABA), water must be added to make an aqueous solution for analysis in CE, hence diluting the sample. Therefore, the CE system used was not suitable for simultaneous analysis of TC and 4-BABA for the enzyme kinetics study in the skin homogenate model.

Two other HPLC systems; the HP1100 ChemStation (Hewlett Packard) and the Waters 2690 (Waters Corporation) systems, were tried. The LOD for 4-BABA and TC were 0.2 ng from both HPLC systems. The LOD of 4-BABA was the same as that from the previous HPLC system. The LOD of TC was slightly better as compared to 0.8 ng in the previous system. However, the LOQs were about the same as those from the previous system.

4.1.1.2 HPLC Method 2

A more sensitive HPLC method was required for the enzyme kinetic study of TC in human skin homogenate as HPLC method 1 could not be further modified to achieve better sensitivity for the application. The Waters 2690 Separations Module, with 996 diode array detector module and Millennium® system control and data acquisition software HPLC system(Waters Corporation) was employed for the new method analysis. Three new HPLC

columns were tried; the first, a Symmetry™ C8, 5 μm, 4.6 x 250 mm (Waters Corporation), the second, a SymmetryShield™ RP18, 5 μm, 3.9 x 150 mm with a 3.9 x 20 mm guard column (Waters Corporation) and thirdly, a Luna™ C18(2), 5 μm, 4.6 x 150 mm column with a 4.6 x 30 mm guard column (Phenomenex, Torrance, CA, USA). These columns were all reversed phase but the silica based bonded phase packing material was smoother, more uniform, higher in purity, low metal content and complete endcapping (coverage of the unbonded silica with small molecules) compared to the previous column used in HPLC method 1. Therefore, the tailing problem of basic analyte (TC) was eliminated.

The composition and the pH of the mobile phase were varied; gradient and isocratic runs of ACN and 10 mM phosphate buffer were performed. The pH of phosphate buffers were 3, 5, 7 and 10, respectively. The type and concentration of the buffer used in mobile phase were also varied; phosphate buffer concentrations of 10 and 25 mM were tried as well as 0.1% trifluoroacetic acid (TFA) or triethyl ammonium acetate as a composition in the mobile phase with ACN or ACN and MeOH mixture. However, none of these systems could simultaneously analyze TC and 4-BABA with a better sensitivity than the HPLC method 1.

When using ion pairing reagent, HSA in the mobile phase, simultaneous analysis of TC and 4-BABA was achieved. The pH of the mobile phase in this system was not adjusted. However, the pH of the mobile phase was found to be between 6 and 7 as compared to pH 6 in method 1. The concentration of the ion pairing reagent was varied as well. HSA 1.25 and 2.5 mM were used and it was found that the 2.5 mM concentration provided better peak shape of the analytes. The composition of the mobile phase was further varied to achieve the best separation of the analytes.

The optimal assay condition for HPLC method 2 was achieved as follows:

HPLC system : Waters 2690 Separations Module, with 996 diode array detector module and Millennium® system control and data acquisition software.

Column : Luna™ 4.6 x 150 mm, 5 μm ODS column with a 4.6 x 30 mm guard column (Phenomenex, Torrance, CA, USA) or SymmetryShield™ RP18, 3.9 x 150 mm, 5 μm with a 3.9 x 20 mm, 5 μm guard column (Waters Corporation).

Column temperature : controlled at the ambient temperature

Mobile phase : ACN : MeOH : 2.5 mM HSA in water (20:55:25)

Flow rate : 1 mL/min

Detection : UV absorbance at wavelength 310 nm

Retention times: 2.6 min for TC, 3.05 min for 4-BABA (Luna™ column with guard)

1.8 min for TC, 2.34 min for 4-BABA (SymmetryShield™ RP18 column with guard)

In the HPLC method 1, 4-BABA peak was very close to the solvent front and overlapping occurred with increasing sample volume or injection volume. In the HPLC method 2, 4-BABA peak moved away from the solvent front hence made it possible to increase aliquot sampling volume from 25 to 100 μL without interference to the 4-BABA peak from the solvent front and the homogenate matrix. Method validation parameters for these systems are shown in Table 4.2 and 4.3. An example of HPLC chromatograms from skin homogenate and heated skin homogenate (negative control) samples is shown in Figure 4.6. The sensitivity of this analytical method was better than the LOQs of 128 ng and 65 ng for TC and 4-BABA, respectively from previous method (Woolfson et al., 1990).

Table 4.2 Method validation parameters for the HPLC analysis, method 2; Luna™ C18(2), 5 µm, 4.6 x 150 mm column with a 30 mm guard column.

Parameter	Tetracaine	4-BABA
Selectivity	Yes	Yes
Limit of quantitation	10 ng	5 ng
Linear regression equation*	Y = 6443.93 X - 12917.33 (n = 3)	Y = 6131.45 X - 1946.32 (n = 3)
r^2	0.9985	0.9987
Range	10 - 90 ng	5 - 60 ng
Accuracy at LOQ, RSD	103.30%, 3.13 % (n = 5)	99.58%, 4.41 % (n = 5)
Precision at LOQ		
Intra-day, RSD	1.1 % (n = 6)	1.1 % (n = 6)
Inter-day, RSD	2.88 % (n = 20)	3.45 % (n = 20)

* X = amount of the analyte, Y = detector response

Table 4.3 Method validation parameters for the HPLC analysis, method 2; SymmetryShield™ RP18, 5 µm, 3.9 x 150 mm with a 20 mm guard column.

Parameter	Tetracaine	4-BABA
Selectivity	Yes	Yes
Limit of detection	0.3 ng	0.5 ng
Limit of quantitation	10 ng	5 ng
Linear regression equation*	Y = 5887.998 X - 1456.61 (n = 3)	Y = 6442.28 X - 2750.10 (n = 3)
r^2	0.9989	0.9970
Range	10 - 120 ng	5 - 60 ng
Accuracy at LOQ, RSD	104.21%, 3.3 % (n = 6)	103.60%, 8.8 % (n = 6)
Precision at LOQ		
Intra-day, RSD	3.9 % (n = 6)	5.6 % (n = 6)
Inter-day, RSD	5.33 % (n = 18)	7.63 % (n = 18)

* X = amount of the analyte, Y = detector response

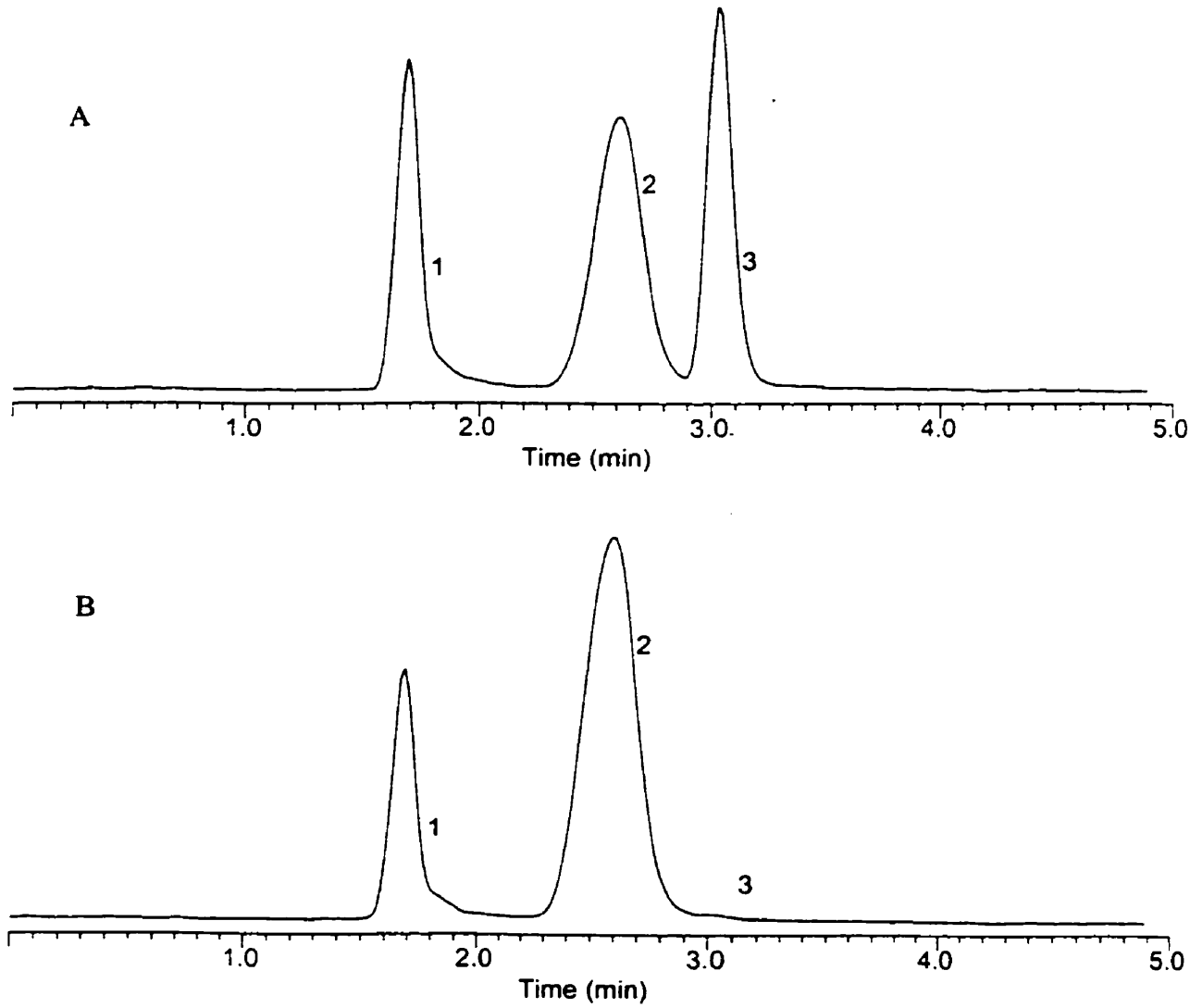

Figure 4.7 Example of HPLC chromatograms from (A) skin homogenate and (B) heated skin homogenate (negative control) samples. Initial tetracaine concentration was 40 μM, samples were analyzed after 2 hours incubation. (1) skin homogenate component, (2) tetracaine peak, (3) 4-BABA peak. The column was Luna™ C18(2), 5 μm, 4.6 x 150 mm column with a 30 mm guard column, the mobile phase was ACN : MeOH : 2.5 mM HSA = 55:20:25, flow rate 1 mL/min.

4.1.2 Identification of the Unknown Peak: Methyl Ester of Tetracaine

An attempt to identify the unknown peak from the previous results was done with the following approaches:

1. Comparing the retention time of the unknown with those of known substances.

Despite 4-BABA, other potential degradation products of TC were PABA and N-butyl aniline (The Pharmaceutical Codex, 1988). However, the comparison of the retention times with PABA and N-butyl aniline showed that the unknown was neither one of these compounds (Figure 4.8).

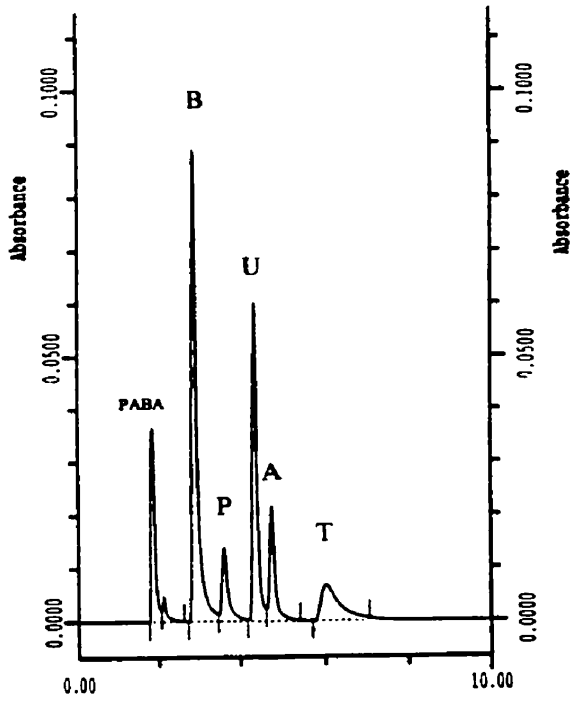

Figure 4.8 HPLC chromatogram of PABA, 4-BABA (B), procaine (P), the unknown (U), N-butyl aniline (A) and tetracaine (T). The column was Ultrasphere™, 4.6 x 150 mm with 45 mm guard column, the mobile phase was MeOH:ACN:5 mM HSA = 40:35:25, pH 6, flow rate 1 mL/min.

2. Reaction with strong reducing agent.

With suspicion that the unknown might be N-oxide of TC as reported by Momose and Fukuda (1976), the solution of TC containing the degradation product was reacted with $TiCl_3$ powder which was a very strong reducing agent (method adapted from Brooks and Sternglanz, 1959). Comparison of the HPLC chromatogram before and after the reaction showed that the unknown was not the N-oxide of TC (Figure 4.9) since the unknown peak did not disappear after the reaction took place.

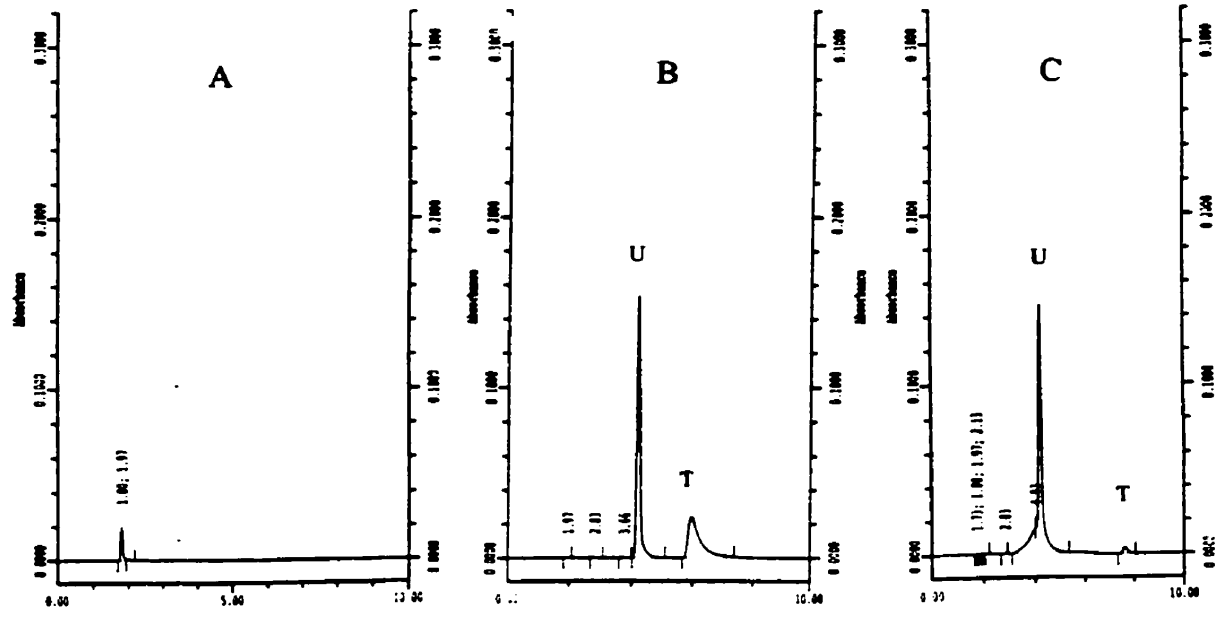

Figure 4.9 Reaction of $TiCl_3$ and tetracaine solution with the unknown; (A) blank, (B) pre-reaction, (C) post-reaction. The column was Ultrasphere™ 4.6 x 150 mm with 45 mm guard column, the mobile phase was MeOH:ACN:2.5mM HSA = 40:35:25, pH 6, flow rate 1 mL/min.

3. Mass spectrometry.

The unknown solution was collected from HPLC after separation from TC and the sample was submitted for mass spectrometry analysis. The electrospray mass spectrometry result had strong signals of a number of peaks but none of the peaks could be identified. It was possible that the unknown concentration was still too low compared to the background (such as substances from the solvents or glassware). The HPLC-electrospray mass spectrometry result of TC powder showed a large peak with the masses of 264 and 175. However, there was a small peak of about 3% of the total area. This peak had a mass of 207 which could be the methyl ester of TC since TC powder was dissolved in MeOH and left overnight before being introduced into the HPLC-Mass Spectrometer. Further experiment was done to verify this as described in the next approach.

4. Changing the solvent for tetracaine.

ACN and DMSO were used to dissolve TC, i.e. to make stock solutions. In order to make the injecting solutions for the HPLC analysis, two mobile phases were used to dilute the stock solutions; one with MeOH, another without MeOH. The unknown peak occurred in the solutions with MeOH and the amount increased with time. However, in the system without MeOH, there was no peak at the same retention time as the unknown peak. This strongly suggested that there were trans-esterification reactions in the systems which contained MeOH. In the preliminary experiment, 95% ethanol was used as one of the solvents for TC and an unknown peak occurred as well. That might be the ethyl ester product of the trans-esterification.

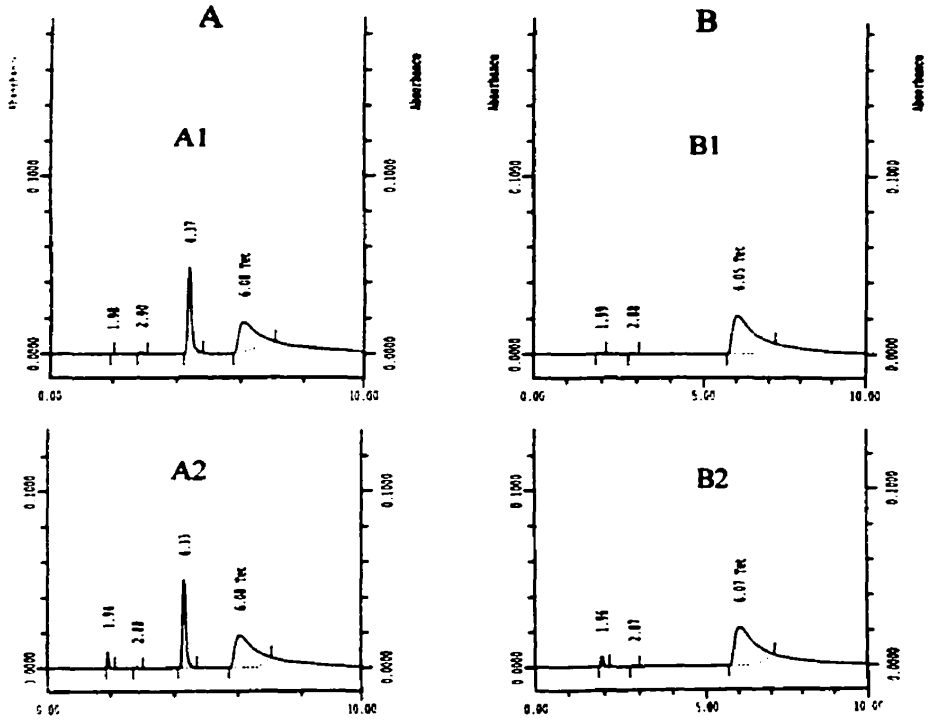

Figure 4.10 Effect of solvent on trans-esterification of tetracaine; (A) diluting solution contained MeOH; (A1) tetracaine in ACN, (A2) tetracaine in DMSO; (B) diluting solution did not contain MeOH; (B1) tetracaine in ACN, (B2) tetracaine in DMSO. Samples were analyzed 20 days after preparation. The column was Ultrasphere™ 4.6 x 150 mm with 45 mm guard column, the mobile phase was MeOH:ACN:2.5mM HSA = 40:35:25, pH 6, flow rate 1 mL/min.

4.1.3 Appropriate Solvent for Tetracaine.

Due to the potential for transesterification, methanol and ethanol must not be present in the solvent for TC. In glycerol, propylene glycol or polyethylene glycol 300 containing

systems, as expected, there were transesterification reactions due to the presence of many hydroxyl groups in their molecules. Several other solvents were also tried for TC and 4-BABA; ACN, DMSO, mobile phase without methanol (ACN:2.5mM HSA = 75:25), phosphate buffered saline (PBS) pH 7.2, and water. The parameters to be considered were the solubility, suitability as the solvent for analysis, and suitability as vehicle for the drug preparation.

For analytical purposes, both ACN and DMSO were suitable solvents. All analytes were very soluble in these solvents. DMSO had a solvent peak around 1.0 min (HPLC method 1, flow rate 2 mL/min) which could interfere with the 4-BABA peak if used in high concentration. ACN also had solvent peak around 1.0 min but it had less interference to 4-BABA peak. Mobile phase without methanol consisted of 75% ACN, hence it was a good solvent for all analytes. Since its composition was very similar to the mobile phase, the solvent peak was very small. TC and 4-BABA are almost insoluble in water and PBS. However, considering the toxicity to cells, ACN should not be used as the vehicle for the preparation (formulation) of the drug. DMSO, although causes irritation, is not toxic to cells. It is widely used in cryopreservation of tissue cultures. In order to reduce the irritation effect and the interference in the analysis, DMSO was used as a solvent to prepare stock solutions of TC and 4-BABA. Further dilution for analysis was done with water, ACN or mobile phase without methanol.

PBS was found to interfere with TC, 4-BABA and PC peaks (Fig. 4.11). This was evident in several experiments such as the metabolism in skin homogenate experiment where TC was dissolved in DMSO then diluted with PBS and used as solution dosage form; in the analysis of the wash from excised skin (permeation study) if PBS was used as the

washing solvent; and in experiments to see the effect of PBS on analysis of TC and 4-BABA. In order to avoid interference from PBS, its concentration must not exceed 0.5 mM in the injected samples.

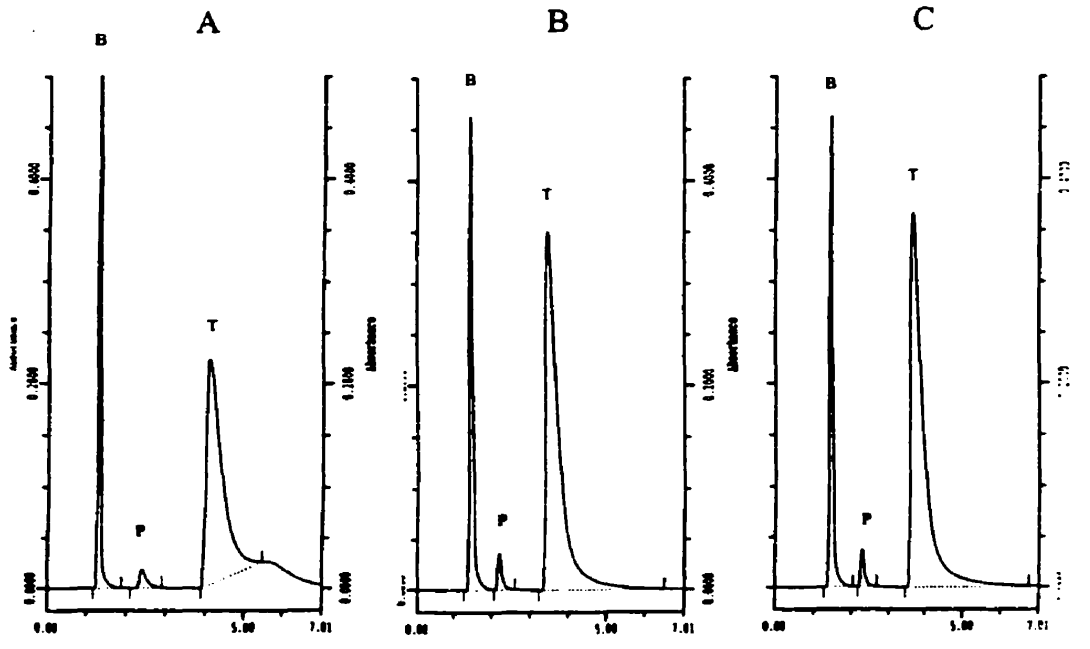

Figure 4.11 Effect of PBS on HPLC analysis of 4-BABA (B), procaine (P) and tetracaine (T). Standard solutions prepared with diluting solvents; (A) PBS, (B) Water (C) Mobile phase without methanol. The column was Ultrasphere™ 4.6 x 150 mm with 45 mm guard column, the mobile phase was MeOH:ACN:2.5mM HSA = 40:35:25, pH 6, flow rate 1 mL/min.

In conclusion, for the preparation of solution dosage form, DMSO was selected as the solvent for TC. For the analysis, DMSO was selected as the solvent for TC and 4-BABA stock solutions and water was the solvent for PC stock solutions. ACN was selected for diluting the solutions for the analysis in general while water was used for the analysis in the wash from excised skin.

4.1.4 Optimal HPLC Analytical Method for Methyl Salicylate and its Metabolites

An HPLC assay method was used for the analysis of MS and its metabolites (SA and SUA). The method was modified from that of Cham et al. (1979). The assay condition was as follows:

The HPLC system consisted of Waters 2690 Separations Module, with 996 diode array detector module and Millennium® system control and data acquisition software. The column was Beckman Ultrasphere™ 4.6 x 250 mm, 5 µm ODS column. The mobile phase was ACN : MeOH: 5% acetic acid in water (30:25:45) with the flow rate of 1 mL/min. Detection was by UV absorbance at wavelength 240 nm. Propyl paraben (PP) solution in MeOH was used as the internal standard. The retention times of SUA, SA, PP and MS were 3.2, 4.5, 7.4 and 9.4 minutes, respectively.

Validation parameters are shown in Table 4.4. Examples of HPLC chromatograms from samples of standard solution, skin homogenate and diffusion cell samples are shown in Figures 4.12 - 4.14.

Table 4.4 Method validation parameters for the assay of methyl salicylate

	SUA	SA	MS
Selectivity	yes	yes	yes
Limit of quantitation	7 ng	15 ng	15 ng
Linear regression equation*	Y=0.0110X-0.0159 (n = 3)	Y=0.00972X-0.0144 (n = 3)	Y=0.00896X-0.0172 (n = 3)
r^2	0.9747	0.9984	0.9975
Range	7-20 ng	15-400 ng	15-600 ng

*X = amount of the analyte, Y = detector response

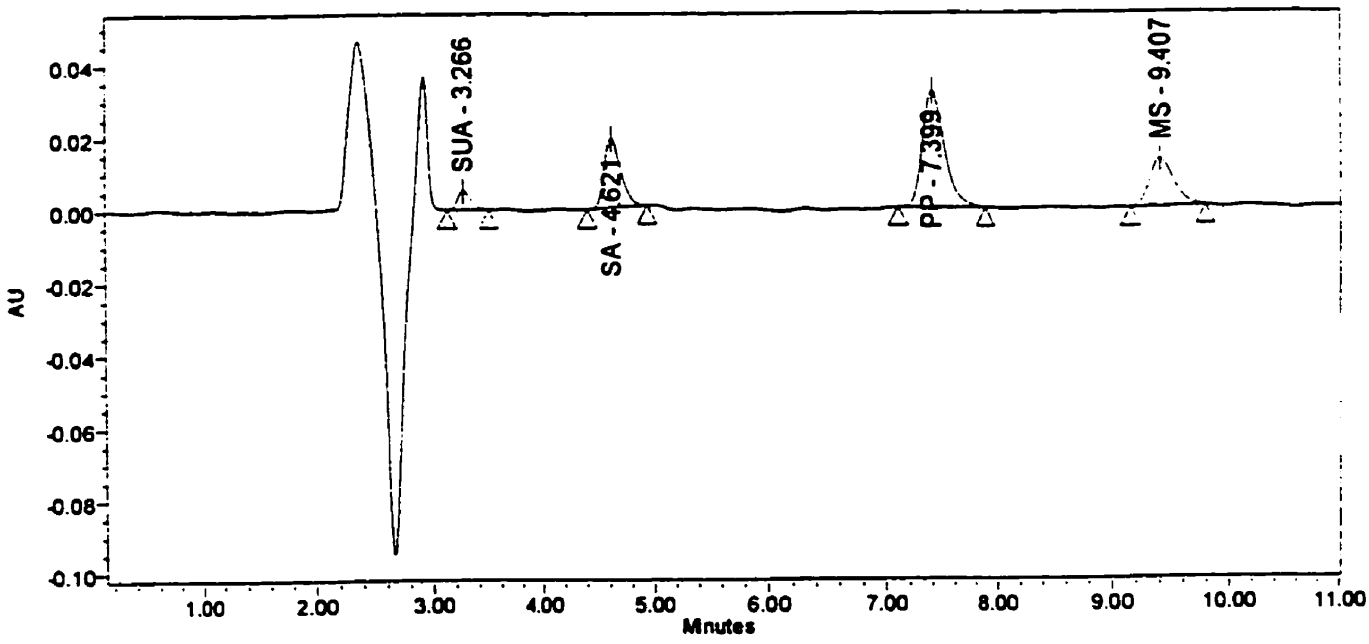

Figure 4.12 HPLC chromatogram from a standard solution which consisted of salicyluric acid (SUA), salicylic acid (SA), propyl paraben (PP, the internal standard) and methyl salicylate (MS). The column was Ultrasphere™ 4.6 x 250 mm, the mobile phase was ACN: MeOH:5% acetic acid in water (30:25:45), flow rate 1 mL/min.

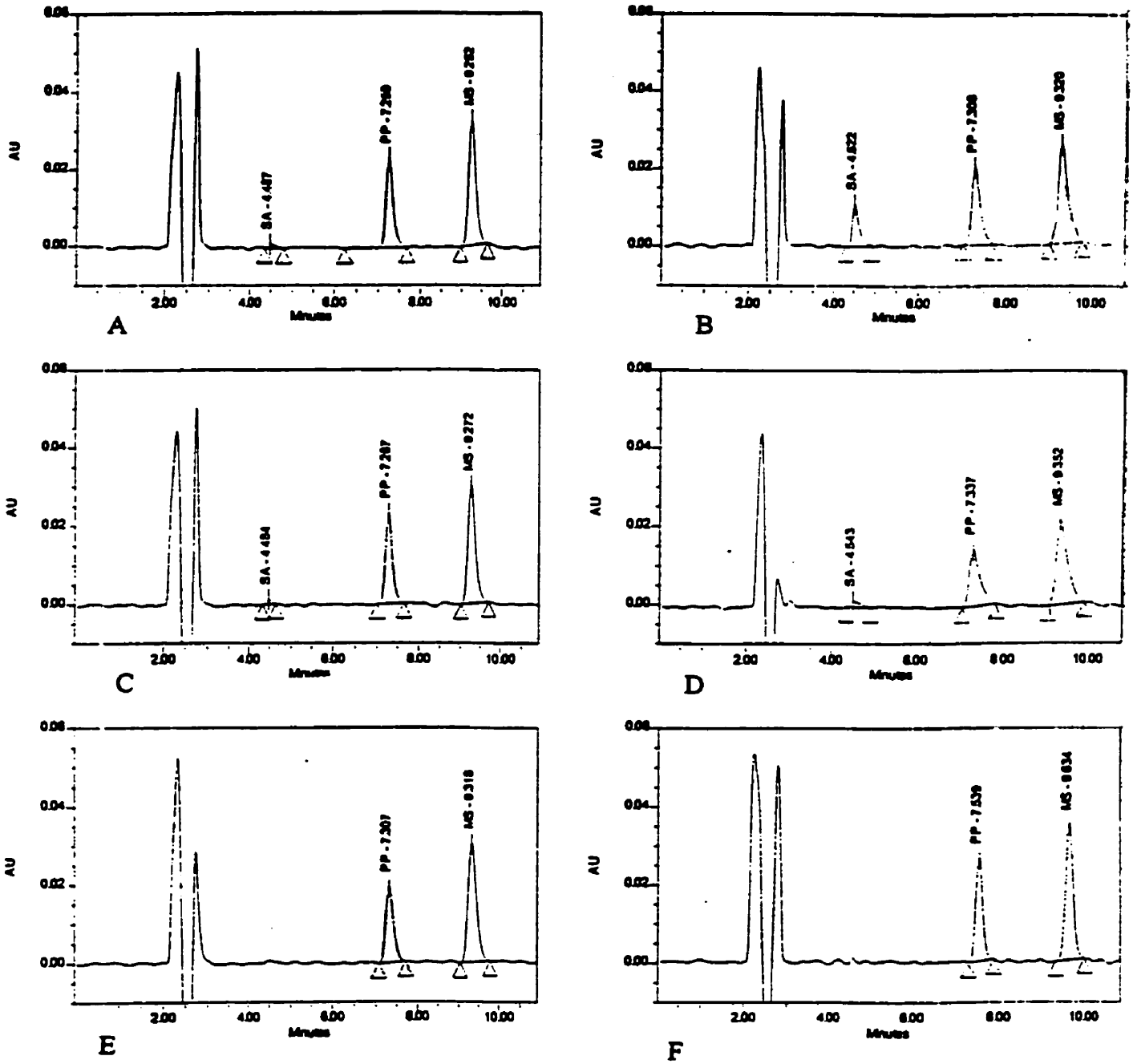

Figure 4.13 HPLC chromatograms from methyl salicylate metabolism in different matrixes from skin homogenate experiment at 4 hours.

(A) Phosphate buffered saline (B) Untreated skin homogenate

(C) Pseudocholinesterase enzyme (13U) (D) Skin homogenate, heated at 60°C, 2 min

(E) Skin homogenate, heated at 100°C, 2 h (F) Skin homogenate, heated at 60°C, 2 h

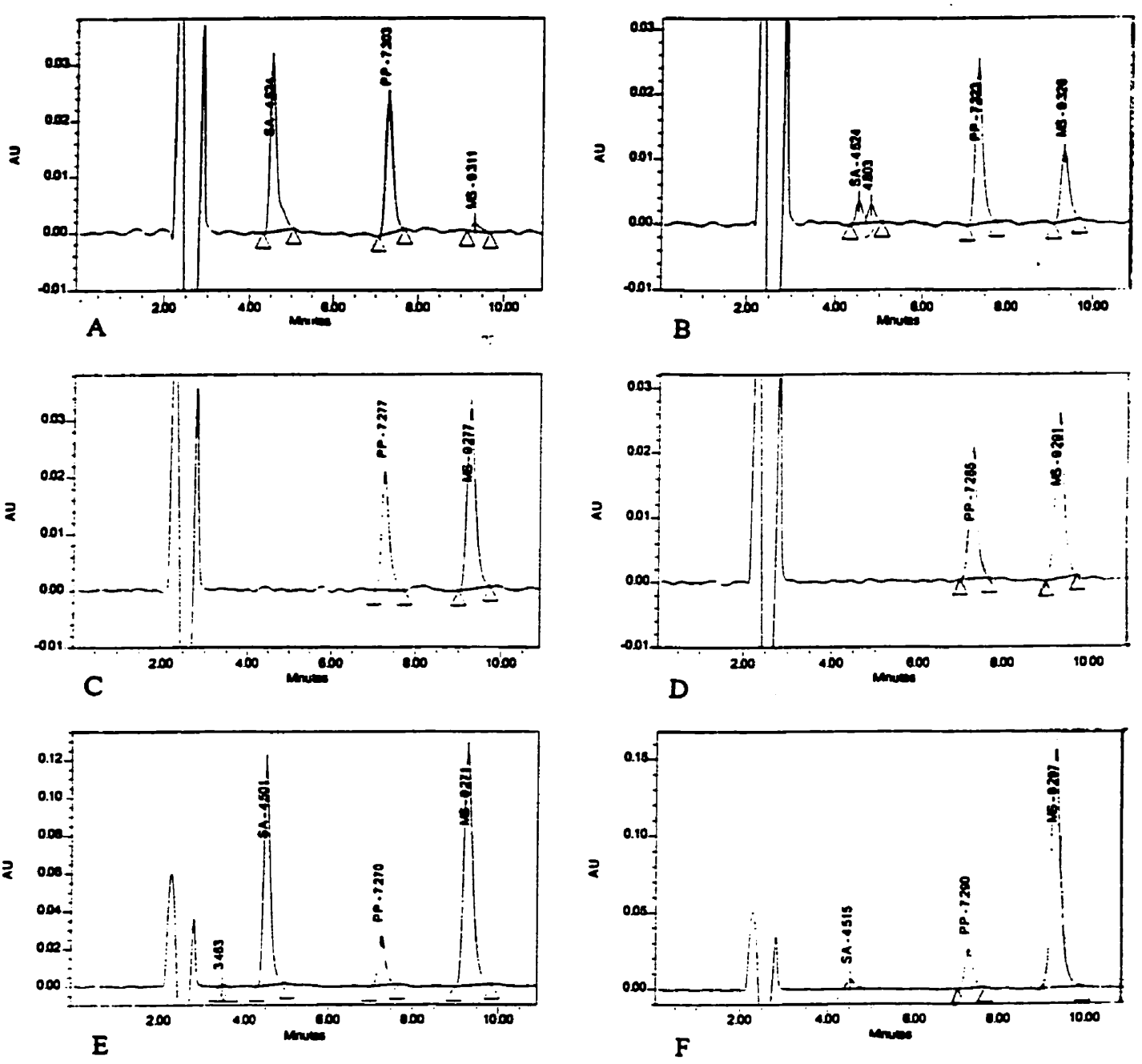

Figure 4.14 HPLC chromatograms from methyl salicylate metabolism in diffusion cell experiments.

(A) 24h fraction from viable skin

(B) 24h fraction from 60°C treated skin

(C) Wash from viable skin

(D) Wash from 60°C treated skin

(E) Skin extract from viable skin

(F) Skin extract from 60°C treated skin

4.2 Human Skin Homogenate Model

Although the concept of making skin homogenate was simple, it was very difficult in practice, especially if the activity of the enzymes in the homogenate must be preserved. The most difficult part was to pulverize the skin before homogenization. The skin was very resilient due to the massive dense fibroelastic connective tissue composed of collagen fibers, elastic fibers, proteoglycans and glycosaminoglycans. Therefore, very high shear was needed to break down the links between these components. However, the temperature had to be controlled so that the enzymes in the skin were not denatured. Mortar and pestle might work for pulverizing very small amount of liquid-nitrogen-frozen skin pieces but not with more than 0.5 g. The Biopulverizer® (Biospec Products Inc., Bartlesville, OK, USA) worked, provided only a small amount of skin was used (less than 1 g). The A10 IKA-Analytical Mill® (IKA Werke, Germany) could grind 5-8 g of frozen skin into powder in less than 10 minutes, therefore, it was used in the preparation of human skin homogenates.

4.2.1 Protein Determinations

The results of protein determinations of skin homogenates from human breast skin of different sources are shown in Table 4.5. These numbers were used in the calculation of specific enzyme activities.

Table 4.5 Protein concentration in skin homogenates from different sources as determined by modified Lowry method using BSA protein standard and absorbance measurement at 750 nm.

Skin source	Protein concentration (mg/mL)
skin 1[a]	8.66 (8.78, 8.53)
skin 2[a]	7.78 (7.55, 8.01)
skin 3[a]	7.38 (7.76, 7.01)
skin 4[b]	3.39 (3.21, 3.56)
skin 5[b]	4.12 (3.89, 4.35)
skin 6[b]	3.21 (3.14, 3.28)
skin 7[b]	3.40 (3.29, 3.52)
skin 8[b]	2.62 (2.45, 2.79)
skin 9[b]	2.95 (2.86, 3.04)

The data are reported as means, n=2, with ranges shown in parentheses.

[a] prepared with the ratio of skin to PBS of 1:2

[b] prepared with the ratio of skin to PBS of 1:5

4.2.2 Hydrolysis of Tetracaine in Human Skin Homogenate

From preliminary results, TC degraded in the incubation condition yielding 4-BABA. The rate of TC hydrolysis in human skin homogenate was higher than that in the negative control (Fig. 4.15), suggesting that the activity of esterases was preserved by the preparation method discussed. However, the hydrolysis rate was very slow compared to that of the purified enzyme Pseudocholinesterase (Fig. 4.16). As shown in Fig. 4.16, it took only 13 hours for the purified enzyme to hydrolyze 80% of TC while it took over 60 hours for the skin homogenate to hydrolyze 30% of TC (Fig. 4.15).

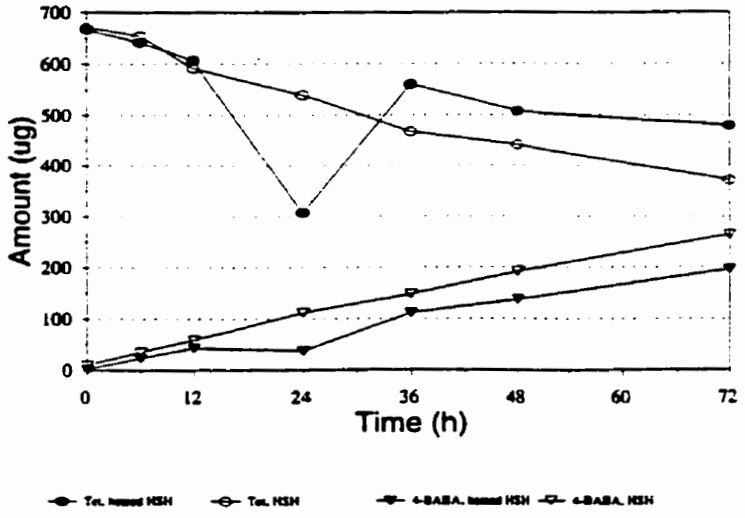

Figure 4.15 Tetracaine hydrolysis in human skin homogenate and its negative control (same skin homogenate which was heated in boiling water for 2 hours and cooled), n = 1. The initial tetracaine concentration was 303 μM.

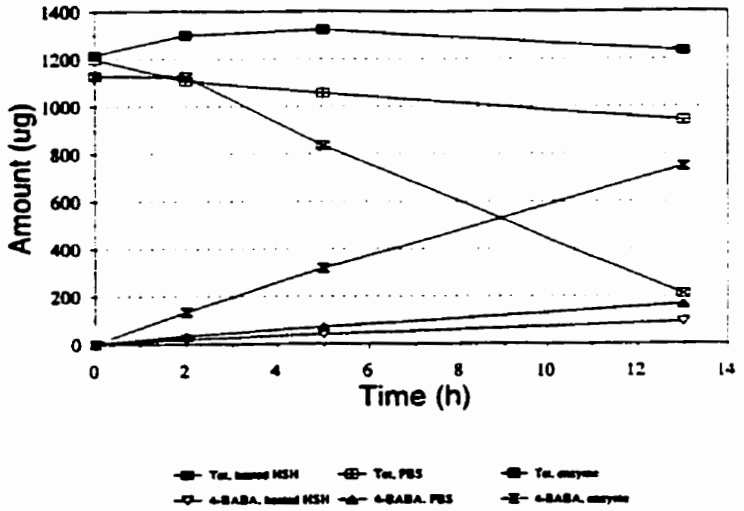

Figure 4.16 Tetracaine hydrolysis in heated human skin homogenate, PBS and purified enzyme pseudocholinesterase, n = 1. The initial tetracaine concentration was 303 μM.

Heating the skin homogenate in boiling water for 2 hours diminished the esterase activity in the skin homogenate. The hydrolysis rate in this system was less than that in PBS (Fig. 4.16).

PBS which was used as the vehicle for the skin homogenate and the purified enzyme, interfered with the analysis (specifically the PC peak, Fig. 4.11) so the aliquot volume must be small but contain enough amount of analytes. This implies the importance of the initial substrate concentration and the sensitivity of the analysis method.

The initial concentration of TC used in the preliminary experiment (303 μM) gave a linear hydrolysis pattern. Compared to the K_m values of 50 μM for human plasma and 2.8 μM for cholase (purified human cholinesterase concentrate) (Foldes et al., 1955), this concentration was much higher therefore assured that the enzyme activity would not be limited by the substrate concentration. It was interesting to conduct an enzyme kinetic study of TC hydrolysis because there was very little information available about the kinetic data for the hydrolysis of TC by esterases, highly purified enzyme became available and the analytical techniques had been improved. This could be done by determining the rate of the reaction while varying the concentration of substrate. The substrate concentration that gives half the maximum rate is the K_m. The substrate concentration used in the experiment must be at least 4-5 K_m.

In order to find where the hydrolytic activity was in the skin layers, the skin sample was separated into the epidermis and the dermis using trypsin or dispase enzyme (Gibco BRL) then homogenate from each layer was made and incubated with TC solution. Comparative hydrolysis rate of TC from different skin layers using different conditions of separating the skin layers is shown in Table 4.6.

Table 4.6 Tetracaine hydrolysis rate per mg skin between 0 and 24 hours in homogenates from different skin layers using different condition of separating the skin layers. Initial tetracaine concentration was 303 μM.

	Hydrolysis rate (μM/h/mg skin) between 0 and 24 hours in homogenate (n = 1) from					
Method of separating skin layers	dermis	heated dermis	epidermis	heated epidermis	whole skin	heated whole skin
1.25% trypsin, 37°C, 8 hours, soaked filter paper method	0.06	0.051	0.029	0.03	0.095	0.074
1.74 U/mL dispase, 37°C, 2.5 hours, soaked filter paper method	0.06	0.104	0.026	0.036	0.126	0.109
2.37 U/mL dispase, 4°C, 15 hours, submerged in enzyme solution method	0.07	0.06	0.038	0.032	0.087	0.065
				Average ± SEM (n = 3)	0.103 ± 0.010	0.083 ± 0.011

As seen from Table 4.6, homogenates from the dermis and the epidermis were inactive. The hydrolysis rate between 0 and 24 hours were about the same as their negative controls. Even with the gentlest method of separating skin layers, i.e. using enzymes, it seemed to inactivate esterase activity. Other methods of separating skin layers such as chemical and heat separation were not suitable for the separation of skin layers in this experiment because the enzyme activity might not be preserved. However, homogenate

from whole skin, which was not treated by enzyme, showed only slightly more hydrolytic activity than its negative control. Longer than 24 hour incubation time was needed to demonstrate more activity from the whole skin and the dermis homogenates than from their respective negative controls (Figure 4.17). Valentino et al. (1981) reported substrate inhibition of enzyme cholinesterase in human sera by TC and some other substrates. They also determined the kinetic parameters for TC. The Michaelis constant (K_m) values for TC for usual and atypical cholinesterase were 0.14 and 8 μM respectively (the buffer was 0.1 M Tris-Cl, pH 7.4, 25 °C). Thus the initial TC concentration of 303 μM was too high and substrate inhibition had occurred. There was no report on the kinetic parameters for TC

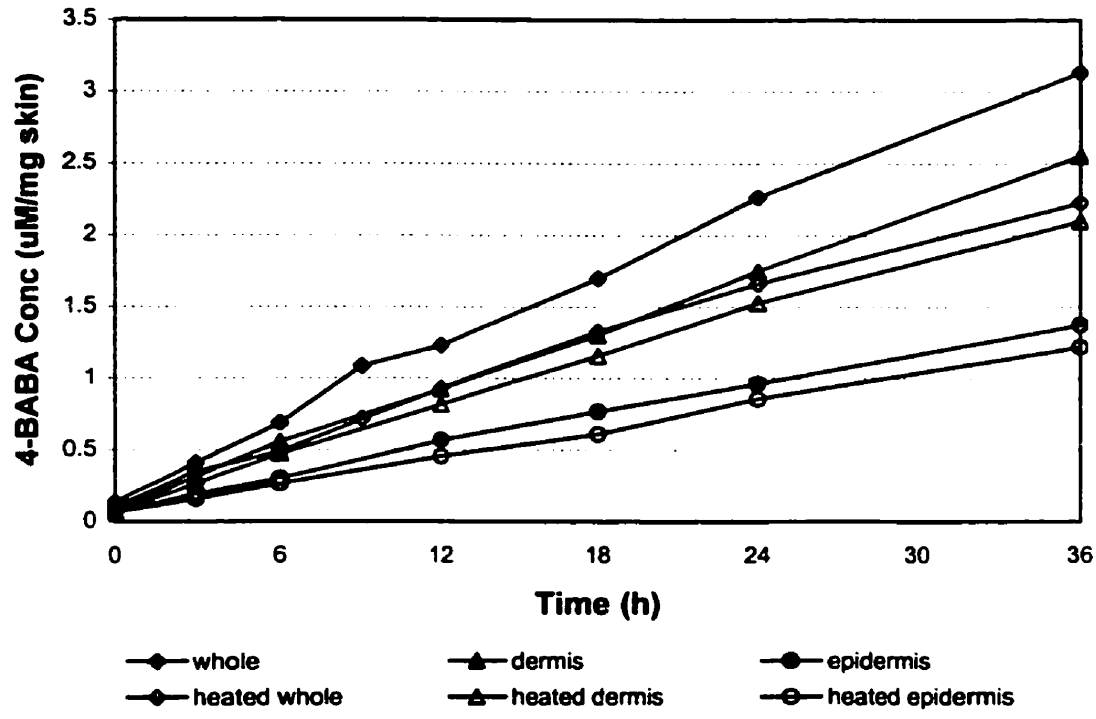

Figure 4.17 4-BABA concentration from tetracaine hydrolysis in homogenates from different layers of human skin up to 36 hours, n = 1. Skin layers were separated by incubation with 2.37 U/mL dispase at 4 °C for 15 hours. Initial tetracaine concentration was 303 μM.

hydrolysis in human skin but it was assumed that its esterase activity would be lower than that in serum. The next step would be to test whether the prepared skin homogenates were active or not, using another substrate. If the homogenates were active, kinetic parameters for hydrolysis of TC in the skin should be determined.

A few experiments were done using methylsalicylate (MS) as substrate to prove whether the skin homogenates were really active. MS was hydrolyzed to SA and methanol. In the preliminary analytical procedure for MS, the HPLC system consisted of the Beckman System Gold programable solvent module 126, Rheodyne injector, Beckman System Gold diode array detector module 168 and a Dell Ultrascan 486P microcomputer to control the conditions and manipulate the data. The column was Beckman Ultrasphere™ 4.6 x 150 mm, 5 μm ODS column with a 45 mm guard column. The mobile phase was water : ACN : trifluoroacetic acid in water (50:50:0.01) at the flow rate of 1 mL/min. Detection was by UV absorbance at wavelength 205 nm. Skin homogenates were incubated with 2% MS in methanol. Aliquots were taken at 0 and 17 hours and analyzed for MS and SA peak areas. The result is shown in Table 4.7. Heating the homogenates in boiling water for 2 hours destroyed the esterase activity. All the negative controls had similar percentage of MS left at 17 hours, about 16%, the same as PBS, except for the epidermis homogenates. The other homogenates had more SA and less MS remained. Even skin homogenates which were thawed and kept at 4°C for 1 month showed more activity than their negative controls, but less activity than the freshly thawed homogenates. Homogenate which was made from frozen whole skin also showed good activity.

Table 4.7 Salicylic acid increase and methyl salicylate remaining from hydrolysis of methyl salicylate in different skin homogenates after 17 hours at 37°C, n=1.

PBS or skin homogenates from	Salicylic acid fold increase from 0 hour	% Methyl salicylate remaining after 17 hours
PBS	12	16.43%
whole skin	231	8.15%
whole skin, thawed for 1month	209	10.57%
whole skin, boiled for 2 hrs	0	16.13%
whole from frozen skin	326	6.82%
whole from frozen skin, boiled for 2 hrs	1	15.85%
dermis	232	8.72%
dermis, thawed for 1 month	138	12.38%
dermis, boiled for 2 hrs	4	15.37%
epidermis	71	17.32%
epidermis, thawed for 1 month	2	18.21%
epidermis, boiled for 2 hrs	0	26.53%

Since the esterase activity in the epidermis homogenate was very low, it was speculated that the enzyme activity was destroyed during the separation of the epidermis from the dermis. Other methods of separation, for example, heating the skin to 60°C for 2-3 minutes and peeling the epidermis off, may also be used. This method was tested with a small piece of skin first. Since heating time and temperature used to separate the epidermis from the dermis was a concern, a quick experiment was done to test the effect of heat on esterase activity. Freshly thawed whole skin homogenate was immersed in 60°C water bath for 5, 10 and 30 minutes before incubation with MS solution along with unheated whole skin homogenate (positive control) and the whole skin homogenate which was heated in boiling water for 2 hours (negative control). Aliquots were taken at 0 and 20 hours and analyzed for MS and SA peak areas. The results are shown in Table 4.8. Exposing

homogenates to 60°C reduced the activity of the enzymes and the longer the exposing time, the less the activity remained. Similar result with the hydrolysis of procaine by human serum was reported by Kisch et al. (1943). According to this study, "the % of total procaine hydrolyzed increased considerably with the temperature increases up to 45 or 50°C and then diminished". Therefore, the separation of the epidermis by heat was not used. Recently Wester et al. (1998) also reported viability lost due to heat separation of the skin layers.

Table 4.8 Effect of exposing time to heat on the hydrolysis of methyl salicylate before incubation with whole skin homogenate, n = 1.

Whole skin homogenate	% Methyl salicylate remaining after incubation at 37°C for 20 hours
not heated	100
exposed to 60°C for 5 minutes	14.82
exposed to 60°C for 10 minutes	10.48
exposed to 60°C for 30 minutes	7.38
exposed to 100°C for 2 hours	6.09

4.2.3 Enzyme Kinetic Study of Tetracaine Hydrolysis in Human Skin Homogenate

As it was found that TC had substrate inhibition at 303 μM, which was in the range of a clinical dose, and there was no report about substrate inhibition by TC in skin, enzyme kinetic study of TC hydrolysis in human whole skin homogenate was conducted by varying the initial TC concentration and then determining the rate of TC hydrolysis. All experiments were carried out with 1 replicate unless stated differently, due to the limited availability of human skin homogenate as well as the nature of experiments which required aliquots to be taken at certain time intervals in series.

1) Initial [TC] were 1, 10, 100, 1000, and 7500 μM; analyzed at time 0 and 1 hour using HPLC method 1. The result is shown in Table 4.9. It was concluded that the assay was not sensitive enough to analyze TC concentrations below 100 μM.

Table 4.9 Hydrolysis of tetracaine in whole skin homogenate : Initial tetracaine concentrations from 1 to 7500 μM, n = 1, analysis by HPLC method 1.

[TC] (μM)	4-BABA concentration assayed (μM)				Tetracaine concentration assayed (μM) and (%recovery)			
	skin homogenate		heated skin homogenate		skin homogenate		heated skin homogenate	
	0 h	1 h	0 h	1 h	0 h	1 h	0 h	1 h
1	6.295	-	0	-	0	-	0	-
10	0	-	0	-	85.578 (855.78%)	-	0	-
100	0	17.584	0	6.103	165.693 (165.69%)	163.301 (163.30%)	171.092 (171.09%)	164.094 (164.09%)
1000	0	22.766	0	17.05	1061.286 (106.13%)	983.859 (98.39%)	984.331 (98.43%)	1033.888 (103.39%)
7500	0	43.035	20.449	38.531	6914.608 (92.19%)	6609.772 (88.13%)	7338.734 (97.85%)	6346.159 (84.62%)

Note 0 = not detected, - = not analyzed.

2) Initial [TC] were 10, 50, 100, and 500 μM; analyzed at time 0 to 20 hours using HPLC method 1. Double sampling volume was performed at initial [TC] of 10 and 50 μM to enable the analysis at these low concentrations. The results are shown in Figures 4.18 and 4.19. The initial [TC] of 10 μM was below the analytical capability of the assay either for

4-BABA or TC. 4-BABA and TC could be analyzed from the initial [TC] of 50 μM or higher. Whole skin homogenate showed higher activity than its negative control. There was no TC present by 12 hours of incubation for the initial [TC] of 50 and 100 μM and the corresponding 4-BABA concentrations were steady as well. TC concentrations in heated skin homogenates remained constant through the incubation period. For the "active" skin homogenates, only the initial [TC] of 500 μM showed enough substrate throughout the experiment. Substrate inhibition might have occurred at this initial concentration since TC remaining was not very different from its negative control although 4-BABA concentration increased and [TC] decreased with time.

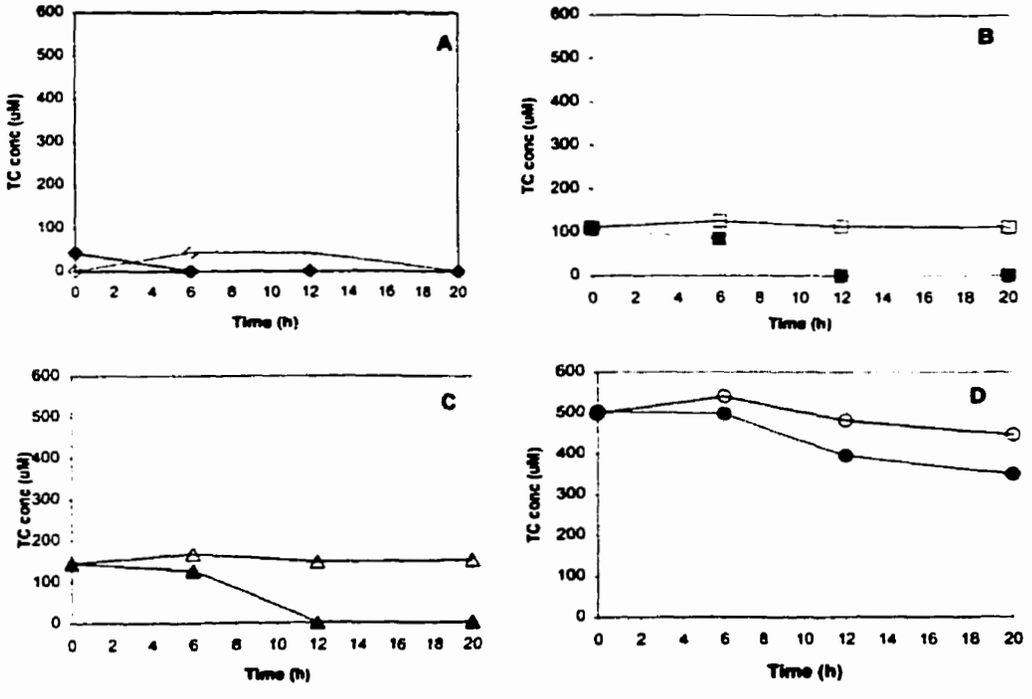

Figure 4.18 Tetracaine concentration in skin homogenate (close symbols) and heated skin homogenates (open symbols) over 20 hours. Initial tetracaine concentrations were (A) 10 μM, (B) 50 μM, (C) 100 μM, (D) 500 μM, n = 1, analysis by HPLC method 1.

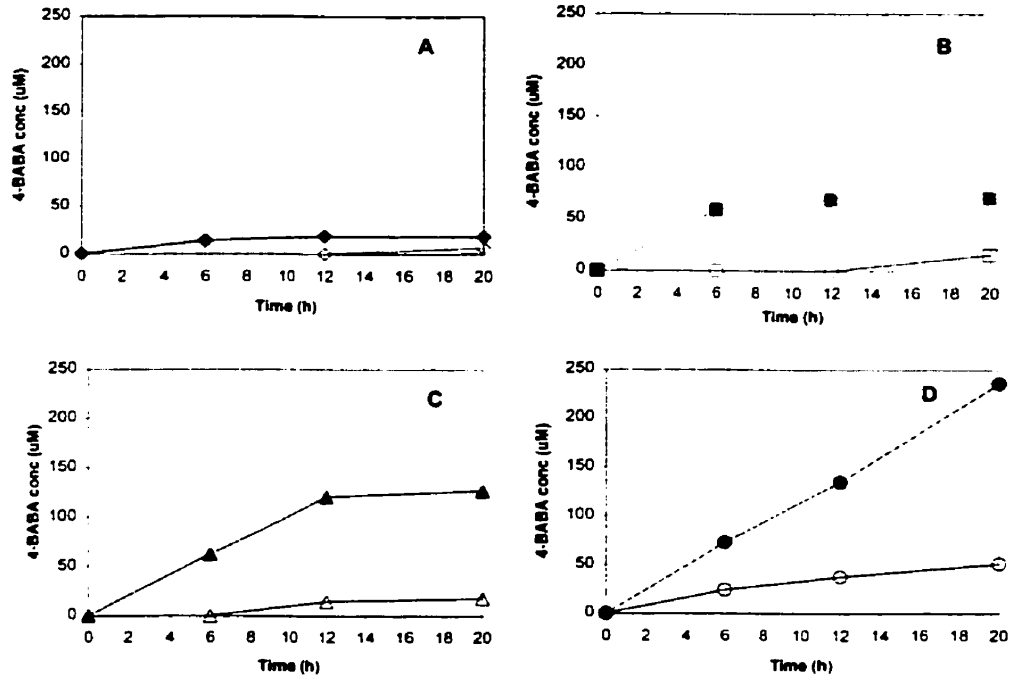

Figure 4.19 4-BABA concentration as the product from tetracaine hydrolysis in skin homogenate (close symbols) and heated skin homogenates (open symbols) over 20 hours. Initial tetracaine concentrations were (A) 10 μM, (B) 50 μM, (C) 100 μM, (D) 500 μM, n = 1, analysis by HPLC method 1.

3) Initial [TC] were 50, 100, 250, 500, 750 and 1000 μM, analyzed at time 0 to 24 hours (6 time points) using HPLC method 1. The results are shown in Table 4.10 and Figures 4.20 to 4.24. From Table 4.10, slopes of plots between corrected concentrations of 4-BABA (concentration in skin homogenate - concentration in heated skin homogenate) and incubation time were determined, then plotted against initial [TC] as in Figure 4.21. Saturation of enzyme occurred at about initial [TC] of 100 μM. Substrate inhibition characteristics was obvious as the rate of the reaction decreased as [TC] increased. This

Table 4.10 Hydrolysis of tetracaine in human skin homogenate : Initial tetracaine concentrations from 50 to 1000 μM, n = 1, analysis by HPLC method 1.

Time (h)	Initial tetracaine concentration					
	50 μM	100 μM	250 μM	500 μM	750 μM	1000 μM
	4-BABA concentration (μM) in skin homogenate					
0	0	0	0	0	0	0
2	0	0	6.1317	16.349	19.701	26.452
4	18.435	18.078	22.324	30.826	33.971	45.531
6	25.987	30.956	31.63	45.532	52.397	59.987
12	51.651	55.505	63.933	84.72	103.61	118.56
24	55.937	104.18	115.53	168.51	196.05	235.6
	4-BABA concentration (μM) in heated skin homogenate					
0	0	0	0	0	0	0
2	0	0	0	0	0	6.7295
4	0	0	0	4.2937	17.06	23.002
6	0	0	0	15.964	23.081	38.461
12	0	0	15.876	27.542	44.58	61.657
24	0	12.793	26.949	51.826	91.437	125.73
	% Tetracaine remaining in skin homogenate					
0	100	100	100	100	100	100
2	90.3	94.19	92.06	93.78	102.03	117.69
4	82.17	87.9	91.13	92.43	96.11	105.8
6	74.71	93.38	86.46	91.54	94.06	93.38
12	48.13	65.28	78.33	83.65	88.05	87.75
24	0	39.78	61.38	67.4	75.28	79.47
	% Tetracaine remaining in heated skin homogenate					
0	100	100	100	100	100	100
2	96.57	106.87	94.79	106.66	96.49	97.89
4	95.65	107.26	92.56	101.54	95.13	95.72
6	95.26	106.04	94.76	100.35	94.06	114.91
12	93.8	103.6	89.99	98.79	92.43	92.72
24	89.31	103.8	89.01	93.45	100.25	94.27

Note 0 = not detected

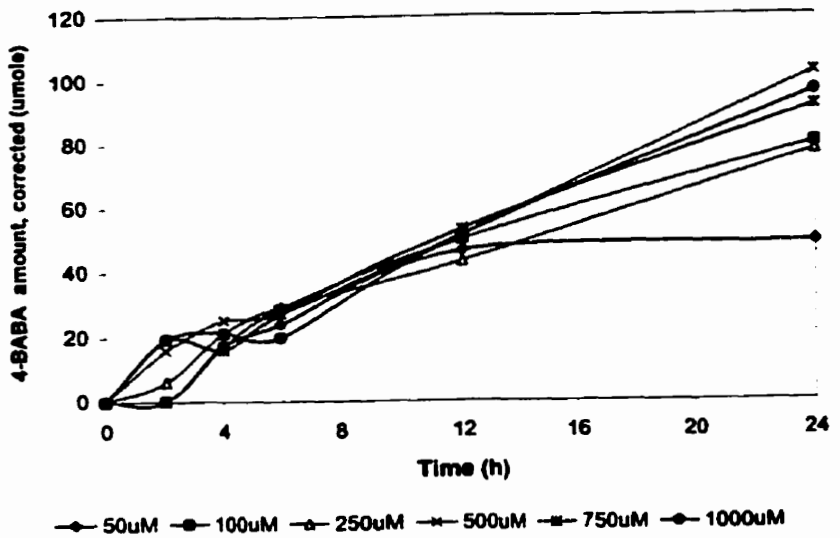

Figure 4.20 4-BABA concentration from tetracaine hydrolysis in skin homogenate in 24 hours. Initial tetracaine concentrations were from 50 to 1000 μM (6 concentrations), n = 1, analysis by HPLC method 1.

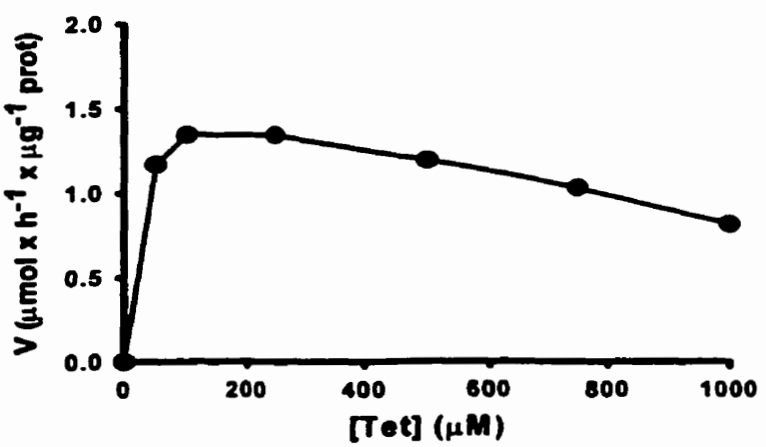

Figure 4.21 Tetracaine hydrolysis rate as a function of initial tetracaine concentrations which were from 50 to 1000 μM (6 concentrations).

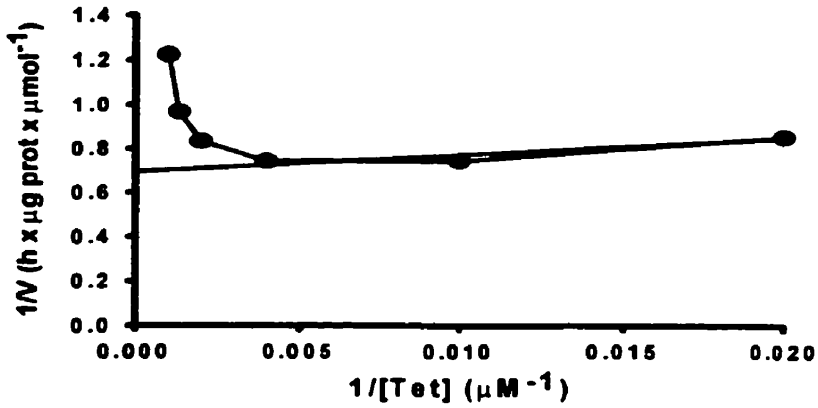

Figure 4.22 Lineweaver-Burk plot from 0-6 hours. Initial tetracaine concentrations were from 50 to 1000 µM (6 concentrations). From the extrapolation of the plot using [TC] of 50 -250 µM; K_m = 1/x-intercept = 12.66 µM, V_{max} = 1/y-intercept = 1.44 µmol/h/µg protein.

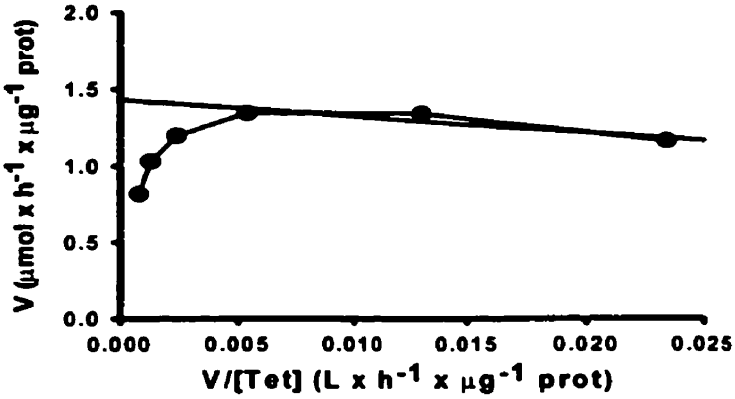

Figure 4.23 Eadie-Hofstee plot from 0-6 hours. Initial tetracaine concentrations were from 50 to 1000 µM (6 concentrations). From the extrapolation of the plot using [TC] of 50 -250 µM; K_m = -slope = 10.20 µM, V_{max} = y-intercept = 1.43 µmol/h/µg protein.

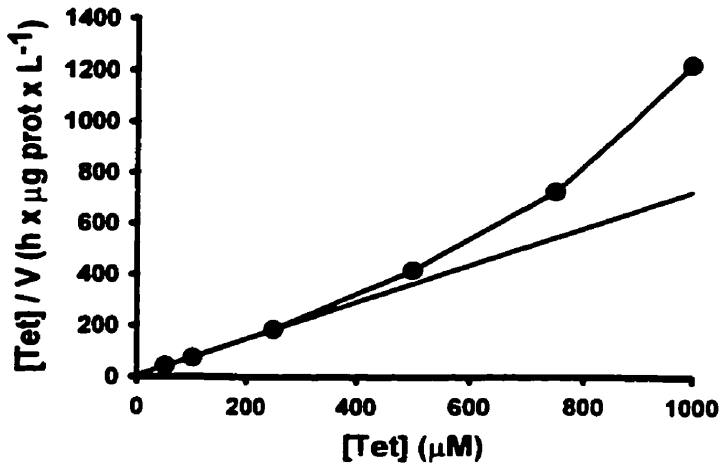

Figure 4.24 Hanes plot from 0-6 hours. Initial tetracaine concentrations were from 50 to 1000 µM (6 concentrations). From the extrapolation of the plot using [TC] of 50 -250 µM; K_m= -x-intercept = 6.58 µM, V_{max}= 1/slope = 1.39 µmol/h/µg protein.

characteristics was also demonstrated in the Lineweaver-Burk plot , Eadie-Hoffstee plot, and Hanes plot from 0 to 6 hours (Figures 4.22-4.24). Extrapolation of the first three [TC] (50-250 µM) provided rough estimations of kinetic data. More data are needed at lower [TC].

4) Initial [TC] at 50, 75, 100, 150, 200, 250, 300, 400, and 500 µM, analyzed at time 0 to 24 hours (9 time points) using HPLC method 1. Since the limit of quantitation (LOQ) of TC was 5 ng, the lowest initial [TC] which still be accurately analyzed at time 0 would be 25 µM. However, once incubated, TC amount will be depleted and the assay would not be accurate anymore. So the lowest [TC] was kept at 50 µM but [TC] were gradually increased to 500 µM. The results are shown in Table 4.11 and Figures 4.25 to 4.29. TC recovery was between 71% and 94% but the data analysis was based on 4-BABA

Table 4.11 Hydrolysis of tetracaine in human skin homogenate : Initial tetracaine concentrations from 50 to 500 μM, n = 1, analysis by HPLC method 1.

Time (h)	Initial tetracaine concentration									
	50μM	75μM	100μM	150μM	200μM	250μM	300μM	400μM	500μM	200μM in PBS
	4-BABA concentration (μM) in skin homogenate									
0	0	0	0	0	0	0	0	0	0	0
1	4.815	0	0	3.95705	6.13558	4.43053	5.73247	6.1066	5.76404	0
2	8.2003	7.7692	8.3581	8.44398	10.7757	8.54489	10.1195	10.2204	11.4044	0
3	11.9	12.383	11.885	12.1863	12.3783	13.629	16.4414	14.9568	15.1912	0
4	16.432	15.069	15.665	17.2414	16.9392	16.7684	18.5299	19.9338	21.1079	0
5	19.817	21.352	20.134	20.5656	20.8652	23.4008	21.6911	23.9803	27.1017	0
6	21.968	22.372	23.643	24.4797	24.5614	25.7889	28.1283	29.6988	31.1436	0
12	29.377	44.089	48.062	49.0665	52.1501	52.1713	52.9785	57.4411	56.9144	7.37025
24	30.648	46.563	63.922	97.4841	98.088	104.129	96.7855	109.17	122.586	13.4215
	4-BABA concentration (μM) in heated skin homogenate									
0	0	0	0	0	0	0	0	0	0	0
1	0	0	0	0	0	0	0	0	0	0
2	0	0	0	0	0	0	0	0	0	0
3	0	0	0	0	0	0	0	0	5.29521	0
4	0	0	0	0	0	0	0	5.43338	6.50401	0
5	0	0	0	0	0	0	4.30168	6.85175	8.06675	0
6	0	0	0	0	3.52083	3.89651	6.41552	7.4577	9.45408	0
12	0	0	0	6.27426	7.78732	8.1956	10.0166	13.3692	18.1821	7.37025
24	0	5.5389	7.3821	11.1405	12.3902	16.0549	18.2918	23.9245	31.1721	13.422
	% Tetracaine remaining in skin homogenate									
0	100	100	100	100	100	100	100	100	100	100
1	101.19	96.08	103.78	101.75	107.46	103.86	100.45	102.61	99.81	97.58
2	87.01	90.72	90.44	91.77	97.9	97.85	93.31	94.9	96.34	100.98
3	73.39	86.8	86.17	87.1	95.78	94.38	104.45	95.88	99.06	102.1
4	68.03	77.19	80.1	82.28	94.3	85.41	85.62	90.94	90.44	97.8
5	61.4	72.95	74.54	77.04	85.85	88.61	84.16	87.15	89.32	99.85
6	41.09	62.41	70.57	75.78	82.95	83.58	85.01	91.66	87.89	99.91
12	0	31.19	38.4	55.41	68.01	65.87	69.14	75.86	74.92	95.16
24	0	0	0	0	32.94	39.74	41.09	52.04	62.69	96.91
	% Tetracaine remaining in heated skin homogenate									
0	100	100	100	100	100	100	100	100	100	100
1	104.06	111.57	98.77	105.75	98.86	98.5	101.84	104.17	102.96	97.58
2	107.46	101.84	104.95	104.75	98.82	100.8	104.39	102.24	103.64	100.98
3	100.19	97.75	100.35	99.31	98.59	100.62	103.32	102.35	112.61	102.1
4	100.01	101.64	99.19	98.22	99.26	101.7	99.27	99.16	97.84	97.8
5	101.78	101.6	95.65	101.79	95.14	95.21	99.02	97.48	99.95	99.85
6	92.06	101.14	96.85	99.2	93.5	99.41	96.03	94.15	99.24	99.91
12	99.13	98.76	97.17	99.4	92.96	99.23	95.98	96.63	97.22	95.16
24	96.63	92.68	100.14	93.18	90.7	90.28	86.95	86.71	90.86	96.91

Note 0 = not detected

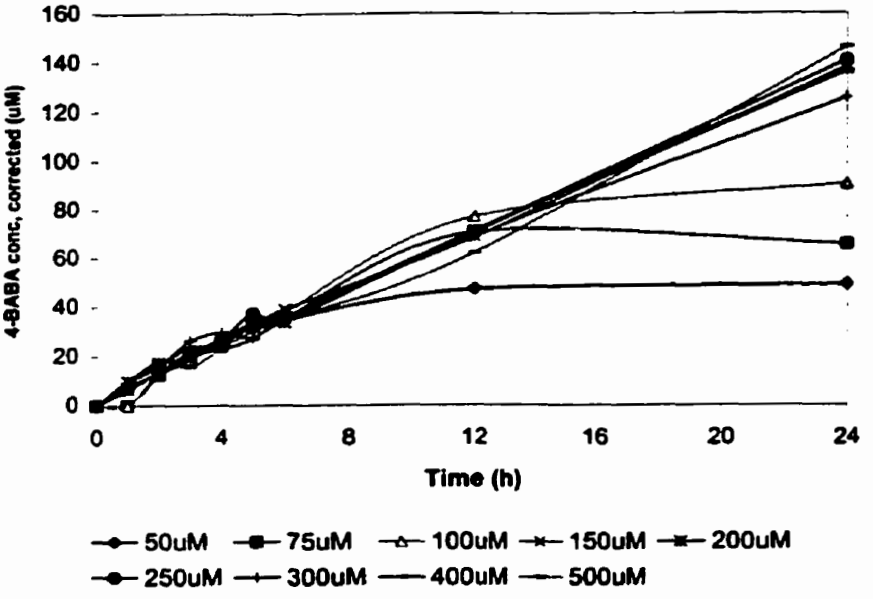

Figure 4.25 4-BABA concentration from tetracaine hydrolysis in skin homogenate in 24 hours. Initial tetracaine concentrations were from 50 to 500 μM (9 concentrations), n = 1, analysis by HPLC method 1.

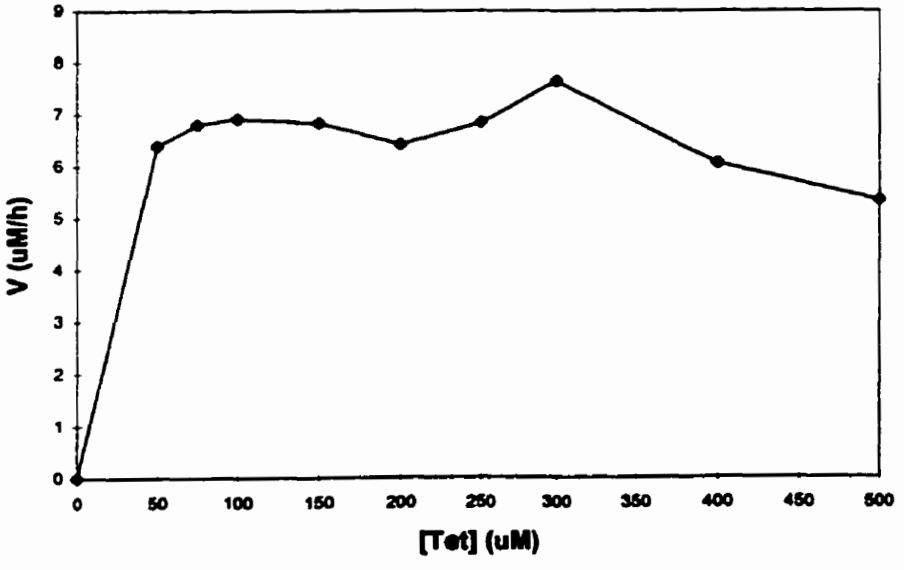

Figure 4.26 Tetracaine hydrolysis rate as a function of initial tetracaine concentrations which were from 50 to 500 μM (9 concentrations).

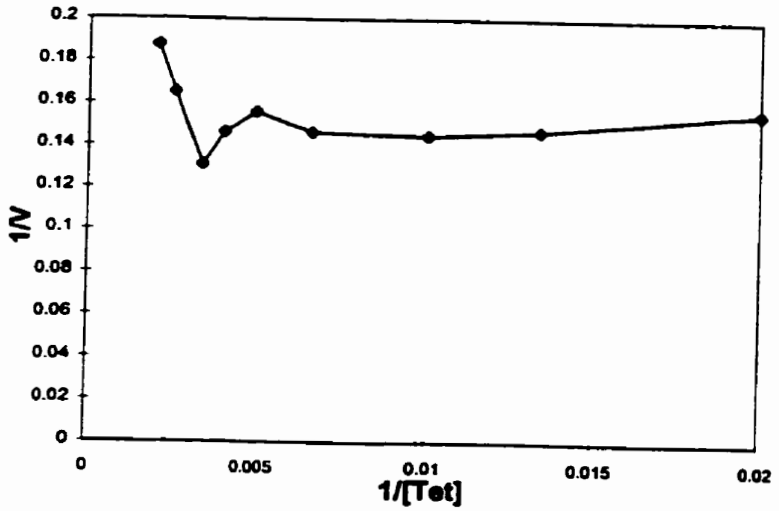

Figure 4.27 Lineweaver-Burk plot from 0-4 hours. Initial tetracaine concentrations were from 50 to 500 μM (9 concentrations). From the extrapolation of the plot using [TC] of 50 -100 μM; K_m = 1/x-intercept = 9.45 μM, V_{max} = 1/y-intercept = 1.72 μmol/h/μg protein.

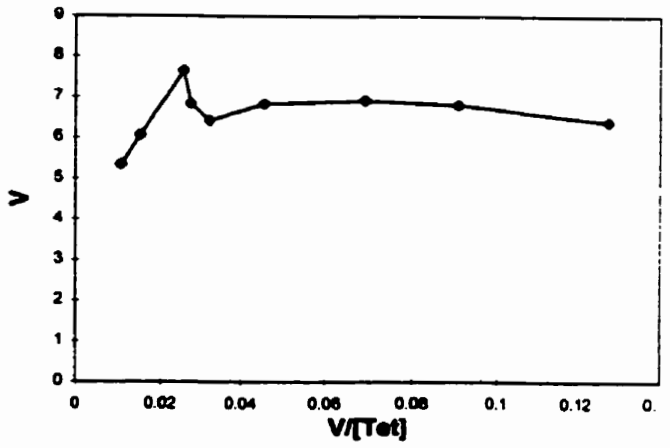

Figure 4.28 Eadie-Hofstee plot from 0-4 hours. Initial tetracaine concentrations were from 50 to 500 μM (9 concentrations). From the extrapolation of the plot using [TC] of 50 -100 μM; K_m = -slope = 9.15 μM, V_{max} = y-intercept = 1.84 μmol/h/μg protein.

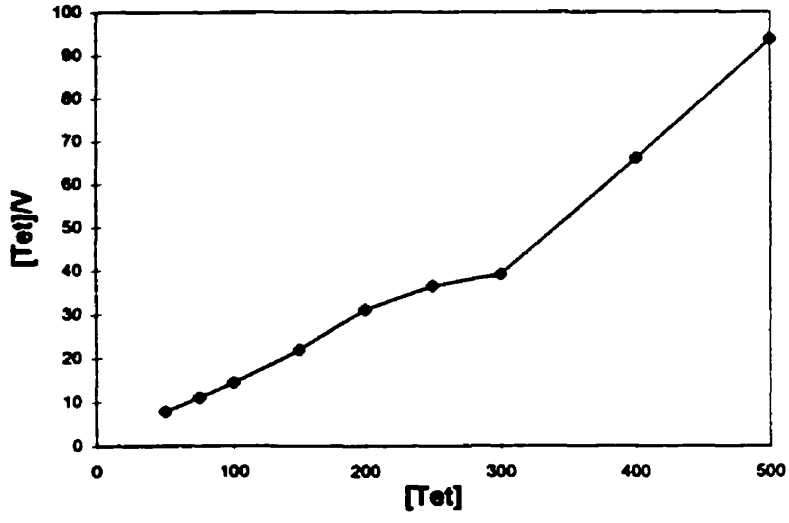

Figure 4.29 Hanes plot from 0-4 hours. Initial tetracaine concentrations were from 50 to 500 μM (9 concentrations). From the extrapolation of the plot using [TC] of 50 -100 μM; K_m= -x-intercept = 8.57 μM, V_{max}= 1/slope = 1.83 μmol/h/μg protein.

concentration assayed. From the plot between the rate of the reaction and [TC] (Figure 4.26), saturation of enzyme was obvious as steady state was already reached at initial [TC] 50 μM. All the secondary plots (Lineweaver-Burk plot, Eadie-Hoffstee plot, and Hanes plot) showed substrate inhibition characteristics. K_m and V_{max} could be determined using the first three initial [TC] (50-100 μM). K_m was in the 9 μM range and V_{max} was about 7.6 μM/h. Again, more data are needed at much lower [TC] to obtain meaningful kinetic data

5. Initial [TC] at 20, 30, 40, 50, 60, 80, 100, 120, 140, 160, 180 and 200 μM, analyzed at time 0 to 6 hours (7 time points) using HPLC method 2. The skin homogenate was two times more concentrated than previous experiments (prepared by increasing the ratio of skin to PBS from 1:5 to 1:2). Data analysis was based on 4-BABA concentration

assayed. Substrate inhibition was observed at initial [TC] above 100 μM as shown in Figure 4.30. Lineweaver-Burk plot, Eadie-Hoffstee plot and Hanes plot (Figures 4.31-4.33) showed substrate inhibition characteristic as well. The K_m and the V_{max} of TC were calculated from the Lineweaver-Burk, Eadie-Hofstee and Hanes plots. These kinetic parameters were calculated separately from data which were obtained from three skin sources. Due to limited availability of the skin homogenate, the experiment with the third set of replicate samples was conducted at initial [TC] of 40, 60, 80, 100, 120 and 140 μM. As the result, the number of data point in this sample set was not sufficient to imply meaningful K_m and V_{max} values. However, this third set of data revealed similar trend of the kinetics of TC hydrolysis in human skin homogenate to the other 2 replicates. The K_m of TC was in the range of 11-28 μM and the V_{max} was in the range of 2.0-2.8 μmol/h/μg protein. Previous K_m reported for Tet were 50 μM for human plasma and 2.8 μM for

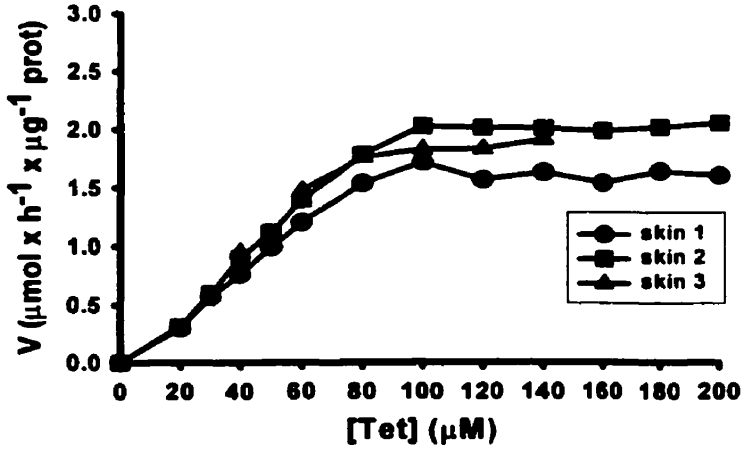

Figure 4.30 Tetracaine hydrolysis rate (V) as a function of initial tetracaine concentrations from 20 to 200 μM (12 or 6 concentrations).

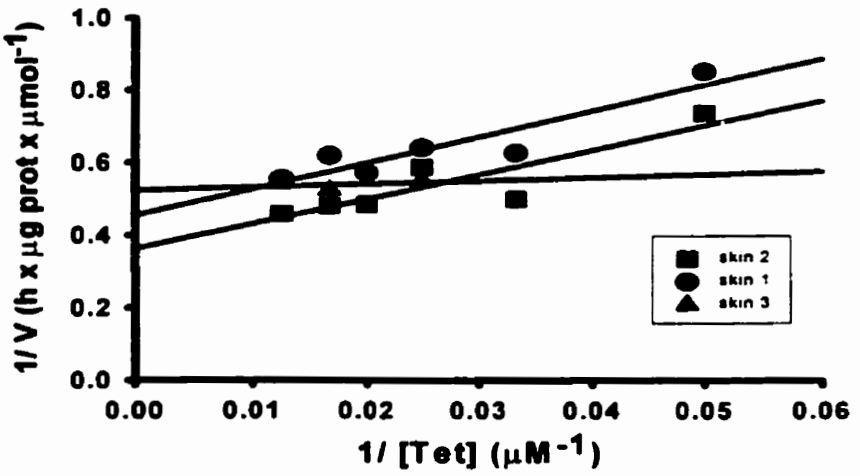

Figure 4.31 Lineweaver-Burk plot from 0-2 hours. Initial tetracaine concentrations were from 20 to 200 µM (12 or 6 concentrations). From the extrapolation of the plot using [TC] of 20-80 µM; K_m = 1/x-intercept = 20.22, 28.27, 11.97 µM for skin 1, 2 and 3, respectively, V_{max} = 1/y-intercept = 2.20, 2.76, 1.91 µmol/h/µg protein for skin 1, 2 and 3, respectively.

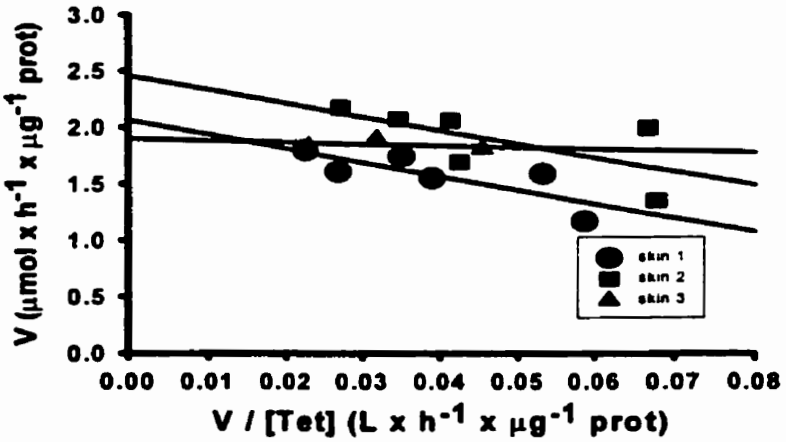

Figure 4.32 Eadie-Hofstee plot from 0-2 hours. Initial tetracaine concentrations were from 20 to 200 µM (12 or 6 concentrations). From the extrapolation of the plot using [TC] of 20-80 µM; K_m = -slope = 12.16, 11.99, 1.41 µM for skin 1, 2 and 3, respectively, V_{max} = y-intercept = 2.07, 2.46, 1.90 µmol/h/µg protein for skin 1, 2 and 3, respectively.

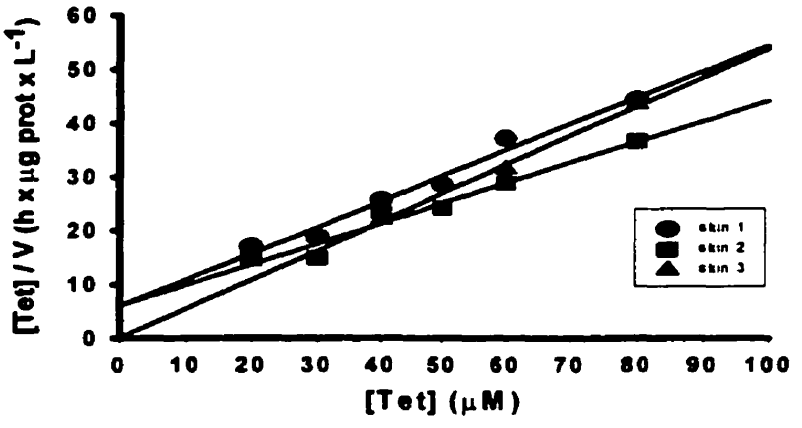

Figure 4.33 Hanes plot from 0-2 hours. Initial tetracaine concentrations were from 20 to 200 µM (12 or 6 concentrations). From the extrapolation of the plot using [TC] of 20-80 µM; K_m= -x-intercept = 11.03, 13.50, 0.20 µM for skin 1, 2 and 3, respectively, V_{max}= 1/slope = 2.06, 2.63, 1.86 µmol/h/µg protein for skin 1, 2 and 3, respectively.

cholase (purified human cholinesterase concentrate) (Foldes et al., 1955), 0.14 and 8 µM for usual and atypical cholinesterase in human sera respectively (the buffer was 0.1 M Tris-Cl, pH 7.4, 25°C)(Valentino et al., 1981).

The initial [TC] used in the preliminary experiments (303 µM) gave a linear hydrolysis pattern in human whole skin homogenate with the rate constant of 21.7 x 10^{-9} mol/mL/h. This is about 5 times higher than the rate constant of 3.4 x 10^{-9} to 4.6 x 10^{-9} mol/mL/h reported by Woolfson et al. (1990). The numbers are quite comparable because the initial [TC] in their experiment was 332 µM and the concentration of the skin homogenate was about 8 times lower than that used in this study. At this range of initial

[TC], substrate inhibition had occurred and TC hydrolysis still happened but at a lower rate than it would have been if there were not any substrate inhibition.

Regarding the substrate inhibition effect of TC, the amount of TC used in topical application should be high enough to inhibit hydrolysis (hence deactivation) of TC in the skin so toxicity would be a concern, especially for people with atypical or silent genotype of pseudocholinesterase enzyme. Beside the rare allergic reaction, systemic toxicity to central nervous and cardiovascular systems is more common. Formulation aspects should concentrate on preparations that deliver TC into the skin, not through the skin.

4.2.4 Hydrolysis of Methyl salicylate in Human Skin Homogenate

Hydrolysis of methyl salicylate in skin homogenates and controls are shown in Figure 4.34 and Table 4.12. There was no substrate inhibition at the MS concentration used

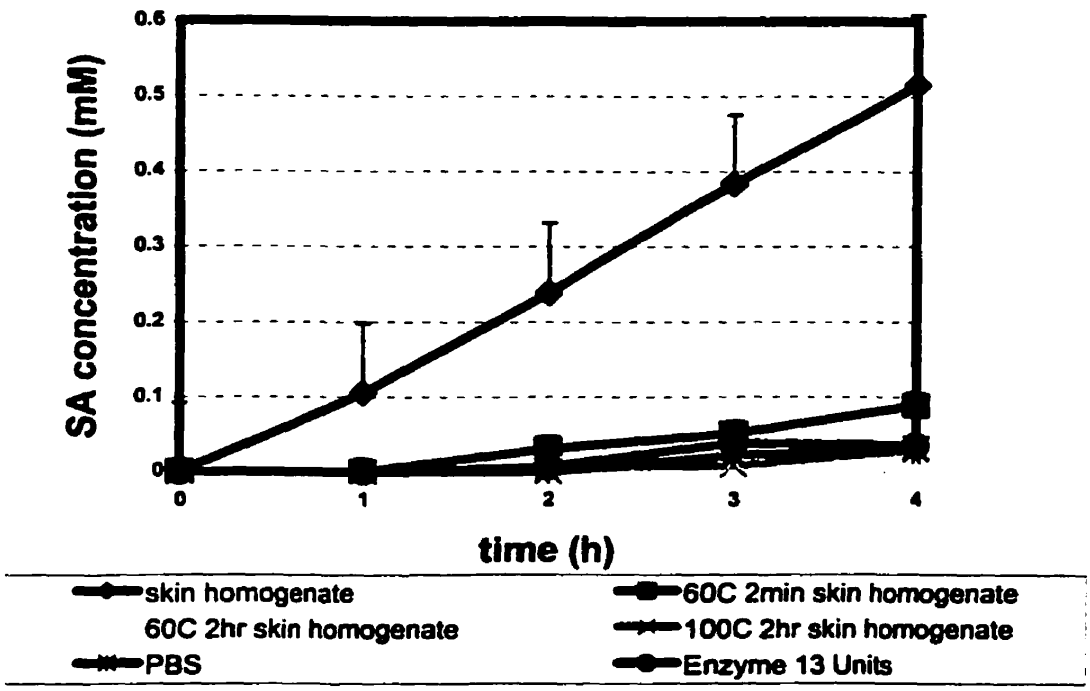

Figure 4.34 Hydrolysis of methyl salicylate in human skin homogenate (n = 3, with 3 replicates each) and controls (n = 3).

Table 4.12 Effect of heat on hydrolysis rate of methyl salicylate in human skin homogenate. The hydrolysis rates were calculated from the slope of the plots between salicylic acid concentration and time (0-4 hours).

Treatment	Hydrolysis rate (μmol/h)	Percent of untreated skin homogenate	Hydrolysis rate (nmol/h/μg protein)	Percent of untreated skin homogenate
Untreated skin homogenate[a]	131.0	100	72.31	100
Heat 60°C for 2 minutes[a]	22.9	17.51	12.88	17.81
Heat 60°C for 2 hours[a]	0	0	0	0
Heat 100°C for 2 hours[a]	6.6	5.05	3.73	5.15
Phosphate buffered saline[b]	8.5	6.52	N/A	N/A
Pseudocholinesterase (13U)[b]	10.8	8.24	45.45	62.85

[a] n = 9

[b] n = 3

(5 mM in the incubation mixture). Untreated skin homogenate showed much higher esterase activity than its negative control and PBS. Pseudocholinesterase enzyme (13 U) hydrolyzed MS at very slow rate while its activity was much higher for the hydrolysis of TC. When the skin homogenate was subjected to 60°C temperature, esterase activity decreased substantially to 17.5% and 0% of untreated homogenate after exposure for 2 minutes and 2 hours respectively. SUA was not detected most likely due to the absence of added cofactor for conjugation in the skin homogenate.

Yano et al. (1991) reported hydrolysis rate of MS in hairless mouse skin homogenate, serum and liver to be 0.031, 0.040 and 1.335 nmol/mg protein/min,

respectively. These numbers are equivalent to 0.517, 0.667 and 22.25 nmol/μg protein/h, respectively. The skin homogenate was prepared with skin to phosphate buffer ratio of 1:9 as compared to 1:5 in this study and the initial MS concentration in the incubation mixture was 2 mM as compared to 5 mM in this study. Therefore, MS was hydrolyzed at higher rate in homogenate from human skin than that from hairless mouse skin. The same authors also mentioned that the hydrolytic activity reduced substantially after exposure to 100°C for 15 minutes. Effect of heat on esterase activity was reported with other drugs and skin preparations from different species as well. For example, the percentage of procaine hydrolyzed by human serum esterase considerably increased with the increase in temperature up to 45 or 50°C, and then diminished (Kisch et al., 1943). Heating at 329°K (56°C)for 30 minutes caused about 60% inhibition of benoxinate and benzoylcholine hydrolysis by human plasma (Dubbels and Schloot, 1983). Pannatier et al. (1981) reported that pretreatment of the 10,000 x *g* skin preparation from mice at 50°C for 10 minutes resulted in only 6% loss of hydrolytic activity for *p*-nitrobenzoate esters. However, treatment at 60°C and higher temperature resulted in 80% and total activity loss, respectively. Similar results from the heat treatment at 50 and 60°C were also mentioned by Ahmed et al. (1995) with the hydrolysis of propranolol prodrugs in the cutaneous 10,000 x *g* preparations from hairless mouse. The relative heat stability of esterase suggested that the enzymes are soluble (Pannatier et al., 1981). In the article about carboxylic ester hydrolase activity in hairless and athymic nude mouse skin, Ghosh and Mitra (1990) described that 35-40% of the total ester hydrolase activity was lost with pretreatment of skin homogenate from athymic nude mouse at 50°C for 15 minutes. More than 80% of esterase activity in skin homogenates from both species was lost at 55°C.

4.3 Excised Human Skin Model

4.3.1 Viability Assessment of the Skin During Diffusion Study

4.3.1.1 Oxygen Consumption Measurement

Aerobic oxygen consumption of the skin samples on diffusion cells was determined. Figure 4.35 displays typical curves obtained from oxygen concentration measurement at time intervals from live and sham samples. As shown in Table 4.13, the slopes of the linear regression curves using data from 100 to 600 seconds (process 1) demonstrate significant difference between live and dead skin ($p=0.0001$). The same highly significant difference is observed using the difference between oxygen concentration at peak and at the 600^{th} second (process 2) as demonstrated in Table 4.14. Although the same conclusion was obtained from 4 experiments conducted on different days, there was some variation in the values of these parameters.

The validity of the oxygen consumption measurement was assessed. Control experiments were conducted in order to compare the two parameters between sham samples (previously frozen skin subjected to the experiment on diffusion cells) and blanks (Parafilm in place of skin). The results are shown in Tables 4.15 and 4.16. Both parameters from the blank and sham samples from three different days were compared. Although there were some differences between each parameters from the blank and sham samples, the extent of the difference was not as high as those between the live and sham samples. These were demonstrated in Figures 4.36 - 4.39 as scatter plots of the differences in the parameters between live *vs* sham and blank *vs* sham samples.

Figure 4.35 Typical profiles of oxygen concentration in the buffer above the skin in the diffusion cell as a function of time: (A) live sample, (B) sham sample.

A

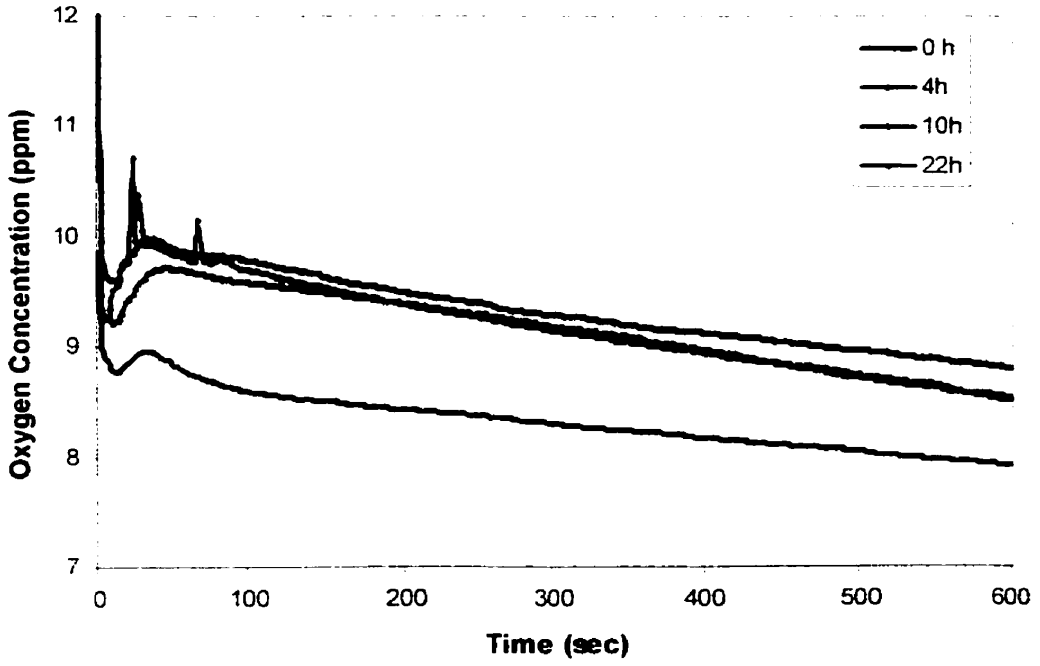

B

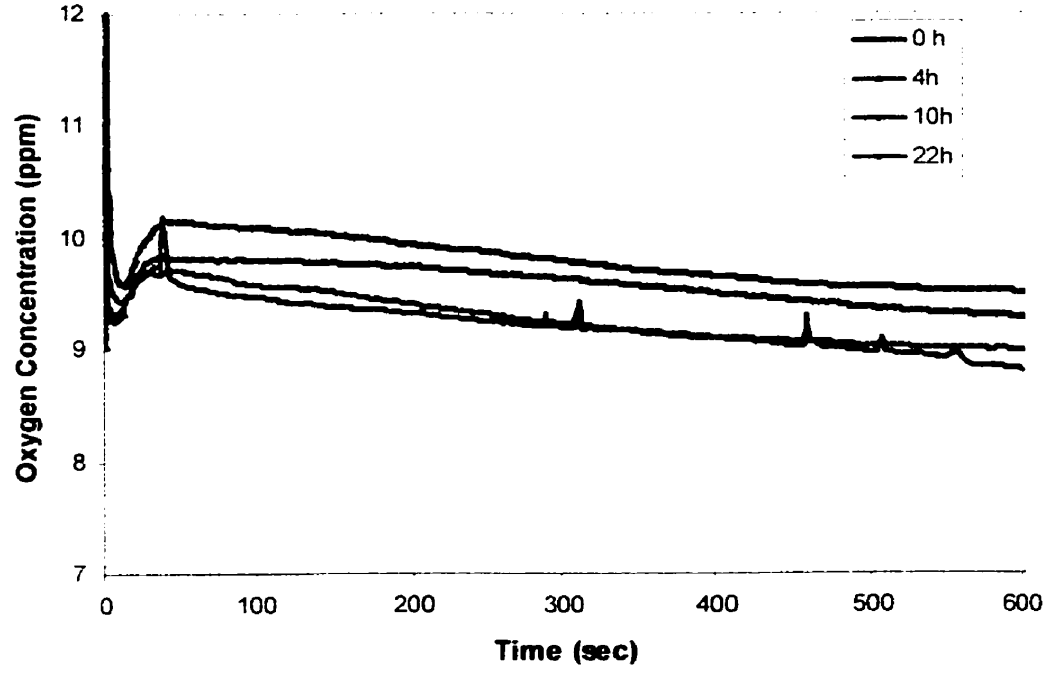

Table 4.13 Slope of the linear regression between oxygen concentration and time using data from 100 to 600 seconds (process 1) : live *vs* sham samples. Values represent mean ± SEM, n = 3. The experiments were conducted on 4 different days with different skin sources.

** p=0.0001 compared to sham sample

* p<0.05 compared to sham sample

A Live *vs* Sham Day 1

Time	Slope x 10^3		Slope difference Live-Sham
	Live	Sham	
0 h	-2.46 ± 0.01	-2.66 ± 0.34	0.2
4 h	-2.21 ± 0.16	-1.82 ± 0.20	0.39
10 h	-2.26 ± 0.18*	-1.50 ± 0.14	0.76
22 h	-3.50 ± 0.28**	-1.32 ± 0.23	2.18
Average (n=12)	-2.61 ± 0.18**	-1.83 ± 0.19	0.78

B Live *vs* Sham Day 2

Time	Slope x 10^3		Slope difference Live-Sham
	Live	Sham	
0 h	-4.32 ± 1.00*	-2.33 ± 0.24	1.99
4 h	-5.24 ± 1.00*	-2.74 ± 0.10	2.5
10 h	-4.07 ± 0.47	-2.51 ± 0.14	1.56
22 h	-5.13 ± 0.30*	-2.89 ± 0.16	2.24
Average (n=12)	-4.69 ± 0.35**	-2.62 ± 0.10	2.07

Table 4.13 (continued)

C Live *vs* Sham Day 3

Time	Slope x 10^3		Slope difference Live-Sham
	Live	Sham	
0 h	-1.71 ± 0.21*	-1.19 ± 0.16	0.52
4 h	-2.22 ± 0.03**	-0.94 ± 0.11	1.28
10 h	-2.04 ± 0.21*	-1.05 ± 0.10	0.99
22 h	-2.36 ± 0.16*	-1.67 ± 0.23	0.69
Average (n=12)	-2.08 ± 0.10**	-1.21 ± 0.11	0.87

D Live *vs* Sham Day 4

Time	Slope x 10^3		Slope difference Live-Sham
	Live	Sham	
0 h	-1.90 ± 0.15	-1.66 ± 0.22	0.24
4 h	-3.26 ± 0.36*	-1.47 ± 0.03	1.79
10 h	-4.57 ± 1.00	-3.34 ± 0.38	1.23
22 h	-4.96 ± 1.00*	-3.14 ± 0.17	1.82
Average (n=12)	-3.67 ± 0.47*	-2.40 ± 0.27	1.27

Table 4.14 Difference between oxygen concentration at peak and at the 600th second (process 2) : live *vs* sham samples.

Values represent mean ● SEM, n = 3. The experiments were conducted on 4 different days with different skin sources.

** p=0.0001 compared to sham sample

* p<0.05 compared to sham sample

A Live *vs* Sham Day 1

Time	$\%[O_2]$ difference		Difference of $\%[O_2]$ difference Live-Sham
	Live	Sham	
0 h	13.79 ● 0.28	12.08 ● 1.10	1.71
4 h	16.49 ± 0.61*	9.75 ± 0.83	6.74
10 h	13.87 ± 0.44*	8.52 ± 0.73	5.35
22 h	23.17 ± 2.07**	8.50 ● 1.31	14.67
Average (n=12)	16.83 ± 1.25**	9.71 ● 0.62	7.12

B Live *vs* Sham Day 2

Time	$\%[O_2]$ difference		Difference of $\%[O_2]$ difference Live-Sham
	Live	Sham	
0 h	32.21 ± 3.42*	20.28 ± 0.86	11.93
4 h	42.45 ± 7.89*	20.85 ± 0.29	21.6
10 h	27.21 ± 2.36*	16.37 ± 1.34	10.84
22 h	37.53 ± 1.88*	22.13 ± 1.16	15.4
Average (n=12)	34.85 ± 2.60**	19.91 ± 0.78	14.94

Table 4.14 (continued)

C Live *vs* Sham Day 3

Time	%[O_2] difference		Difference of %[O_2] difference Live-Sham
	Live	Sham	
0 h	14.50 ± 1.85*	7.93 ± 0.53	6.57
4 h	12.72 ± 0.82**	5.69 ± 0.30	7.03
10 h	12.19 ± 0.98*	6.56 ± 0.17	5.63
22 h	13.32 ± 0.51	10.81 ± 1.51	2.51
Average (n=12)	13.18 ± 0.56**	7.75 ± 0.68	5.43

D Live *vs* Sham Day 4

Time	%[O_2] difference		Difference of %[O_2] difference Live-Sham
	Live	Sham	
0 h	13.15 ± 1.18	9.32 ± 1.31	3.83
4 h	22.99 ± 2.54*	11.34 ± 1.24	11.65
10 h	36.87 ± 6.21*	24.93 ± 2.42	11.94
22 h	32.62 ± 3.35*	21.11 ± 2.13	11.51
Average (n=12)	24.61 ± 3.20*	16.67 ± 2.12	7.94

Table 4.15 Slope of the linear regression between oxygen concentration and time using data from 100 to 600 seconds (process 1) : blank *vs* sham samples. Values represent mean ● SEM, n = 3. The experiments were conducted on 3 different days with different sources of frozen skin samples.

** p=0.0001 compared to sham sample

* p<0.05 compared to sham sample

A Blank *vs* Sham Day 5

Time	Slope x 10^3		Slope difference Blank-Sham
	Blank	Sham	
0 h	-0.39 ± 0.10*	-0.91 ● 0.04	0.52
4 h	-0.54 ± 0.03*	-1.13 ● 0.25	0.59
10 h	-1.45 ● 0.06	-1.18 ± 0.09	0.27
22 h	-1.57 ● 0.26	-1.71 ± 0.19	0.14
Average (n=12)	-0.99 ± 0.17*	-1.23 ± 0.11	0.24

B Blank *vs* Sham Day 6

Time	Slope x 10^3		Slope difference Blank-Sham
	Blank	Sham	
0 h	-0.71 ± 0.09**	-1.49 ± 0.04	0.78
4 h	-1.18 ± 0.12	-1.37 ± 0.09	0.19
10 h	-1.12 ± 0.07	-1.26 ± 0.12	0.14
22 h	-0.78 ± 0.05**	-1.48 ± 0.05	0.7
Average (n=12)	-0.95 ● 0.07**	-1.40 ± 0.04	0.45

Table 4.15 (continued)

C Blank *vs* Sham Day 7

Time	Slope x 10^3		Slope difference Blank-Sham
	Blank	Sham	
0 h	-1.12 ± 0.21	-1.46 ± 0.28	0.34
4 h	-0.74 ± 0.02	-1.18 ± 0.11	0.44
10 h	-0.77 ± 0.15	-1.14 ± 0.16	0.37
22 h	-0.50 ± 0.42*	-1.61 ● 0.19	1.11
Average (n=12)	-0.78 ± 0.12*	-1.35 ± 0.10	0.57

Table 4.16 Difference between oxygen concentration at peak and at the 600th second (process 2) : blank *vs* sham samples.

Values represent mean ± SEM, n = 3. The experiments were conducted on 3 different days with different sources of frozen skin samples.

** p=0.0001 compared to sham sample

* p<0.05 compared to sham sample

A Blank *vs* Sham Day 5

Time	%[0_2] difference		Difference of %[0_2] difference Blank-Sham
	Blank	Sham	
0 h	2.30 ± 0.49*	6.13 ± 0.18	3.83
4 h	3.29 ± 0.14*	6.67 ± 1.56	3.38
10 h	7.22 ± 0.78	7.31 ± 1.14	0.09
22 h	8.45 ± 1.27	10.94 ± 1.23	2.49
Average (n=12)	5.32 ± 0.85*	7.76 ± 0.75	2.44

Table 4.16 (continued)

B Blank *vs* Sham Day 6

Time	%[O_2] difference		Difference of %[O_2] difference Blank-Sham
	Blank	Sham	
0 h	6.28 ± 2.05	8.65 ± 0.37	2.37
4 h	7.81 ± 0.48	8.77 ± 0.49	0.96
10 h	7.69 ± 0.53	9.01 ± 0.44	1.32
22 h	5.45 ± 0.28*	10.88 ± 0.82	5.43
Average (n=12)	6.81 ± 0.55*	9.33 ± 0.36	2.52

C Blank *vs* Sham Day 7

Time	%[O_2] difference		Difference of %[O_2] difference Blank-Sham
	Blank	Sham	
0 h	7.77 ± 2.15	8.17 ± 1.18	0.4
4 h	5.82 ± 0.75	6.25 ± 1.16	0.43
10 h	5.94 ± 1.35	7.22 ± 1.08	1.28
22 h	2.81 ± 1.74*	11.22 ± 1.77	8.41
Average (n=12)	5.59 ± 0.86*	8.22 ± 0.80	2.63

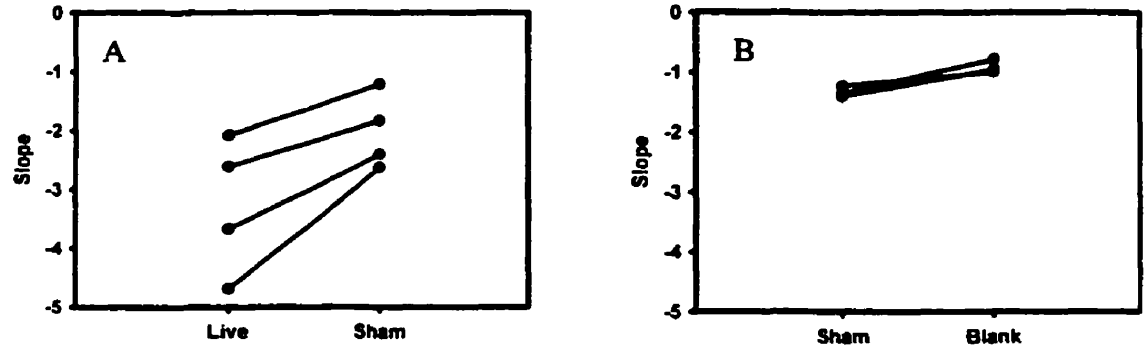

Figure 4.36 Scatter plot of the average values of the slopes (process 1) from (A) live and sham samples, (B) sham and blank samples from different experimental days. Lines co-ordinate values from the same day.

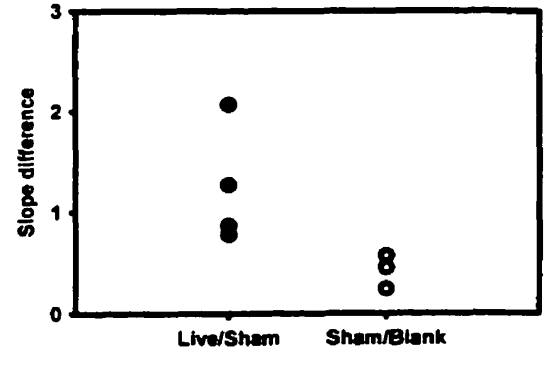

Figure 4.37 Summary of the difference between slopes of live *vs* sham and sham *vs* blank samples from all experiments.

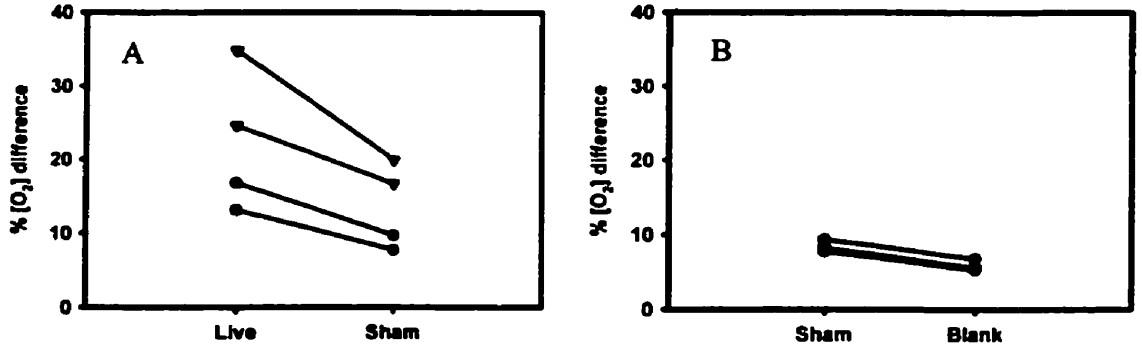

Figure 4.38 Scatter plot of the average % [O_2] difference (process 2) from (A) live and sham samples, (B) sham and blank samples from different experimental days. Lines co-ordinate values from the same day.

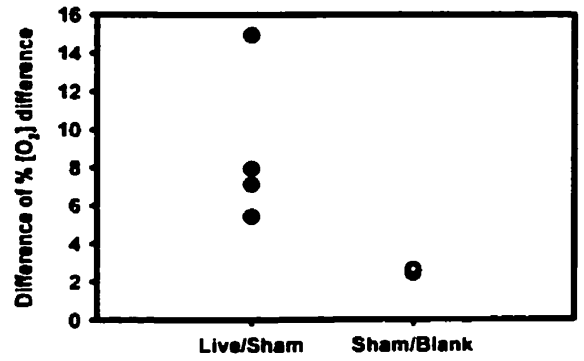

Figure 4.39 Summary of the difference between % [O_2] difference of live *vs* sham and sham *vs* blank samples from all experiments.

At this point, it might be inferred that there is a certain range of the numbers in the parameters to be considered live or dead. Within these ranges, there is some variation which is acceptable since the difference of the parameters between live and sham samples was high compared to that of the sham and blank samples. These variations might come from some uncontrolled factors such as the change in the ambient temperature over 24 hours, the change in barometric pressure (even within the time of calibration of the oxygen probe and measurement, approximately 20 minutes/measurement/sample).

The oxygen electrode was calibrated in water-saturated air before measuring the oxygen concentration in the buffer above the skin in diffusion cell. Normally, the response time of the oxygen electrode is less than 30 seconds when going from oxygen free to air-saturated water but a response time of up to 90 seconds may occur if the temperature of the sample is 5 to 10°C different from the air temperature (from the instruction manual of the oxygen electrode). In this experiment, the electrode was calibrated at ambient temperature but measured at about 28°C (within 10°C difference) hence the data from 100 to 600 seconds was selected to use for the determination of the slope of the linear regression.

Typical curve characteristic is shown in Figure 4.35. The sharp decline in the oxygen concentration at the beginning of the measurement was the equilibration of the electrode once it was placed in the bore of the top part of the diffusion cell. Then the oxygen concentration increased to a "flat" peak and started to decline again in the linear manner. The difference of the oxygen concentration between this "peak" and at the 600th seconds was used as a parameter to compare the viability of the samples. The oxygen concentration in the medium was always declining which means that the back diffusion of oxygen into the system is negligible, similar to the results from the system of Zieger et al.

(1993).

The diffusion cell experiment was conducted under a semi-sterile environment. The fresh skin samples were obtained under sterile conditions (in the operating room) and were collected in a sterile buffer. The frozen skin was thawed and washed in sterile buffer just before placing in the diffusion cells. The skins were handled in a sterile environment until the start of the permeation study. The buffer was sterile and the diffusion cell and the tubing were continuously washed with sterile water at least for 10 hours before starting the experiment. The buffer, in which the measurement was done, was pipetted out after each measurement. With these precautions in sample handling, microbial contamination is considered minimal and should not contribute to any significant difference of the results.

The oxygen concentration-time curves in the experiment of Zeiger et al. (1993) were exponential between the 100^{th} and 600^{th} seconds but those in this experiment were straight lines. This might be due to the difference in designing of the small environment where the oxygen probe was during the measurement. The size and thickness of skin samples in their experiment was much smaller than those used in this experiment. Therefore the buffer completely covered the whole skin sample in their experiment while only a portion of the skin sample was covered by the HHBSS in this study. Full thickness skin was used in this experiment and the oxygen concentration was measured in the buffer on top of the skin on diffusion cell. Skin oxygen consumption rate is the function of all cells and cell types within the tissue. It depends on the number of respiring cells and the level of the respiration of all cells in the tissue, or the combination of both. The quantity of the skin and the volume of the medium must be optimized to achieve appropriate range of values which can distinguish the live and dead samples without stirring the medium during the measurement.

With the nature of the experiment, measurement of skin oxygen consumption during permeation study, larger piece of skin is required. As a result, higher variation occurred from biological variation of the skin itself (even from the same source and anatomical site) and from the variation of the number of cells in each piece. The latter could be controlled by the uniformity of the exposed surface area of the top part of the diffusion cells to the skin sample and the medium.

Although noninvasive, the measurement with a transcutaneous oxygen electrode requires steady contact with the skin during measurement (after the first calibration) which makes it unsuitable to measure the oxygen concentration of skin samples in 6 diffusion cells in a timely manner. Moreover, measurement with transcutaneous oxygen electrode must be done at 44°C which is quite higher than 32°C (normal skin surface temperature) and it might damage the skin samples if the measurement is to be conducted for 24 hours. Intracutaneous measurement of oxygen with a fine needle electrode is invasive and not suitable for repeated measurements over time.

This method measures oxygen consumption of skin samples which reflects aerobic respiration hence viability of the skin. It is nondestructive, easy to perform, fairly reproducible and requires only simple instruments. No complex processing or radioactive compounds are required. Data analysis is also simple.

4.3.1.2 Confocal Laser Scanning Microscopy Study

In this study, two fluorescent probes; CAM and EthD-1, were used to evaluate the viability of intact human skin in diffusion cells. CAM, which is virtually nonfluorescent, permeated and was well retained within live cells. It was hydrolyzed by ubiquitous intracellular esterases to calcein which produced an intense uniform green fluorescence.

EthD-1 could not enter live cells but passed through the damaged membranes of dead cells. Upon binding to nucleic acids, it underwent a 40-fold enhancement of fluorescence and produced a bright red fluorescence . The viability of tissue was quantified by comparing the light intensities of both probes in the samples to those in the live and dead controls.

4.3.1.2.1 Optimal Staining Protocols

The optimum staining protocol for thick sections is as follows:

Skin samples were washed in 3% BSA solution in normal saline 3 times. They were incubated in 10 μM EthD-1 in 1% PBS at 37°C for 20 minutes then in the mixture of 10 μM EthD-1 and 4 μM CAM in 1% PBS at 4°C for 90 minutes. The samples were washed in normal saline 3 times then hydrolyzed in normal saline for at least 10 minutes before being examined with CLSM.

The optimum staining protocol for 100-μm sections is as follows:

Skin sections were washed in 3% BSA solution in normal saline 3 times. The sections were incubated in 10 μM EthD-1 in 1% PBS at 37°C for 10 minutes then in the mixture of 10 μM EthD-1 and 4 μM CAM in 1% PBS at 4°C or room temperature for 45 minutes. The samples were washed in normal saline 3 times then hydrolyzed in normal saline for at least 10 minutes before being examined with CLSM.

A lot of non-specific staining of calcein was found which could come from the hydrolysis of CAM by leached esterases from damaged cutting surface of the skin samples. However, this could be reduced by washing the sample in 3% BSA before staining with the fluorescent probes. Moreover, the background fluorescence was deducted from the calculation of the intensity values of the probes. Example of two dimensional confocal images of live control, dead control, and skin sample from diffusion cell are presented in

Figure 4.40.

Figure 4.40 Two dimensional confocal images of tissue samples

A) Dead control biopsy showing part of the epidermis (white arrow) and the dermis. The intense red stain is produced by ethidium homodimer-1.

B) Magnified image of the boxed region shown in panel A. The structure of the dermis appears less dense than in normal tissue.

C) Live control biopsy showing intense green staining due to calceine. The epidermis appears as a wavy line (white arrow). The rest of the stained region is the dermis.

D) Enlargement of boxed area in panel C shows areas of overlap with the two dyes (yellowish appearing cells).

E) Example of a skin sample from a diffusion cell after a 24-hour experiment. The yellowish-orange areas are regions of overlap between the dyes.

F) Magnified image of the boxed region in panel E showing regions of overlap as well as healthy (pale green) and necrotic (pale red) foci (see arrows). The structure of the tissue appears quite fibrous.

Scale bars for panels A, C, E are 200 μm

Scale bars for panels B, D, F are 50 μm.

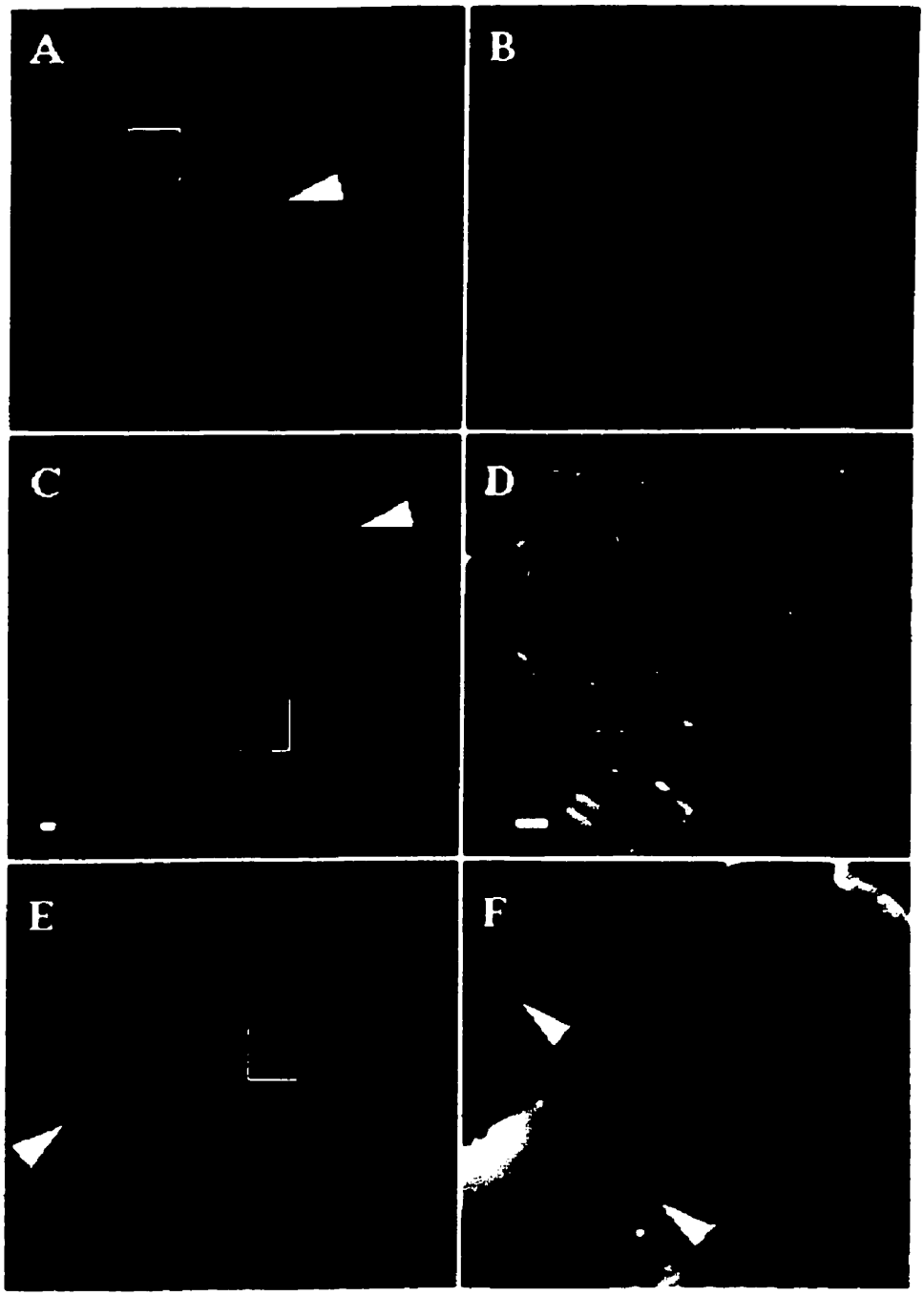
A
B
C
D
E
F

4.3.1.2.2 Effect of Scan Depth and Tissue Thickness on the Light Intensities of Probes in the Skin Samples

This experiment utilized the ability of CLSM to obtain dual-channel optical section inside the skin (avoiding the damaged cut surface), combined with the mechanical cross-sectioning of the skin sample to expose different layers of the skin for scanning by the CLSM at the same depth, hence providing better assessment of the results. Sample thickness is an important factor because the tissue must be sufficiently thin to permit penetration of the laser light. How deep one can scan and still obtain useful information depends on the instrument used, the quality of the objective lens of the microscope, the working distance of the lens used and the absorbance of the light in the tissue sample.

From the scan depth and tissue thickness results in Figure 4.41 and Tables 4.17 and 4.18, CLSM could distinguish live samples from dead samples regardless of the thickness of tissue or the scan depth used in this experiment. Scan depth from 5 to 100 μm had no significant effect on the CLSM results except for the epidermis of thick samples where it could distinguish between live and dead samples at the same scan depth.

Thick samples were sufficient for viability evaluation and the sample preparation time was much shorter compared to the 100-μm samples. However, the 100-μm sections provided better detailed image because they were more transparent and more uniform in thickness. Thickness uniformity is important in order to be less subjective during the analysis of the fluorescent intensities of the probes.

Figure 4.41 Two dimensional confocal images of live and dead skin samples: scan depth and tissue thickness effect.

Panel 1 - Live, thick (200-400 μm) sample; Panel 2 - Dead, thick (200-400 μm) sample;

Panel 3 - Live, 100-μm sample; Panel 4 - Dead, 100-μm sample.

Each sample was scanned at the following depths:

A - 5 μm; B - 10 μm; C - 20 μm, D - 40 μm; E- 80 μm; F - 100 μm.

Scale bars are 500 μm.

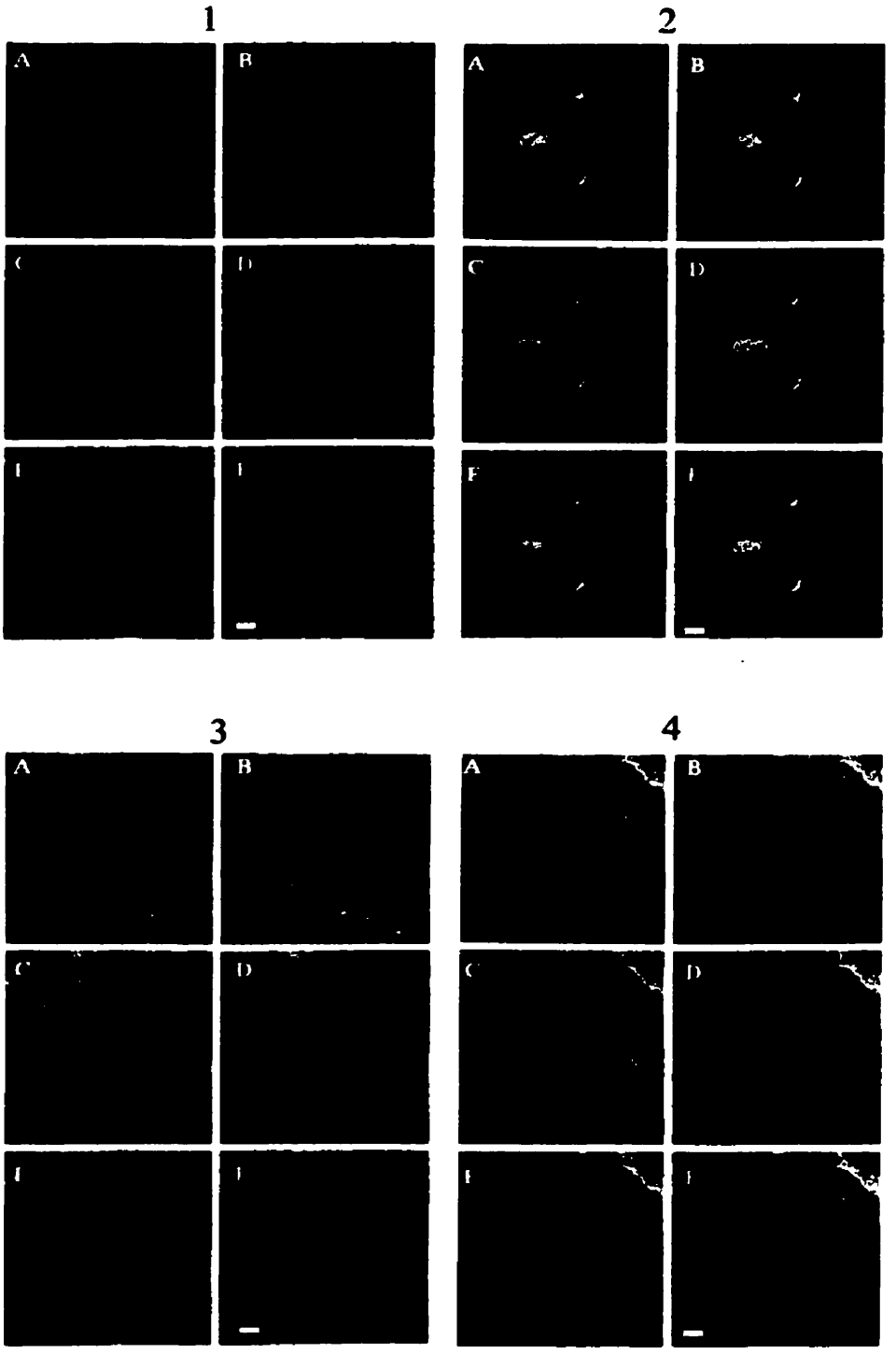
1
2
3
4
A
B
C
D
E
F

Table 4.17 Live/dead differential staining of the epidermis : Scan depth and thickness of section[a].

Scan depth (μm)	Thick (200- to 400-μm) section		100-μm section	
	Live[**]	Dead	Live[*]	Dead
5	1.703 ± 0.184	1.067 ± 0.150	1.350 ± 0.330	0.940 ± 0.127
10	1.693 ± 0.192	1.073 ± 0.143	1.307 ± 0.303	0.947 ± 0.130
20	1.690 ± 0.195	0.947 ± 0.054	1.303 ± 0.278	0.947 ± 0.126
40	1.683 ± 0.182	1.063 ± 0.139	1.347 ± 0.323	0.937 ± 0.119
80	1.687 ± 0.188	1.070 ± 0.151	1.353 ± 0.334	0.937 ± 0.129
100	1.703 ± 0.199	1.077 ± 0.165	1.377 ± 0.352	0.940 ± 0.118

[a] Values represent mean ± SEM, n = 3 (one reading from 3 different sources).

[**] $p=0.0001$ when compared to respective dead sample.

[*] $p<0.05$ when compared to respective dead sample.

Table 4.18 Live/dead differential staining of the dermis : Scan depth and thickness of section[a].

Scan depth (μm)	Thick (200- to 400-μm) section		100-μm section	
	Live[**]	Dead	Live[**]	Dead
5	1.293 ± 0.124	0.900 ± 0.064	1.333 ± 0.277	0.927 ± 0.027
10	1.297 ± 0.127	0.897 ± 0.058	1.333 ± 0.264	0.930 ± 0.051
20	1.300 ± 0.127	1.010 ± 0.173	1.370 ± 0.311	0.937 ± 0.042
40	1.300 ± 0.133	0.897 ± 0.064	1.340 ± 0.271	0.937 ± 0.037
80	1.300 ± 0.130	0.893 ± 0.067	1.347 ± 0.277	0.927 ± 0.043
100	1.297 ± 0.130	0.890 ± 0.064	1.353 ± 0.283	0.927 ± 0.043

[a] Values represent mean ± SEM, n = 3 (one reading from 3 different sources).

[**] $p<0.0002$ when compared to respective dead sample.

none were significantly different regarding the scan depth or thickness of section.

4.3.1.2.3 Viability Results

Comparison of the live/dead differential staining of different skin samples is shown in Tables 4.17 to 4.19. CLSM can differentiate live and dead skin samples and the difference can be seen in both the epidermis and the dermis. As shown in Table 4.18, live skin samples survived on diffusion cells for 24 hours. Some viability loss could be interpreted in the dermis for the diffusion cell sample and the skin which was stored at 4°C in HHBSS for 24 hours. However, the differential staining of the diffusion cell sample was still significantly different from the dead control. The skin which was stored at 4°C in HHBSS for 24 hours did not show significant difference from the dead control or sham although the intensity ratios were similar to those of live control and diffusion cell samples.

Table 4.19 Live/Dead differential staining of 100-μm skin sample from diffusion cell after 24-hour experiment as compared to controls[a].

	Diffusion cell sample [b]	Live control [c]	Live 24h control [d]	Dead control [e]	Dead sham [f]
Epidermis	1.109±0.077*+	1.107±0.119*+	1.020±0.060	0.783±0.068	0.799±0.064
n	11	4	4	7	11
Dermis	0.933±0.046*	1.026±0.079*+	0.942±0.056	0.777±0.061	0.809±0.039
n	15	5	5	9	14

[a] values represent mean ● SEM. The scan depth was 5 μm from the cutting surface.

[b] fresh skin sample on diffusion cell for 24 hours.

[c] fresh skin, processed within 7 hours from surgery.

[d] live control sample which was stored in HHBSS at 4°C for 24 hours.

[e] 5- to 16-month old skin, stored at -20°C until used.

[f] dead control sample subjected to 24-hour experiment on diffusion cell.

* $p<0.05$ when compared to respective dead control.

+ $p<0.05$ when compared to respective dead sham.

The use of fluorescent probes with CLSM for the evaluation of cell viability has been described, for example, simultaneous staining with fluorescein diacetate and propidium iodide to assess viability of mice spleen cell suspensions (Jones and Senft, 1985). Boderke et al. (1997) used propidium iodide to check the dead or dying cells (viability control) in the experiment to localize enzyme aminopeptidase activity in freshly excised human skin. However, there was no live probe control in this experiment and the aminopeptidase activity was used to imply the activity of the live cells instead. CAM and EthD-1 combination was developed for use with eukaryotic cell types, including adherent cells and certain tissues. The applications include measurement of cytotoxic effects of compounds, proteins, etc., quantitation of apoptotic cell death and cell-mediated cytotoxicity (Molecular Probes, Inc., 1996; Moore et al., 1990). Applications to animal and human tissues include the investigation of viability, morphology and organization of keratocytes in intact living cornea (Poole et al., 1993), viability assessment of excised rabbit corneas (Imbert and Cullander, 1997) and porcine buccal mucosa (Imbert and Cullander, 1999). In this study, CAM and EthD-1 were successfully applied in the viability evaluation of intact excised human skin in diffusion cells.

Oxygen consumption measurement and CLSM methods described in this experiment can distinguish live and dead samples. Combination of the results from both methods provides another means of evaluating the viability of skin samples on diffusion cells during permeation study. This is particularly important for compounds which are highly metabolized in the skin.

4.3.2 Metabolism of Methyl Salicylate During Permeation Study in Diffusion Cells

Results from the percutaneous absorption of MS through human breast skin in diffusion cells are shown in Table 4.20 and Figure 4.42. Most of MS was recovered in the wash (96-98% of the applied amount). Absorbed MS was found mainly in the skin and was found slightly more in viable skin than in the 60°C treated skin but it was not statistically significant ($p>0.05$). Only 12% of the absorbed amount was recovered in the percutaneous fractions from viable skin while 27% was found in the fractions from the 60°C treated skin. This is because MS was hydrolyzed to SA in viable skin at higher extent than in the 60°C treated skin.

Results from the metabolism studies of MS to SA in human breast skin in diffusion cells are shown in Figure 4.43 and Table 4.21. From Table 4.21, SA amount recovered in the percutaneous fractions and skin was significantly higher in viable skin than in the 60°C treated skin ($p<0.0001$). However, when calculated as the percentage of SA recovered amount in the skin and in the percutaneous fractions, there was no significant difference between the viable and the 60°C treated skin. This can be explained that the permeation of SA is determined by a diffusion process, i.e. the diffusion rate of SA is the same in both viable and 60°C treated skins. The only difference is the metabolism rate and extent of MS which generates SA.

In the study conducted by Boehnlein et al. (1994), radioactivity assay was used to quantitate the analytes and SUA was found only in viable skin. In this study SUA was not found. This might be due to the lower sensitivity of the assay. However, the difference in the amount of SA recovered between the viable and the 60°C treated skin was significantly high enough to tell the difference between both skins.

Table 4.20 Percutaneous absorption of methyl salicylate (MS) in human breast skin in diffusion cells[a]

	MS amount recovered (μg)			% of recovered amount			% of absorbed amount		
	Viable skin	60°C treated skin	skin stored at -20°C[b]	Viable skin	60°C treated skin	skin stored at -20°C[b]	Viable skin	60°C treated skin	skin stored at -20°C[b]
Fractions[c]	24.6 ± 5.8	87.1 ± 19.5*	6.5	0.24 ± 0.06	1.20 ± 0.27*	0.10	11.8 ± 3.3	26.9 ± 6.1*	5.6
Skin	196.1 ± 18.9	209.0 ± 16.5	110.6	1.93 ± 0.17	2.73 ± 0.22*	1.74	88.2 ± 3.3	73.1 ± 6.1*	94.4
Wash[d]	9888 ± 145	7416 ± 278*	6246	97.83 ± 0.17	96.07 ± 0.34*	98.16	N/A	N/A	N/A

[a] Values are mean ● SEM, n = 3 with 4 replicates each

[b] n = 1

[c] 0-24 h fractions were combined

[d] wash combined with recovered cream after 24 h experiment

* significantly different from the paired viable skin at $p<0.05$ using 2 tailed, paired t-test

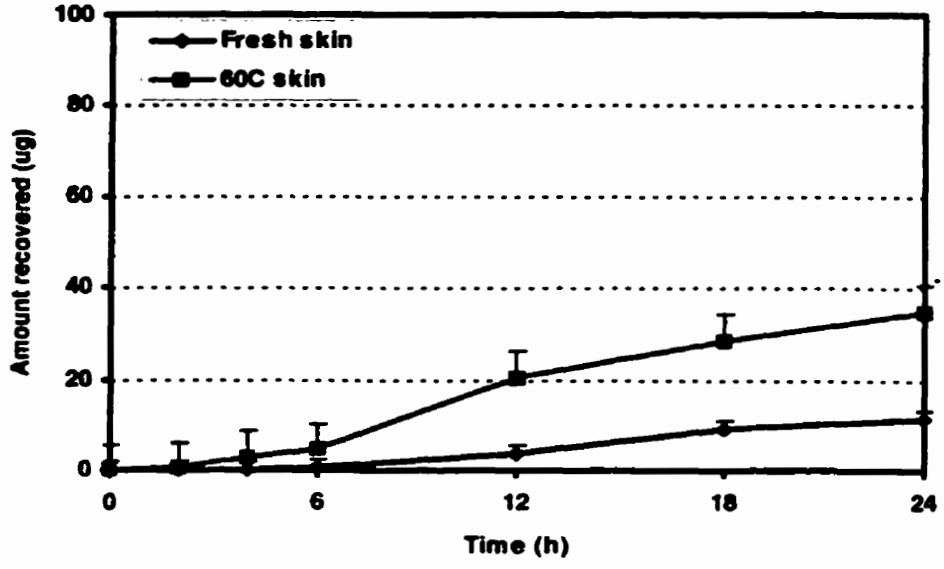

Figure 4.42 Methyl salicylate recovery in the percutaneous fractions through excised human breast skin in diffusion cells (n = 3, with 4 replicates each).

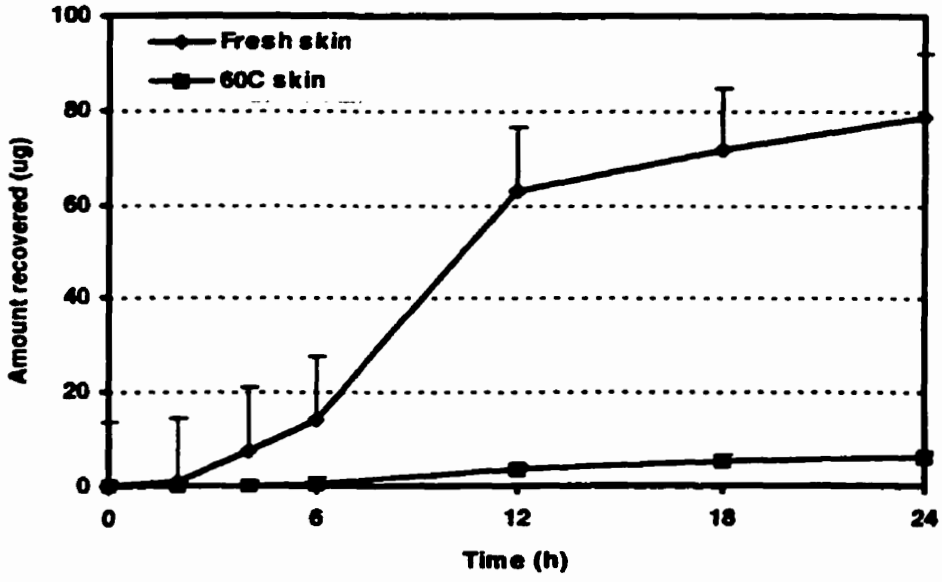

Figure 4.43 Salicylic acid recovery in the percutaneous fractions through excised human breast skin in diffusion cells (n = 3, with 4 replicates each).

Table 4.21 Metabolism of methyl salicylate in human breast skin in diffusion cells[a]

	Salicylic acid amount recovered (μg)			% of recovered amount		
	Viable skin	60°C treated skin	skin stored at -20°C[b]	Viable skin	60°C treated skin	skin stored at -20°C[b]
Fractions[c]	235.4 ± 26.4	15.4 ± 4.5*	393.8	63.3 ± 5.1	51.9 ± 8.8	72.6
Skin	134.9 ± 19.0	9.4 ± 1.4*	148.9	36.7 ± 5.1	48.1 ± 8.8	27.4
Wash[d]	0 ± 0	0 ± 0	0	N/A	N/A	N/A

[a] Values are mean ± SEM, n = 3 with 4 replicates each

[b] n = 1

[c] 0-24 h fractions were combined

[d] wash combined with recovered cream after 24 h experiment

* significantly different from the paired viable skin at $p<0.05$ using 2 tailed, paired t-test

Total recovery of MS was about 50% of the amount applied. Evaporation of MS was the main reason despite the fact that the diffusion cells were well covered with Parafilm during the experiment. However, with the amount of MS applied (100 mg of 20% w/w MS in Glaxal base), infinite dose was maintained. This could be seen from the amount of MS recovered in the wash (which includes recovered cream after 24 h experiment).

Regarding the effect of temperature on esterase activity, considerable reduction in esterase activity from the exposure to 60°C heat was again demonstrated. According to Wester et al. (1998), exposure to 60°C temperature resulted in skin viability loss. This occurred during the process of heat separation of the skin layers. On the other hand, esterase activity appeared to be preserved at low storage temperatures. In an MS diffusion cell experiment, the skin which was stored at -20°C for 17 days exhibited high esterase activity. As shown in Table 4.22, only 5.6% of MS absorbed was recovered in the percutaneous fractions from the skin which was stored at -20°C while 12% and 27% were recovered from viable skin and the 60°C treated skin, respectively. From Table 4.23, SA amount recovered in the percutaneous fractions from the skin which was stored at -20°C was comparable to (or even higher than) those recovered from the viable skin. This suggests that esterase activity was preserved in frozen skin. MS might even be metabolized at a higher extent in previously frozen skin than in the viable skin because freeze-thaw process might damage the skin cells and exposed esterases inside the cells. In a pilot study, MS metabolism in human skin homogenate which was made from frozen skin (stored at -20°C) also demonstrated high esterase activity (Table 4.7). Skin homogenate which was thawed and stored at 4°C for 1 month still showed good esterase activity although not as much as freshly thawed skin homogenate.

Among many percutaneous absorption and metabolism studies of ester-type drugs and prodrugs using excised skin from animals and humans, only a few used the experimental conditions which maintained the skin viability during permeation and found the difference in the metabolism between viable and non-viable skins. For example, MS absorption and metabolism in hairless guinea pig skin (Boehnlein et al., 1994). In most investigations the skin viability was not maintained because improper receptor fluid was employed (such as normal or physiological saline, phosphate or acetate buffers, 20% ethanol in water), sometimes in combination with the use of non-viable skin (previously frozen or rehydrated frozen skins). However, hydrolysis still occurred. The length of the experiments ranged from 6-10 hours (Liu et al., 1990; Nacht et al., 1981; Ahmed et al., 1996), 24 hours (Seki et al., 1990; Sato and Mine, 1996; Cross et al., 1998), 40 hours (Potts et al., 1989), 60 hours (Stinchcomb et al., 1996) to 90 hours (Johansen et al., 1986). When PBS with 0.1% (w/v) glucose was used as the receptor fluid, rat skin viability decreased steadily from the beginning of the experiment and was diminished after 12-15 hours as per $^{14}CO_2$ detection and lactate formation results (Collier et al., 1989). If distilled water was used as the receptor fluid, human scalp skin was essentially non-viable after 5 hours (Cornwell et al., 1997) and hairless guinea pig skin viability was abolished within 1 hour (Nathan et al., 1990) as detected by lactate formation. Therefore, it is assumed that skin viability was not maintained in those experiments. Still, hydrolysis took place. Esterases are relatively stable enzyme and can function in nonliving cells such as the cells in the stratum corneum. Moreover, degradation occurred in non-viable skin and this process might cause different localization of enzymes in the skin (Nathan et al., 1990). Bundgaard et al. (1983) found that, during a permeation experiment, the hydrolytic enzyme activity in the

receptor phase remained constant for at least an additional 70 hours after completion of leaching from the excised skin into the receptor fluid (which took about 20 hours). Therefore, results from ester hydrolysis in the skin during permeation study must be interpreted cautiously. While ester hydrolysis in skin may be valid qualitatively, quantitation of the rate and extent of the bioconversion must be carefully interpreted.

The importance of skin viability maintenance during percutaneous absorption study was more pronounced in other enzyme systems such as the oxidation of estradiol and testosterone in female fuzzy and Osborne-Mendel rat skins (Collier et al., 1989), the *N*-acetylation of benzocaine in hairless guinea pig skin (Nathan et al., 1990). Even in human skin homogenates, glucose-6-phosphate dehydrogenase activities reduced by half when the experiment was carried out with human skin homogenates which were stored at -30°C overnight (Raab and Gmeiner, 1976).

4.4 Localization of Esterases in Human Skin

Skin samples, fixed in formalin solution, from the viability studies on diffusion cells were submitted to the Department of Pathology for morphology and staining for esterases.

The morphology results from paraffin sections stained with hematoxylin and eosin (H&E) in Figure 4.44 revealed subtle difference between fresh skin, skin which was kept in HHBSS at 4°C for 24 hours, and skin samples on diffusion cells with the fresh skin being in the best condition, followed by the 4°C skin and the skin on diffusion cells. Frozen skin showed some deterioration but still stayed intact, while shams showed edematous and autolyzed cells and separation between the epidermis and the dermis. This might result from the freezing process and aggravated by treatment on the diffusion cell for 24 hours. Although the morphology result using H&E staining showed some difference between the

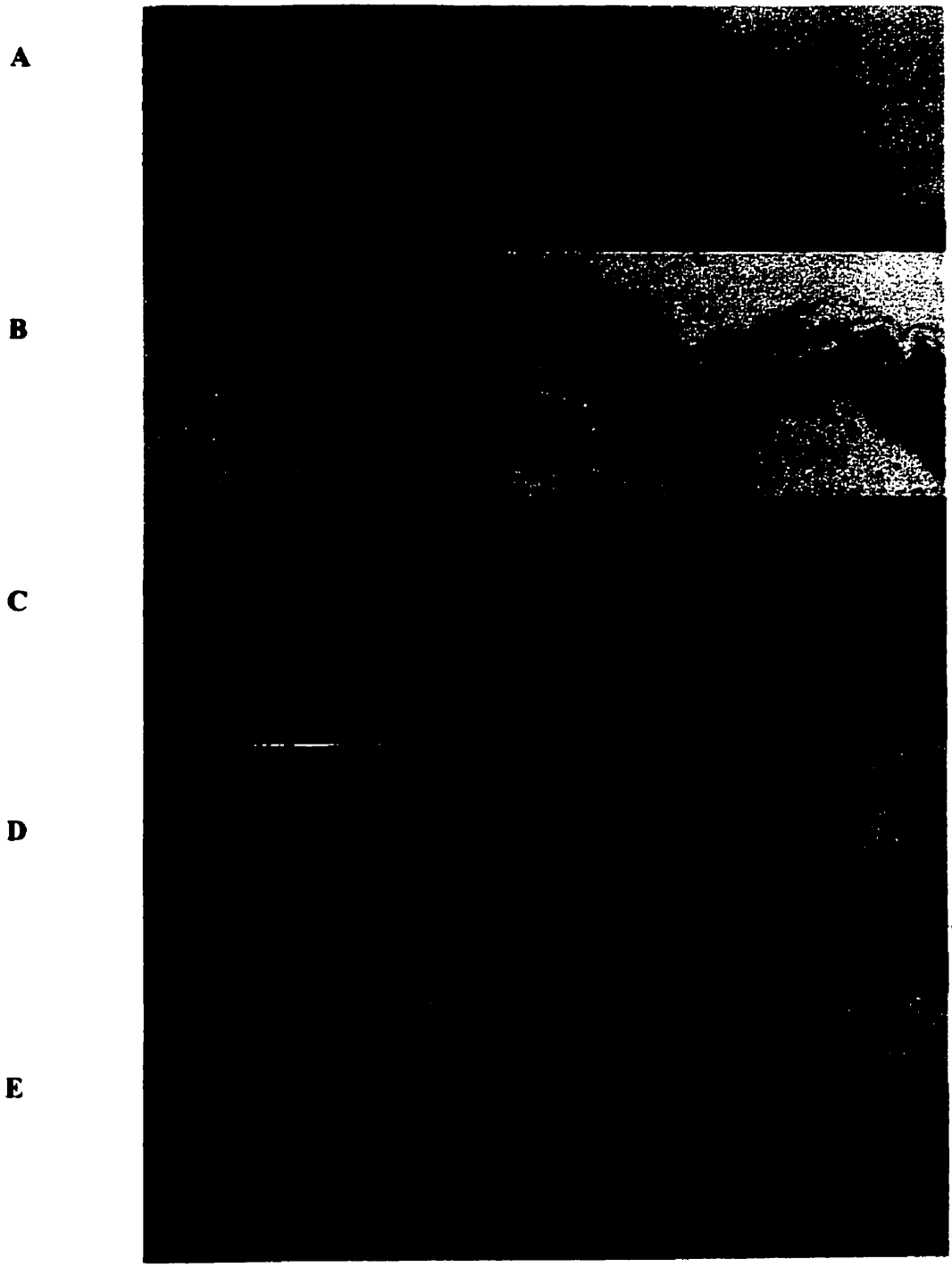

Figure 4.44 H&E staining results from diffusion cell experiment; (A) fresh skin, (B) fresh skin after 24 h on diffusion cell, (C) fresh skin kept at 4°C for 24 h, (D) previously frozen skin, (E) sham (previously frozen skin after 24 h on diffusion cell). Magnification x 100.

live and previously frozen skins in this experiment, it is not conclusive since the freezing process might introduce an artifact.

Figures 4.45 and 4.46 show the NSE staining results of fresh skin sample, live skin on diffusion cell, skin which was kept in HHBSS at 4°C for 24 hours, sham and frozen skin sample. Weak to moderate positive NSE activity was found as a band between the stratum granolosum and the stratum corneum in the epidermis of fresh skin sample, live skin on diffusion cell and 24 hours skin kept at 4°C in HHBSS. Moderate to strong positive NSE activity was found staining the fibroblasts in the dermis. Frozen skin sample also showed strong positive NSE staining in the fibroblasts in the dermis but weak and patching positive staining in the epidermis. Shams showed weak positive and diffused pattern in the epidermis and also weak positive staining in the fibroblasts in the dermis. Pearse et al. (1986) showed that NSE activity in normal human subjects was found exclusively in the stratum granulosum and the enzyme density decreased towards the basal layer. Treatment with etretinate (an aromatic retinoid) significantly increased the NSE activity. Betz (1994) reported that NSE activity in normal human skin was found as a band-shape but weak positive staining between the stratum granulosum and stratum corneum while strong reactions were shown in skin appendages such as the sheath of hair roots, hair follicles, sweat glands as well as the musculi arrectores pilorum and dermal fibroblasts. A clear increase in NSE activity of dermal fibroblasts was first detectable in a vital skin wound aged 1 hour and positive results were found in 40% of the cases with a post infliction interval between 1 hour and 5 days. However, postmortem induced injuries showed no increased activities. Contrarily, there were reports of possible postmortem increase in the activity of NSE (Dachun and Jiazhen, 1992; Pioch, 1969). Yoshimura and Mori (1970)

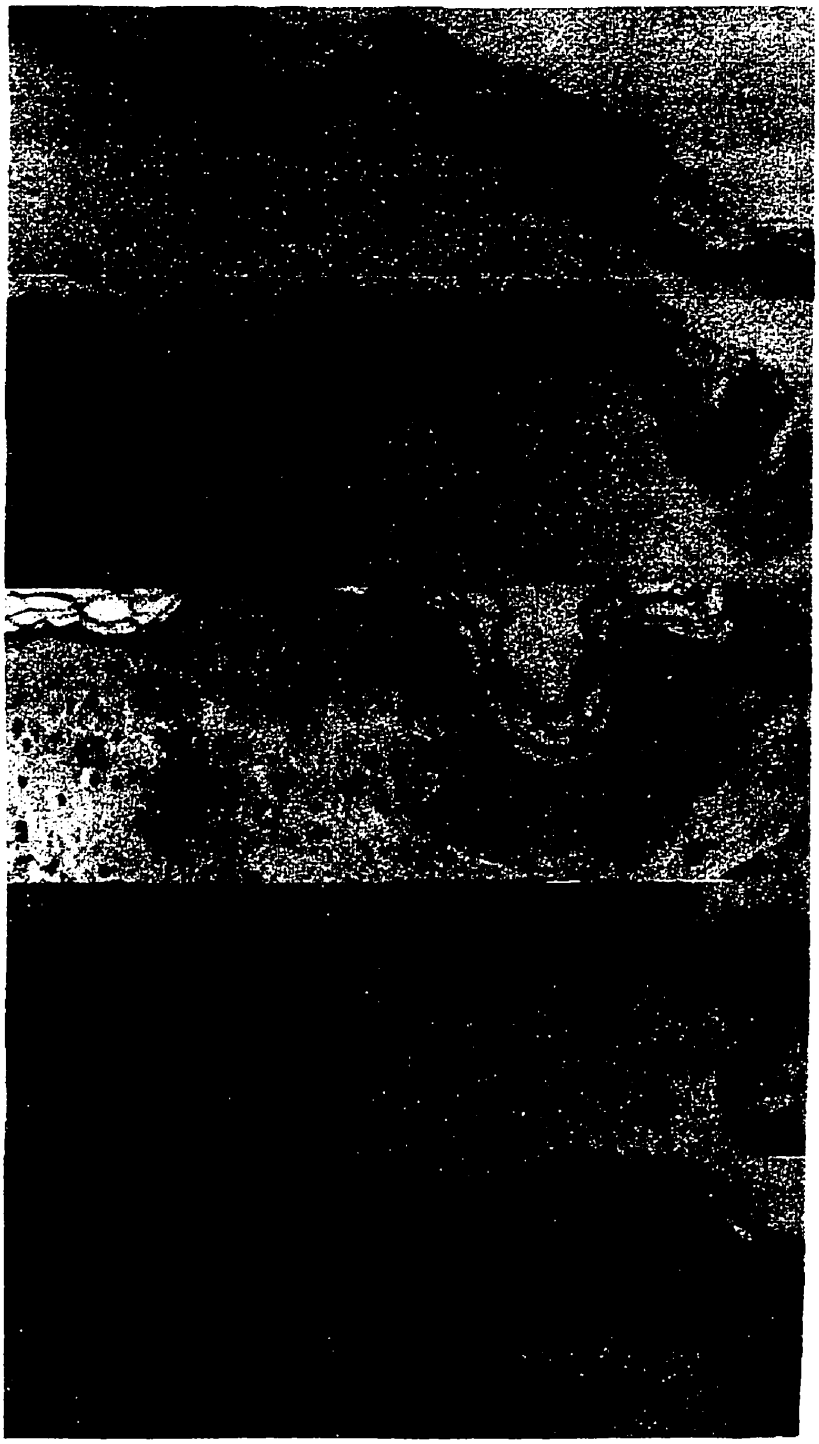

Figure 4.45 NSE staining results from diffusion cell experiment; (A) fresh skin (x 100), (B) fresh skin after 24 h on diffusion cell (x 100), (C) fresh skin kept at 4 °C for 24 h (x200), (D) previously frozen skin (x 100), (E) sham (previously frozen skin after 24 h on diffusion cell) (x200).

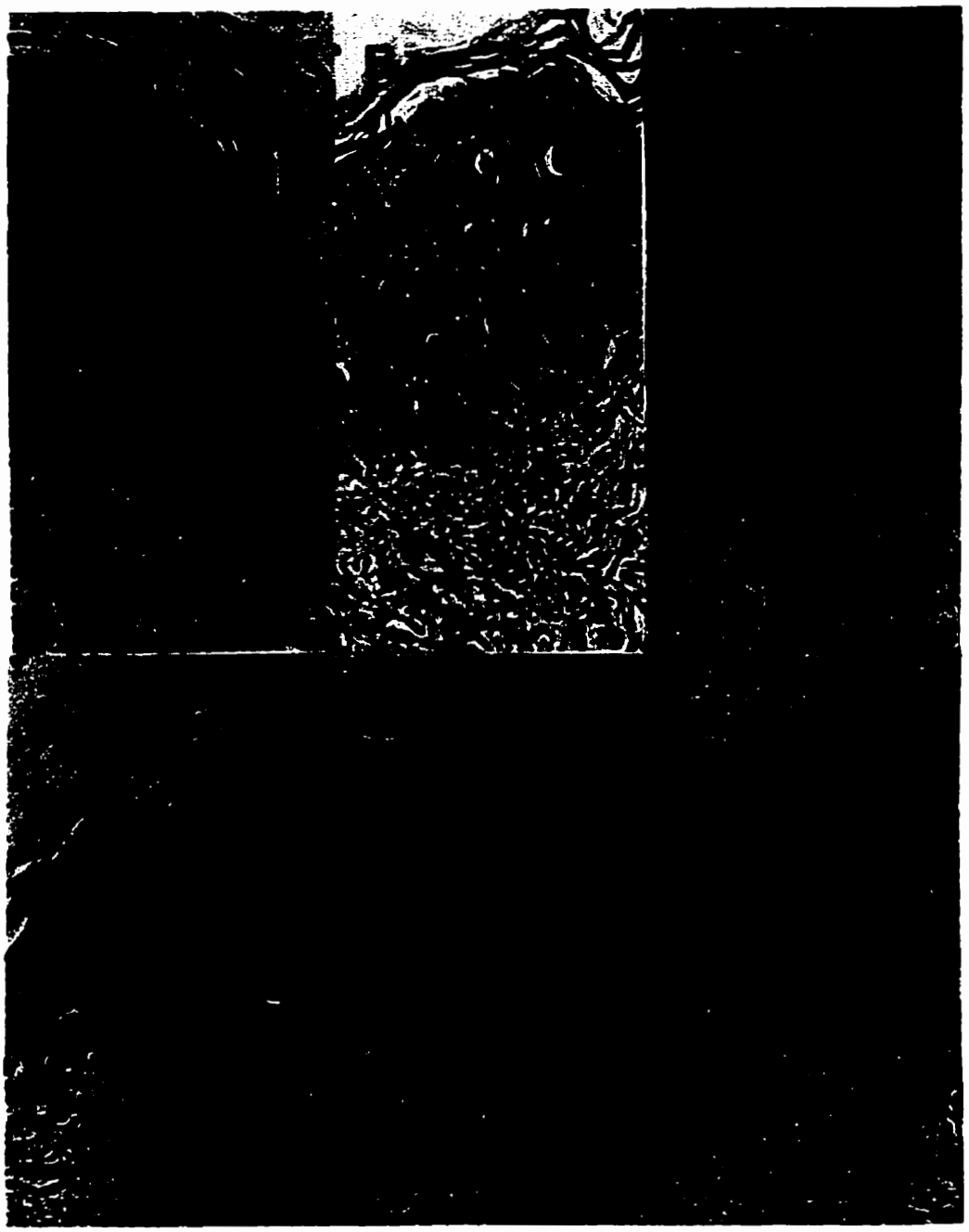

Figure 4.46 NSE staining results from diffusion cell experiment (x 400); (A) fresh skin, (B) fresh skin after 24 h on diffusion cell, (C) fresh skin kept at 4°C for 24 h, (D) previously frozen skin, (E) sham (previously frozen skin after 24 h on diffusion cell).

described a strong NSE activity in the basal cell and granular cell layers but no activity in the cornified layer of normal mouse skin. NSE activity was also found in the epithelial appendages and subepithelial connective tissue fibres.

CHAPTER FIVE

CONCLUSIONS

The goal of this study is to develop a viable *in vitro* skin model for the assessment of cutaneous delivery and metabolism of ester type compounds. Several steps were taken to characterize the model.

A sensitive reversed phase ion-pairing HPLC assay was developed to simultaneously analyze tetracaine (TC) and its metabolite (4-BABA). Several factors were varied during the method development to achieve optimal analysis conditions. Factors affecting HPLC analysis in this system were the type of the HPLC column, pH of the mobile phase, the composition of the mobile phase, the concentration of the ion-pairing reagent, salts/buffer components, temperature and flow rate. The need for sensitive analytical method arose from kinetic study of TC hydrolysis in human skin homogenate. Since TC had a very low K_m (11-28 μM range, from this study) and also showed substrate inhibition, the kinetic study had to be carried out from very low initial substrate concentrations and cover appropriate range of initial substrate concentrations. Therefore, a very sensitive analytical method had to be used to analyze the samples from these experiments. The optimal condition of the HPLC method 2 in this study used the Waters 2690 Separations Module, with 996 diode array detector module and Millennium® system control and data acquisition software (Waters Corporation) HPLC system. The column used was a Luna™ 4.6 x 150 mm, 5 μm ODS column with a 4.6 x 30 mm guard column

was a Luna™ 4.6 x 150 mm, 5 μm ODS column with a 4.6 x 30 mm guard column (Phenomenex, Torrance, CA, USA) or a SymmetryShield™ RP18, 3.9 x 150 mm, 5 μm column with a 3.9 x 20 mm, 5 μm guard column (Waters Corporation). The column temperature was controlled at the ambient temperature. The mobile phase was ACN : MeOH : 2.5 mM HSA in water (20:55:25), flow rate 1 mL/min and detection by UV absorbance at wavelength 310 nm. This method provided LODs of 0.3 ng and 0.5 ng for TC and 4-BABA, respectively. The LOQs for TC and 4-BABA were 10 ng and 5 ng, respectively. The linear regression was obtained in the range of 10 - 120 ng for TC and 5 - 60 ng for 4-BABA with good accuracy and precision. The sample preparation method for the analysis was simple. ACN was mixed with an aliquot of skin homogenate in order to simultaneously precipitate proteins and extract the compounds in the skin homogenate, followed by centrifugation. The supernatant was then directly injected to the HPLC. This method is sensitive enough for a kinetic study of TC in human skin homogenate. More sensitive assay may be achieved with more sensitive methods such as gas chromatography, mass spectrometry, and radioactivity assays provided the instruments and/or resources are available.

Excised intact human skin in diffusion cells was used to evaluate cutaneous delivery and metabolism of methyl salicylate (MS). The viability of the skin must be maintained in order to correctly determine the metabolism of compounds in the skin during percutaneous absorption. Two methods to assess viability during diffusion cell study were developed; oxygen consumption measurement and confocal laser scanning microscopic (CLSM) methods. Both could distinguish between live and dead skin samples. In this investigation, the procedure used to conduct metabolism and permeation study in diffusion cells could

maintain the viability of fresh skin for 24 hours. The features of this viable *in vitro* excised skin model as well as the instrumental setup and the factors to be controlled are summarized as follows:

The diffusion cell system was the flow-through type. The receptor fluid was sterile HHBSS, pH 7.4, gassed with oxygen and maintained at 37°C. The perfusion rate was 3.5 mL/h. Fresh skin from surgery must be stored in sterile HHBSS, on ice, during the transportation and handling of the skin and to be processed as soon as possible (within 7 hours from surgery in this study). The excised and cleaned skin was cut to appropriate size and mounted, epidermis side up, in the diffusion cells with were maintained at 37°C but yielding the skin surface temperature of about 32°C. The preparation of the model compound was applied and the receptor fluid was collected at time intervals and analyzed. At the end of the experiment, the skins in the diffusion cells were retrieved, washed and analyzed. The viability assessment could be done along side the permeation and metabolism study using oxygen consumption measurement. Two more diffusion cells with the top part which accommodates the oxygen probe could be set up with fresh skin as the live control and frozen skin as the sham. At any time during the experiment, sterile HHBSS 300-400 µL could be pipetted into the bore of the top part of the diffusion cell and let equilibrated for 5 minutes. The calibrated oxygen probe, which is connected to a pH/ion meter, could then be inserted into the bore and the oxygen concentration in the HHBSS above the skin could be measured. The pH meter is linked to a computer to collect data on file. The collected data could be processed in a spreadsheet program. The two parameters, the slope of the linear regression using data from 100 to 600 seconds (process 1) and the difference between the oxygen concentrations at peak of the graph and at the 600th second (process 2),

could be derived and compared to those of the live and sham samples (Tables 4.13 and 4.14). It is better to have both live and sham controls in this case as there is some variation in the absolute values of the oxygen concentration in each day. However, the difference in the oxygen concentration values between live and sham samples in the same day was normally very high. At the end of the experiment both control skin samples could be processed for the CLSM. Then the intensity ratio of calcein to EthD-1 could be compared to those of the live and sham samples (Table 4.19). If the intensity ratio is in the 1.0 range for the dermis and 1.1 range for the epidermis, then it could be assumed that the skin is viable up to that time of the experiment. Should the intensity ratio falls below 0.8, it could be assumed that the skin is non-viable.

The oxygen consumption measurement method was simple, nondestructive, economical and fairly reproducible. No complex instrument, processing method or radioactive compounds were required. The measurement can be done over and over at any time during the experiment. However, the experimental conditions must be optimized prior to being utilized in the viability assessment experiments. Once optimized, the experimental procedure and data analysis were simple.

CLSM is a new alternative for skin viability assessment. Its optical sectioning ability enables visualization of deeper layers in the skin without mechanical damage to the sample. Fresh skin can be examined without pre- freezing or embedding which could alter the viability status of the sample. Two fluorescent probes (live and dead) were required as well as the confocal laser scanning microscope. The viability of a skin sample can be assessed only once by this method.

The morphology results from hematoxylin and eosin (H&E)staining revealed subtle difference between fresh skin, skin which was kept in HHBSS at 4°C for 24 hours, and skin samples on diffusion cells with the fresh skin being in the best condition, followed by the 4°C skin and the skin on diffusion cells. Frozen skin showed some degradation but still stayed intact while shams showed edematous and autolyzed cells and separation between the epidermis and the dermis. From the enzyme histochemical study, weak to moderate nonspecific esterase (NSE) activity was found as a band between the stratum granulosum and stratum corneum in the epidermis of fresh skin sample while moderate to strong NSE activity was found in the dermis. Shams showed weak positive and diffused pattern in the epidermis and also weak positive staining in the fibroblasts in the dermis.

MS was hydrolyzed to salicylic acid (SA) during absorption through human excised skin in diffusion cells. The extent of MS hydrolysis was significantly higher in viable skin than non-viable skin (the same skin was exposed to 60°C temperature for 2 hours prior to the experiment). This also demonstrated that temperature was an important factor in the investigation of esterase activity. The extent of absorption of MS through full thickness human breast skin into the receptor fluid was 12% and 27% of the total MS amount absorbed for the viable skin and the 60°C treated skin, respectively. The extent of absorption of SA was 64% and 52% of the total SA amount absorbed in the viable skin and the 60°C treated skin, respectively (the difference was not statistically significant). This suggests that the permeation of SA through human skin was governed by a diffusion process and the diffusion rate of SA was the same in both viable and 60°C treated skins.

Human skin homogenate was selected as a comparative *in vitro* model to the excised skin model. Metabolism of two compounds were evaluated with this model; MS and TC.

At the initial concentration of 5 mM, MS did not have a substrate inhibition effect on esterases in human skin homogenate. The hydrolysis rate of MS in human skin homogenate was 72.31 nmol/h/μg protein. MS hydrolysis in phosphate buffered saline was very low. TC hydrolysis in human skin homogenate was not extensive due to substrate inhibition especially at clinical doses used for topical application. From the kinetic study of TC hydrolysis in human skin homogenate, K_m was in the 11-28 μM range and V_{max} was in the 2.0-2.8 μmol/h/μg protein range. Exposure to heat (60°C and higher) substantially reduced esterase activity in the skin homogenate even when the exposure time was as short as 2 minutes. Therefore caution must be taken in the preparation and handling of tissue samples during investigation involving esterases to make sure that esterase activity is preserved.

The human skin homogenate model is simpler than the viable excised skin model. The homogenate can be prepared once the fresh human skin sample is available then kept at -70°C until needed for the experiment without activity loss. However, harsh method is needed to homogenize the skin. Consequently, intact cells might be damaged and intracellular contents including esterases might be exposed. This might cause the over-estimation of skin hydrolytic activity. The selection of supernatant or certain portion of the skin homogenate after centrifugation at certain force can result in over- or under-estimation of the enzyme activity, depending on the portion which is selected. The skin structure is maintained in the viable excised skin model thus make it closer resemblance to the real situation than skin homogenate model.

The limitation of the viable *in vitro* model in this study is that the viability of the skin was maintained under the described conditions and was tested for 24 hours only. After being excised from the body, skin starts to degenerate. The rate and extent of the

deterioration depends on the treatment of the skin after the removal from the live body in order to maintain the skin viability. Any changes in the experimental conditions have to be justified and tested if necessary, to ensure that the skin viability is properly maintained.

CHAPTER SIX

SIGNIFICANCE OF FINDINGS

Although numerous percutaneous absorption studies have been conducted with many substances to understand the absorption of the compounds into and through the skin, only some of the studies emphasized metabolism in the skin. Among those studies, few paid attention to the viability of the skin during the experiment. In order to correctly determine the metabolism of compounds in the skin during percutaneous absorption study, viability of the skin must be maintained. In this study, the importance of skin viability in the *in vitro* excised skin model was demonstrated. Two new methods to assess viability during diffusion cell study were developed; oxygen consumption measurement and confocal laser scanning microscopic methods. Both were able to distinguish between the viable and non-viable skin samples in diffusion cells. This *in vitro* viable excised skin model is useful in the characterization of metabolism of compounds in the skin as one of the aspects to be considered in topical and transdermal drug development.

The HPLC method 2, which was developed in this study, enabled simultaneous determination of low amounts of TC and its metabolite in skin homogenates. Subsequently, enzyme kinetic parameters of TC hydrolysis in human skin homogenate were determined. Although the V_{max} and K_m of TC were reported in serum of human and animals and in purified pseudocholinesterase, these parameters in human skin homogenate were not

available before. Substrate inhibition of TC could be explained by the low K_m, hence high affinity of the substrate to the enzyme. This could be another reason for the long duration of action of topically applied TC. More important aspect would be the awareness of possible toxicity in persons with atypical or silent type of pseudocholinesterase should local anesthesia be needed.

CHAPTER SEVEN

RESEARCH PERSPECTIVE

Metabolism in the skin, although a slow process, does occur. This cannot be overlooked as it involves detoxification of compounds (typical and soft drugs), activation of some prodrugs and may generate toxic metabolites. Substrate inhibition can compromise the ability of the body to detoxify and eliminate toxic substances. In the worst situation, toxicity can occur with normally safe drugs if the person has enzyme deficiency, either inherited as the atypical and silent genotypes of cholinesterase enzyme or acquired by organophosphate poisoning, liver disease, or if the enzyme system is not fully developed. In case of local anesthetics of aminobenzoic derivatives, allergic sensitivity reactions were reported. On the other hand, compounds which are expected to show their effect after undergoing metabolism (such as hydrolysis) may not be activated to the extent needed for its therapeutic activity. This aspect should be taken into consideration in the development of new drug and drug delivery systems.

In vitro models have the advantages of simplicity, economy and speed over *in vivo* models. However, care must be taken in the interpretation of the data. A skin homogenate model can either over- or under-estimate the maximum metabolic rates as the structure of the skin is disrupted and the preparation process may lead to selection and/or exclusion of some cell components. Caution must be taken as well in the preparation of the skin homogenate, especially the temperature control and the pulverization of the skin prior to

homogenization. Excised skin model is one step closer to the real situation. The skin structure is maintained. Simultaneous permeation and metabolism can be investigated provided the viability of the skin is maintained during the study. This is particularly important for compounds which are highly metabolized in the skin. Although viability maintenance of the skin during percutaneous absorption study may seemed not so critical for esterase activity qualitatively, there is a need to verify whether this is the case for the quantitation of ester metabolism in the skin, especially when adequate activation of prodrugs is essential for the activity of the drugs. For the excised skin in diffusion cells model, a sensitive assay is normally required to quantitate the analytes in the receptor fluid. Both the viable excised human skin in diffusion cell and the human skin homogenate models provide information about metabolism by esterases in the skin and will be useful in the development of dermal and transdermal preparations.

Future investigation could be done to further characterize the models; for example, regarding the viability assessment of the skin in diffusion cells, further validation may be conducted by comparing the newly developed methods in this study with standard viability test for skin such as the MTT assay. For the skin homogenate model, activity of the enzymes from different skin layers may be examined, provided a suitable method for the separation of skin layers is used. Temperature was found to be an important factor in the assessment of esterase activity, i.e. temperature higher than 60°C substantially reduced esterase activity while (from pilot studies) low temperatures preserved the activity. Therefore, it should be examined whether these enzymes will still be active at low temperatures generally used in the storage of skin samples such as 4°, -20° or -70°C; and if the enzyme activity is preserved at low temperature, how long in the storage would still

be useful in the evaluation of skin metabolism. The viable excised skin model can be used to better evaluate the permeation and metabolism of other ester compounds, especially prodrugs to see if the activity of the drugs can be activated. Peptide delivery and metabolism may be tested since peptidases which cleave peptides are also hydrolytic enzymes. Different dosage forms may be compared as well. The *in vitro* models may be applied to other metabolizing enzyme systems either phase I or phase II reactions. However, some cofactors, such as NAD^+ or some metal ions, in an appropriate concentrations may be required (in the receptor fluid of the diffusion cell system or in the skin homogenate) for systems using oxidation-reduction reaction or conjugation pathway.

LIST OF REFERENCES

Ademola, J. I., Chow, C. A., Wester, R. C. and Maibach, H. I. (1993). "Metabolism of propranolol during percutaneous absorption in human skin." *J Pharm Sci* **82**(8): 767-70.

Ademola, J. I., Wester, R. C. and Maibach, H. I. (1992). "Cutaneous metabolism of theophylline by the human skin." *J Invest Dermatol* **98**(3): 310-4.

Agarwal, R., Raza, H., Allyn, D. L., Bickers, D. R. and Mukhtar, H. (1992). "Glutathione S-transferase-dependent conjugation of leukotriene A4-methyl ester to leukotriene C4-methyl ester in mammalian skin." *Bioche. Pharmacol* **44**(10): 2047-53.

Ahmed, S., Imai, T. and Otagiri, M. (1995). "Stereoselective hydrolysis and penetration of propranolol prodrugs: *in vitro* evaluation using hairless mouse skin." *J Pharm Sci* **84**(7): 877-83.

Ahmed, S., Imai, T. and Otagiri, M. (1996). "Evaluation of stereoselective transdermal transport and concurrent cutaneous hydrolysis of several ester prodrugs of propranolol: mechanism of stereoselective permeation." *Pharm Res* **13**(10): 1524-9.

Ahmed, S., Imai, T. and Otagiri, M. (1997). "Stereoselectivity in cutaneous hydrolysis and transdermal transport of propranolol prodrug." *Enantiomer* **2**(3-4): 181-91.

Aldrige, W. N. (1953). "Serum esterases 1. Two types of esterases (A and B) hydrolysing *p*-nitrophenyl acetate, propionate and butyrate, and a method for their determination." *Biochem J* **53**: 110-7.

Anderson, C., Andersson, T. and Andersson, R. G. G. (1992). "*In vivo* microdialysis estimation of histamine in human skin." *Skin Pharmacol* **5**: 177-83.

Anderson, C., Andersson, T., Boman, A. and Molander, M. (1996). "Cutaneous microdialysis for the measurement *in vivo* of the percutaneous absorption of organic solvents." *Curr Probl Dermatol* **25**: 37-46.

Anderson, C., Andersson, T. and Molander, M. (1991). "Ethanol absorption across human skin measured by *in vivo* microdialysis technique." *Acta Derm Venereol* **71**(5): 389-93.

Asselineau, D., Bernard, B. A. and Darmon, M. (1987). "Three-dimensional culture of human keratinocytes on a dermal equivalent." *Models Dermatol.* **3**: 1-7.

Augustinsson, K. B. (1959). "Electrophoresis studies on blood plasma esterases I. Mammalian plasmata." *Acta Chem Scand* **13**(3): 571-92.

Augustinsson, K. B. (1961). "Multiple forms of esterase in vertebrate blood plasma." *Ann N Y Acad Sci* **94**: 844-60.

Baron, J., Voigt, J. M., Whitter, T. B., Kawabata, T. T., Knapp, S. A., Guengerich, F. P. and Jakoby, W. B. (1986). "Identification of intratissue sites for xenobiotic activation and detoxication." *Adv Exp Med Biol* **197**: 119-44.

Bauer, M., Degude, C. and Mailhe, L. (1984). "Simultaneous determination of chlorhexidine, tetracaine and their degradation products by ion-pair liquid chromatography." *J Chromatogr* **315**: 457-64.

Behrendt, H. and Kampffmeyer, H. G. (1989). "Absorption and ester cleavage of methyl salicylate by skin of singla-pass perfused rabbit ears." *Xenobiotica* **19**: 131-141.

Behrendt, H. and Korting, H. C. (1990). "Experimental evidence for amide hydrolysis of indomethacin in rabbit skin." *Skin Pharmacol* **3**(1): 41-4.

Bergmann, F., Segal, R. and Rimon, S. (1957). "A new type of esterase in hog-kidney extract." *Biochem J* **67**: 481-6.

Berti, J. J. and Lipsky, J. J. (1995). "Transcutaneous drug delivery: a practical review." *Mayo Clin Proc* **70**(6): 581-6.

Betz, P. (1994). "Histological and enzyme histochemical parameters for the age estimation of human skin wounds." *Int J Leg Med* **107**: 60-8.

Bickers, D. R., Dutta-Choudhury, T. and Mukhtar, H. (1982). "Epidermis: a site of drug metablism in neonatal rat skin. Studies on cytochrome P-450 contant and mixed-function oxidase and epoxide hydrolase activity." *Mol Pharmacol* **21**: 239-247.

Bickers, D. R., Mukhtar, H., Meyer, L. W. and Speck, W. T. (1985). "Epidermal enzyme-mediated mutagenicity of the skin carcinogen, 2-aminoanthracene." *Mutat Res* **147**: 37-43.

Boderke, P., Merkle, H. P., Cullander, C., Ponec, M. and Bodde, H. E. (1997). "Localization of aminopeptidase activity in freshly excised human skin: direct visualization by confocal laser scanning microscopy." *J Invest Dermatol* **108**(1): 83-6.

Boehnleine, J., Sakr, A., Lichtin, J. L. and Bronaugh, R. L. (1994). "Characterization of esterase and alcohol dehydrogenase activity in skin. Metabolism of retinyl palmitate to retinol (vitamin A) during precutaneous absorptoin." *Pharm Res* **11**: 1155-1159.

Bongard, O. and Bounameaux, H. (1993). "Clinical investigation of skin microcirculation." *Dermatology* **186**(1): 6-11.

Boyce, S. T. and Ham, R. G. (1985). "Cultivation, frozen storage, and clonal growth of normal human epidermal keratinocytes in serum-free media." *J Tiss Cult Met.* **9**: 83-93.

Brimfield, A. A., Zweig, L. M., Novak, M. J. and Maxwell, D. M. (1998). "*In vitro* oxidation of the hydrolysis product of sulfur mustard, 2,2'-thiobis-ethanol, by mammalian alcohol dehydrogenase." *J Biochem Mol Toxicol* **12**(6): 361-9.

Brooks, R. T. and Sternglanz, P. D. (1959). "Titanometric determination of the N-oxide group in pyridine-N-oxide and related compounds." *Anal Chem* **31**: 561-5.

Bundgaard, H., Hoelgaard, A. and Mollgaard, B. (1983). "Leaching of hydrolytic enzymes from human skin in cutaneous permeation studies as determined with metronidazole and 5-fluorouracil prodrugs." *Int J Pharm* **15**: 285-292.

Chalardsunthornvatee, P. and Thomas, R. E. (1961). "The stability of solutions of amethocaine hydrochloride." *Australian Journal of Pharmacy* (Aug 30, 1961): 800-2.

Cham, E. B., Johns, D., Bochner, F., Imhoff, D.M. and Rowland, M. (1979). "Simultaneous liquid-chromatographic quantitation of salicylic acid, salicyluric acid, and gentisic acid in plasma." *Clin Chem* **25**(8): 1420-5.

Collier, S. W., Sheikh, N. M., Sakr, A., Lichtin, J. L., Stewart, R. F. and Bronaugh, R. L. (1989). "Maintenance of skin viability during *in vitro* percutaneous absorption/metabolism studies." *Toxicol Appl Pharmacol* **99**(3): 522-33.

Constantinides, P. (1974). Functional electronic histology. Elsevier Scientific Publishing Co.

Coomes, M. W., Norling, A. H., Pohl, R. J., Muller, D. and Fouts, J. R. (1983). "Foreign compound metabolism by isolated skin cells from the hairless mouse." *J Pharmacol Exp Ther* **225**(3): 770-7.

Corcuff, P. and Leveque, J. L. (1993). "*In vivo* vision of the human skin with the tandem scanning microscope." *Dermatology* **186**(1): 50-4.

Corcuff, P. and Pierard, G. E. (1998). "Skin imaging: state of the art at the dawn of the year 2000." *Curr Probl Dermatol* **26**: 1-11.

Cornish-Bowden, A. (1995). Fundamentals of enzyme kinetics. Portland Press, London, UK.

Cornwell, P. A., van Gompel, A. H. P., Blount, M. A. and Wiechers, J. W. (1997). "Maintenance of human skin viability in flow-through diffusion cells; absorption and metabolism of benzyl alcohol in scalp skin." *J. Controlled Release* **48**: 289-363.

Cross, S. E., Anderson, C. and Roberts, M. S. (1998). "Topical penetration of commercial salicylate esters and salts using human isolated skin and clinical microdialysis studies." *Br J Clin Pharmacol* **46**(1): 29-35.

Cross, S. E., Anderson, C., Thompson, M. J. and Roberts, M. S. (1997). "Is there tissue penetration after application of topical salicylate formulations?" *Lancet* **350**(9078): 636.

Cross, S. E., Zhenyu, W. and Roberts, M. S. (1996). "The effect of protein binding on the deep tissue penetration and efflux of dermally applied salicylic acid, lidocaine and diazepam in the perfused rat hindlimb." *J Pharmacol Exp Ther* **277**: 366-374.

Cullander, C. (1996). The laser-scanning confocal microscope. *In* Handbook of Skin Bioengineering. 3. Skin Imaging and Analysis. Edited by K. P. Wilhelm, P. Elsner, E. Barardesca and H. I. Maibach, CRC Press: 23-37.

Cumpstone, M. B., Kennedy, A. H., Harmon, C. S. and Potts, R. O. (1989). "The water permeability of primary mouse keratinocyte cultures grown at the air-liquid interface." *J Invest Dermatol* **92**: 598-600.

Dachun, W. and Jiazhen, Z. (1992). "Localizationand quantificationof the non-specific esterase in injured skin for timing of wounds." *Forensic Science International* **53**: 203-13.

Darling, C. A. (1991). Local anesthetic agents. *In* Wilson and Gisvold's Textbook of Organic Medicinal and Pharmaceutical Chemistry : 585-602.

Das, M., Asokan, P., Don, P. S., Krueger, G. G., Bickers, D. R. and Mukhtar, H. (1986b). "Carcinogen metabolism in human skin grafted onto athymic nude mice: a model system for the study of human skin carcinogenesis." *Biochem Biophys Res Commun* **138**(1): 33-9.

Das, M., Bickers, D. R. and Mukhtar, H. (1986a). "Epidermis: the major site of cutaneous benzo(a)pyrene and benzo(a)pyrene 7,8-diol metabolism in neonatal BALB/c mice." *Drug Metab Dispos* **14**(6): 637-42.

de Carvalho, H. F. and Taboga, S. R. (1996). "Fluorescence and confocal laser scanning microscopy imaging of elastic fibers in hematoxylin-eosin stained sections." *Histochem Cell Biol* **106**(6): 587-92.

Deimling, O. V. and Bocking, A. (1976). "Esterases in histochemistry and ultrahistochemistry." *Histochemical Journal* **8**: 215-252.

Drug Information (1988). American Society of Hospital Pharmacists, Madison : 1857.

Dubbels, R. and Schloot, W. (1983). "Studies on the metabolism of benoxinate by human pseudocholinsterase." *Metabolic, Pediatric and Systemic Ophthalmology* **7**: 37-43.

Emilson, A., Lindberg, M., Forslind, B. and Scheynius, A. (1993). "Quantitative and 3-dimensional analysis of Langerhans' cells following occlusion with patch tests using confocal laser scanning microscopy." *Acta Derm Venereol* **73**(5): 323-9.

Emilson, A., Lindberg, M. and Scheynius, A. (1998). "Differential epidermal expression of the invariant chain in allergic and irritant contact dermatitis." *Acta Derm Venereol* **78**(6): 402-7.

Emilson, A. and Scheynius, A. (1995). "Quantitative and three-dimensional analysis of human Langerhans cells in epidermal sheets and vertical skin sections." *J Histochem Cytochem* **43**(10): 993-8.

English, J. C., Deisinger, P. J. and Guest, D. (1998). "Metabolism of 2-ethylhexanoic acid administered orally or dermally to the female Fischer 344 rat." *Xenobiotica* **28**(7): 699-714.

Fawcett, D. W. (1981). The cell, 2nd ed. W. B. Saunders Company, Toronto.

Fink Puches, R., Hofmann Wellenhof, R., Smolle, J. and Kerl, H. (1995). "Confocal laser scanning microscopy: a new optical microscopic technique for applications in pathology and dermatology." *J Cutan Pathol* **22**(3): 252-9.

Finnen, M. J. (1987). Skin metabolism by oxidation and conjugation. *In* Skin Pharmacokinetics, Vol 1, Pharmacology and the Skin. Edited by B. Shroot and H. Schaefer, Karger, Basel : 163-169.

Finnen, M. J. and Shuster, S. (1985). "Phase I and phase II drug metabolism in isolated epidermal cells from adult hairless mice and in whole human follicles." *Biochem Pharmacol* **34**: 3571-3575.

Flynn, G. L. (1996). Topical drug absorption and topical pharmaceutical systems. *In* Modern Pharmaceutics, 3rd ed. Edited by G. S. Banker and C. T. Rhodes., Marcel Dekker, Inc., New York, : 239-298.

Foldes, et al. (1955). "Hydrolysis of ester-type local anesthetics and their halogenated analogs by purified plasma cholinesterase." **77**: 5149-51.

Foye, W. O., Lemke, T. L. and Williams, D. A. (1995). Principles of medicinal chemistry. Williams & Wilkins, Philadelphia.

Fuchs, J. and Thiele, J. (1998). "The role of oxygen in cutaneous photodynamic therapy." *Free Radic Biol Med* **24**(5): 835-47.

Geesin, J. C., Gordon, J. S. and Berg, R. A. (1990). "Retinoids affect collagen synthesis through inhibition of ascorbate-induced lipid peroxidation in cultured human dermal fibroblasts." *Arch Biochem Biophys* **278**(2): 350-5.

Ghosh, M. K. and Mitra, A. K. (1990). "Carboxylic acid ester hydrolase activity in hairless and athymic nude mouse skin." *Pharm Res* **7**: 251-255.

Gonzalez, S. and Pathak, M. A. (1996). "Inhibition of ultraviolet-induced formation of reactive oxygen species, lipid peroxidation, erythema and skin photosensitization by polypodium leucotomos." *Photodermatol Photoimmunol Photomed* **12**(2): 45-56.

Gray, G. M., Tabiowo, A. and Trotter, M. D. (1977). "Studies on the soluble and membrane-bound amino acid 2-naphthylamidases in pig and human epidermis." *Biochem J* **161**: 667-675.

Gray, P. N. and Dana, S. L. (1979). "GABA synthesis by cultured fibroblasts obtained from persons with Huntington's disease." *J Neurochem* **33**(5): 985-92.

Grouls, R. J. E., Ackerman, E. W., Korsten, H. H. M., Hellebrekers, L. J. and Breimer, D. D. (1997). "Partition coefficients (*n*-octanol/water) of *N*-butyl-*p*-aminobenzoate and other local anesthetics measured by reversed-phase high-performance liquid chromotography." *J Chromatography B* **694**: 421-5.

Guy, R. H., Hadgraft, J. and Bucks, D. A. (1987). "Transdermal drug delivery and cutaneous metabolism." *Xenobiotica* **17**(3): 325-43.

Guzek, D. B., Kennedy, A. H., McNeill, S. C., Wakshull, E. and Potts, R. O. (1989). "Transdermal drug transport and metabolism. I. Comparison of *in vitro* and *in vivo* results." *Pharm Res* **6**: 33-39.

Hakanson, R. and Moller, H. (1963). "On metabolism of noradrenaline in the skin: Activity of catechol-o-methyl transferase and monoamine oxidase." *Acta Derm-Venerol* **43**: 552-5.

Hanthamrongwit, M., Wilkinson, R., Osborne, C., Reid, W. H. and Grant, M. H. (1996). "Confocal laser-scanning microscopy for determining the structure of and keratinocyte infiltration through collagen sponges." *J Biomed Mater Res* **30**(3): 331-9.

Harper, K. H. and Calcutt, G. (1960). "Conjugation of 3:4-benzpyrenols in mouse skin." *Nature* **186**: 80-1.

Hegemann, L., Forstinger, C., Partsch, B., Lagler, I., Krotz, S. and Wolff, K. (1995). "Microdialysis in cutaneous pharmacology; Kinetic analysis of transdermally delivered nicotine." *J Invest Dermatol* **104**: 839-43.

Henrikus, B. M. and Kampffmeyer, H. G. (1992). "Ester hydrolysis and conjugation reactions in intact skin and skin homogenate, and by liver esterase of rabbits." *Xenobiotica* **22**(12): 1357-66.

Higo, N., Hinz, R. S., Lau, D. T., Benet, L. Z. and Guy, R. H. (1992). "Cutaneous metabolism of nitroglycerin *in vitro*. I. Homogenized versus intact skin." *Pharm Res* **9**(2): 187-90.

Higo, N., Sato, S., Irie, T. and Uekama, K. (1995). "Percutaneous penetration and metabolism of salicylic acid derivatives across hairless mouse skin in diffusion cell *in vitro*." *S.T.P. Pharma Sciences* **5**(4): 302-8.

Holland, J. M., Kao, J. Y. and Whitaker, M. J. (1984). "A multisample apparatus for kinetic evaluation of skin penetration *in vitro*: the influence of viability and metabolic status of the skin." *Toxicol Appl Pharmacol* **72**(2): 272-80.

Hopsu-Havu, V. K., Fraki, J. E. and Jarvinen, M. (1977). Proteolytic enzymes in the skin. *In* Proteinases in mamalian cells and tissues. A. J. Barret., Elsevier, Amsterdam, : 545-581.

Hopsu-Havu, V. K. and Tuohimaa, P. (1970). "Quantitative and radioautographic studies on the penetration kinetics of 9alpha-fluoro-16-methylene-prednisolone-21-acetate-7-T in human skin." *Arch Klin Exp Dermatol* **239**(3): 252-65.

Hsia, S. L. and Hao, Y. L. (1966). "Metabolic transformations of cortisol-4-^{14}C in human skin." *Biochemistry* **5**(5): 1469-74.

Ichikawa, K., Takashima, A., Yasuda, S. and Mizuno, N. (1989b). "Enhanced rabbit skin plasmin activity by UV irradiation." *Dermatologica* **179 Suppl 1**: 132.

Ichikawa, T., Hayashi, S., Noshiro, M., Takada, K. and Okuda, K. (1989a). "Purification and characterization of cytochrome P-450 induced by benz(a)anthracene in mouse skin microsomes." *Cancer Res* **49**(4): 806-9.

Imbert, D. and Cullander, C. (1997). "Assessment of cornea viability by laser scanning confocal microscopy and MTT assay." *Cornea* **16**(6): 666-74.

Imbert, D. and Cullander, C. (1999). "Buccal mucosa *in vitro* experiments. I. Confocal imaging of vital staining and MTT assays for the determination of tissue viability." *J Controlled Release* **58**(1): 39-50.

Imoto, H., Zhou, Z., Stinchcomb, A. L. and Flynn, G. L. (1996). "Transdermal prodrug concepts: permeation of buprenorphine and its alkyl esters through hairless mouse skin and influence of vehicles." *Biol Pharm Bull* **19**(2): 263-7.

International Union of Biochemistry (1984). Enzyme Nomenclature - Recommendation of the Nomenclature Committee of the International Union of Biochemistry. Academic Press, New York.

Ito, Y., Fukuyama, K., Horie, N. and Epstein, W. L. (1984). "Enzymatic activity of metal-binding proteins in epidermal cells." *Mol Cell Biochem* **60**(2): 183-8.

Ji, C. and Marnett, L. J. (1992). "Oxygen radical-dependent epoxidation of (7S,8S)-dihydroxy-7,8-dihydrobenzo[a]pyrene in mouse skin *in vivo*. Stimulation by phorbol esters and inhibition by antiinflammatory steroids." *J Biol Chem* **267**(25): 17842-8.

Johansen, M., Mollgaard, B., Wotton, P. K., Larsen, C. and Hoelgaard, A. (1986). "*In vitro* evaluation of dermal prodrug delivery- transport and bioconversion of a series of aliphatic esters of metronidazole." *Int J Pharm* **32**: 199-206.

Jones, K. H. and Senft, J. A. (1985). "An improved mrthod to determine cell viability by simultaneous staining with fluorescein diacetate-propidium iodide." *J Histochem Cytochem* **33**(1): 77-9.

Kalow, W. and Genest, K. (1957). "A method for the detection of atypical forms of human serum cholinesterase, determination of dibucaine numbers." *Can J Biochem Physiol* **35**: 339-46.

Kao, J. (1990). Validity of skin absoption and metabolism studies. *In* Methods for skin absorption. Edited by B. W. Kemppainen and W. G. Reifenrath., CRC Press., Inc., U.S.A. : 191-212.

Kao, J., Hall, J. and Holland, J. M. (1983). "Quantitation of cutaneous toxicity: an *in vitro* approach using skin organ culture." *Toxicol Appl Pharmacol* **68**(2): 206-17.

Kao, J., Hall, J., Shugart, L. R. and Holland, J. M. (1984). "An *in vitro* approach to studying cutaneous metabolism and disposition of topically applied xenobiotics." *Toxicol Appl Pharmacol* **75**(2): 289-98.

Katagata, Y. and Aso, K. (1986). "Intermediates in the conversion of prekeratin into keratin molecules in psoriatic epidermis." *Arch Dermatol Res* **278**(5): 419-22.

Katagata, Y. and Aso, K. (1988). "The presumption of proteolytic enzymes related to the formation of intermediates during the terminal differentiations." *FEBS Letters* **230**: 151-154.

Kikuchi, M., Fukuyama, K. and Epstein, W. L. (1988). "Soluble dipeptidyl peptidase IV from terminal differentiated rat epidermal cells: purification and its activity on synthetic and natural peptides." *Arch Biochem Biophys* **266**: 369-376.

Kirjavainen, M., Urtti, A., Valjakka Koskela, R., Kiesvaara, J. and Monkkonen, J. (1999). "Liposome-skin interactions and their effects on the skin permeation of drugs." *Eur J Pharm Sci* **7**(4): 279-86.

Kisch, B., Koster, H. and Strauss, E. (1943). "The procaine esterase." *Experimental Medicine and Surgery* **1**(1): 51-65.

Klein, M. B., Shaw, D., Barese, S., Chapo, G. A. and Cuono, C. B. (1996). "A reliable and cost-effective *in vitro* assay of skin viability for skin banks and burn centers." *J Burn Care Rehabil* **17**(6 Pt 1): 565-70.

Klink, F., Husstedt, W., von Klitzing, L., Friedrich, H., Seoudy, A. and Oberheuser, F. (1982). "The transcutaneous PO2 measurement as an additional evaluation index to the physiological and pathological conditions under delivery." *Int J Gynaecol Obstet* **20**(6): 427-31.

Kubota, K., Ademola, J. and Maibach, H. I. (1994). "Metabolism and degradation of betamethasone 17-valerate in homogenized living skin equivalent." *Dermatology* **188**(1): 13-7.

Kuroki, T., Hosomi, J., Chida, K., Hosoi, J. and Nemoto, N. (1987). "Inter-individual variations of aryl-hydrocarbon hydroxylase activity in cultured human epidermal and dermal cells." *Jpn J Cancer Res* **78**: 45-53.

Laerum, O. D. (1969). "Oxygen consumption of basal and differentiating cells from hairless mouse epidermis. A new method for obtaining almost pure selections of basal and differentiating cells respectively." *J Invest Dermatol* **52**(2): 204-11.

Lamb, K. A., Denyer, S. P., Sanderson, F. D. and Shaw, P. N. (1994). "The metabolism of a series of ester pro-drugs by NCTC 2544 cells, skin homogenate and LDE testskin." *J Pharm Pharmacol* **46**(12): 965-73.

Larson, T. A., Uden, D. L. and Schilling, C. G. (1996). "Stability of epinephrine hydrochloride in an extemporaneously compounded topical anesthetic solution of lidocaine, racepinephrine, and tetracaine." *Am J Health-Syst Pharm* **53**(6): 659-62.

Leeson, C. R., Leeson, T. S. and Paparo, A. A. (1985). Textbook of histology. W.B. Saunders Company, Toronto.

Liu, K. J., Mader, K., Shi, X. and Swartz, H. M. (1997). "Reduction of carcinogenic chromium(VI) on the skin of living rats." *Magn Reson Med* **38**(4): 524-6.

Liu, P., Higuchi, W. I., Ghanem, A., Kurihara Bergstrom, T. and Good, W. R. (1990). "Quantitation of simultaneous diffusion and metabolism of beta-estradiol in hairless mouse skin : Enzyme distribution and intrinsic diffusion/metabolism parameters." *Int J Pharm* **64**: 7-25.

Lockridge, O., Mottershaw-Jackson, N., Eckerson, H. and La Du, B. N. (1980). "Hydrolysis of diacetylmorphine (heroine) by human serum cholinesterase." *J Pharmacol Exp Ther* **215**(1): 1-8.

Lojda, Z., Gossrau, R. and Schiebler, T. H. (1976). Enzymhistochemische Methoden. Springer-Verlag, Berlin.

Long, C. (1961). Biochemist Handbook. E.&F.N. SPON, Ltd., London.

Mahoney, S. E., Paddock, S. W., Smith, L. C., Lewis, D. E. and Duvic, M. (1994). "Three-dimensional laser-scanning confocal microscopy of *in situ* hybridization in the skin." *Am J Dermatopathol* **16**(1): 44-51.

Martin, R. J., Denyer, S. P. and Hadgraft, J. (1987). "Skin metabolism of topically applied compounds." *Int J Pharm* **39**: 23-32.

May, S. R. and DeClement, F. A. (1980). "Skin banking. Part III. Cadaveric allograft skin viability." *J Burn Care Rehab* **2**: 128.

Mazumda, B., Tomlinson, A. A. and Faulder, G. C. (1991). "Preliminary study to assay plasma amethocaine concentrations after topical application of a new local anaesthetic cream containing amethocaine." *British J Anaesth* **67**: 432-6.

Menon, G. N. and Norris, B. J. (1981). "Simultaneous determination of tetracaine and its degradation product, *p-n*-butylaminobenzoic acid, by high-performance liquid chromatography." *J Pharm Sci* **70**(5): 569-70.

Merk, H., Rumpf, M., Bolsen, K., Wirth, G. and Goerz, G. (1984). "Inducibilityof arylhydrocarbon-hydroxylase activity in human hair follicles by topical application of liquor carbonis detergens (coal tar)." *Br J Dermatol* **111**: 279-84.

Merk, H. F., Mukhtar, H., Kaufmann, I., Das, M. and Bickers, D. R. (1987). "Human hair follicle benzo(a)pyrene and benzo(a)pyrene 7,8-diol metabolism: Effect of exposure to a coal tar-containing shampoo." *J Invest Dermatol* **88**: 71-6.

Mershon, M. M. and Callahan, J. F. (1975). Exploiting the differences. *In* Animal models in dermatology. H. I. Maibach., Churchill Livingston, New York : 36-52.

Molecular Probes, Inc. (1996). LIVE/DEAD® Viability/Cytotoxicity Kit (L-3224) for animal cells. Product Information Sheet.

Momose, A. and Fukuda, J. (1976). "A new metabolite of tetracaine." *Chem Pharm Bull* **24**(7): 1637-40.

Montagna, W. and Parakkal, P. F. (1974). The structure and function of skin. Academic Press.

Moore, P. L., Mac Coubrey, I. C. and Haughland, R. P. (1990). "A rapid, pH insensitive, two color fluorescence viability (cytotoxicity) assay." *J Cell Biol* **111**(5 part 2): 58A.

Morra, P., Bartle, W. R., Walker, S. E., Lee, S. N., Bowles, S. K. and Reeves, R. A. (1996). "Serum concentrations of salicylic acid following topically applied salicylate derivatives." *The Annals of Pharmacotherapy* **30**: 935-9.

Muller, M., Schmigt, R., Wagner, O., Osten, B. V., Shayganfar, H. and Eichler, H. G. (1995). "*In vivo* characterization of transdermal transport by microdialysis." *J Contr Rel* **57**: 49-57.

Murphy, G. F. (1997). Histology of the skin. *In* Lever's Histopathology of the skin. Edited by D. Elder, R. Elenitsas, C. Jaworsky and B. Johnson, Jr., Lippincott-Raven Publishers, Philadelphia : 5-50.

Nasseri Sina, P., Hotchkiss, S. A. and Caldwell, J. (1997). "Cutaneous xenobiotic metabolism: glycine conjugation in human and rat keratinocytes." *Food Chem Toxicol* **35**(3-4): 409-16.

Natcht, S., Yeung, D., Beasley, J. N., Anjo, M. D. and Maibach, H. I. (1981). "Benzoyl peroxide: percutaneous penetration and metabolic disposition." *Am Acad Dermatol* **4**(1): 31-7.

Nathan, D., Sakr, A., Lichtin, J. L. and Bronaugh, R. L. (1990). "*In vitro* skin absorption and metabolism of benzoic acid, p-aminobenzoic acid, and benzocaine in the hairless guinea pig." *Pharm Res* **7**(11): 1147-51.

Nicolau, G. and Yacobi, A. (1989). "Transdermal absorption and skin metabolism of viprostol, a synthetic prostaglandin E2 analogue." *Drug Metab Rev* **21**(3): 401-25.

Noonan, P. K. and Wester, R. C. (1989). Cutaneous metabolism of xenobiotics. *In* Percutaneous absorption : mechanisms, methodology and drug delivery. Edited by R. L. Bronaugh and H. I. Maibach., Marcel Dekker Inc., New York : 53-75.

Norred, W. P. and Akin, F. J. (1976). "Induction of aryl hydrocarbon hydroxylase and carbon monoxide-binding hemoproteins in mouse epidermis by tobacco carcinogens." *Biochem Pharmacol* **25**(6): 732-4.

Odland, G. (1991). Structure of the skin. *In* Biochemistry of the skin, Vol 1: 3-29.

Ortiz de Solorzano, C., Garcia Rodriguez, E., Jones, A., Pinkel, D., Gray, J. W., Sudar, D. and Lockett, S. J. (1999). "Segmentation of confocal microscope images of cell nuclei in thick tissue sections." *J Microsc* **193**(Pt 3): 212-26.

Overman, D. O. and White, J. A. (1983). "Comparative teratogenic effects of methyl salicylate applied orally or topically to hamsters." *Teratology* **28**: 421-426.

Pannatier, A., Jenner, P., Testa, B. and Etter, J. C. (1978). "The skin as a drug-metabolizing organ." *Drug Metab Rev* **8**(2): 319-43.

Pannatier, A., Testa, B. and Etter, J. C. (1981). "Enzymatic hydrolysis by mouse skin homogenates: Structure-metabolism relationship of para-nitrobenzoate esters." *Int J Pharm* **8**: 167-74.

Parkinson, E. K. and Newbold, R. F. (1980). "Benzo(a)pyrene metabolism and DNA adduct formation in serially cultivated strains of human epidermal keratinocytes." *Int J Cancer* **26**(3): 289-99.

Pearse, A. D., Gaskell, S. A. and Marks, R. (1986). "The effects of an aromatic retinoid (etretinate) on epidermal cell production and metabolism in normal and ichthyotic skin." *Br J Dermatol* **114**: 285-94.

Pershing, L. K. and Krueger, G. G. (1989). Human skin sandwich flap model for percutaneous absorption. *In* Percutaneous absorption, 2nd ed. Edited by R. L. Bronaugh and H. I. Maibach., Marcel Dekker, Inc., New York : 397-414.

Petry, J. J. and Wortham, K. A. (1984). "The anatomy of the epigastric flap in the experimental rat." *Plast Reconstr Surg* **74**: 410-5.

Pham, M., Magdalou, J., Siest, G., Lenoir, M., Bernard, B. A., Jamoulle, J. and Shroot, B. (1990). "Reconstituted epidermis: a novel model for the study of drug metabolism in human epidermis." *J Invest Dermatol* **94**: 749-752.

Pioch, W. (1969). "Epidermale Esterase-Aktivitat als Beweis der vitalen Einwirkung von stumpfer Gewalt." *Beitr. Gerichtl. Med.* **25**: 136-145.

Pohl, R. J., Coomes, M. W., Sparks, R. W. and Fouts, J. R. (1984). "7-Ethoxycoumarin O-deethylation activity in viable basal and differentiated keratinocytes isolated from the skin if the hairless mouse." *Drug Metab Dispos* **12**: 25-34.

Pohl, R. J., Philipot, R. M. and Fouts, J. R. (1976). "Cytochrom P-450 content and mixed function oxidase activity in microsomes isolated from mouse skin." *Drug Metab Dispos* **4**: 442-450.

Poole, C. A., Brookes, N. H. and Clover, G. M. (1993). "Keratocyte networks visualised in the living cornea using vital dyes." *J Cell Sciences* **106**: 685-92.

Porter, K. R. and Bonneville, M. A. (1972). Fine structure of cells and tissues. Lea & Febiger .

Porush, I., Shimamura, A. and Takahashi, L. T. (1965). "Determination of tetracaine in blood." *J Pharm Sci* : 1809-10.

Potts, R. O., McNeill, S. C., Desbonnet, C. R. and Wakshull, E. (1989). "Transdermal drug transport and metabolism. II. The role of competing kinetic events." *Pharm Res* **6**: 119-124.

Powell, M. F., Magill, A., Chu, N., Hama, K., Mau, C. I., Foster, L. and Bergstrom, R. (1991). "Chemical and enzymatic degredation of ganciclovir prodrugs: enhanced stability of the diadamantoate prodrug under acid conditions." *Pharm Res* **8**: 1418-1423.

Price, N. C. and Steven, L. (1993). Fundamentals of Enzymology. Oxford University Press, New York.

Raab, W. P. and Gmeiner, B. M. (1976). "The influence of D-penicillamine on enzymatic activities: glucose-6-phosphate dehydrogenase. Correlation with serum levels measured in humans." *J Clin Chem Clin Biochem* **14**(4): 173-6.

Rajadhyaksha, M., Grossman, M., Esterowitz, D., Webb, R. H. and Anderson, R. R. (1995). "*In vivo* confocal scanning laser microscopy of human skin: melanin provides strong contrast." *J Invest Dermatol* **104**(6): 946-52.

Ramaiah, A. (1996). "Lag kinetics of tyrosinase: its physiological implications." *Indian J Biochem Biophys* **33**(5): 349-56.

Ree, K., Johnson, S., Rugstrad, H. E., Bakka, A. and Hovig, T. (1981). "Characterization of human epithelial cell line with special reference to its ultrastructure." *Acta Pathol Microbiol Scand Sect A* **89**: 73-80.

Reynolds, J. E. F. (1996). Martindale the Extra Pharmacopoeia. The Pharmaceutical Press, London.

Rheinwald, J. G. and Green, H. (1975). "Serial cultivation of strains of human epidermal keratinocytes: the formation of keratinizing colonies from single cells." *Cell* **6**: 331-344.

Rhodin, J. A. G. (1963). An atlas of ultrastructure. W. B. Saunders Company.

Rittirod, T., Hatanaka, T., Uraki, A., Hino, K., Katayama, K. and Koizumi, T. (1999). "Species difference in simultaneous transport and metabolism of ethyl nicotinate in skin." *Int J Pharm* **178**(2): 161-9.

Riviere, J. E., Bowman, K. F. and Monteiro Riviere, N. A. (1987). "On the definition of viability in isolated perfused skin preparations." *Br J Dermatol* **116**(5): 739-41.

Riviere, J. E., Bowman, K. F., Monteiro Riviere, N. A., Dix, L. P. and Carver, M. P. (1986). "The isolated perfused porcine skin flap (IPPSF). I. A novel *in vitro* model for percutaneous absorption and cutaneous toxicology studies." *Fundam Appl Toxicol* **7**(3): 444-53.

Roberts, M. S., Favretto, W. A., Meyer, A., Reckmann, M. and Wongseelachote, T. (1982). "Topical bioavailability of methyl salicylate." *Australian and New Zealand J Med* **12**: 303-305.

Rochat, M. C., Payne, J. T., Pope, E. R., Wagner Mann, C. C. and Pace, L. W. (1993). "Evaluation of skin viability in dogs, using transcutaneous carbon dioxide and sensor current monitoring." *Am J Vet Res* **54**(3): 476-80.

Roy, S. D., Fujiki, J. and Fleitman, J. S. (1993). "Permeabilities of alkyl p-aminobenzoates through living skin equivalent and cadaver skin." *J Pharm Sci* **82**(12): 1266-8.

Sato, K. and Mine, T. (1996). "Analysis of *in vitro* rat skin permeation and metabolism of SM-10902, prodrug of synthetic prostacyclin analogue." *Int J Pharm* **135**: 127-36.

Scheynius, A. and Lundahl, P. (1990). "Three-dimensional visualization of human Langerhans' cells using confocal scanning laser microscopy." *Arch Dermatol Res* **281**(8): 521-5.

Seki, T., Kawaguchi, T. and Juni, K. (1990). "Enhanced delivery of zidovudine through rat and human skin via ester prodrugs." *Pharm Res* **7**(9): 948-52.

Seppa, H. E. J., Jansen, C. T. and Hopsu-Havu, V. K. (1971). "Proteolytic enzymes in the skin." *Acta Derm Venereol* **51**: 35-40.

Simonetti, O., Hoogstraate, A. J., Bialik, W., Kempenaar, J. A., Schrijvers, A. H., Bodde, H. E. and Ponec, M. (1995). "Visualization of diffusion pathways across the stratum corneum of native and *in-vitro*-reconstructed epidermis by confocal laser scanning microscopy." *Arch Dermatol Res* **287**(5): 465-73.

Slivka, S. R. (1992). "Testosterone metabolism in an *in vitro* skin model." *Cell Biol Toxicol* **8**(4): 267-76.

Steinstrasser, I. and Merkle, H. P. (1995). "Dermal metabolism of topically applied drugs: pathways and models reconsidered." *Pharm Acta Helv* **70**(1): 3-24.

Stinchcomb, A. L., Paliwal, A., Dua, R., Imoto, H., Woodard, R. W. and Flynn, G. (1996). "Permeation of buprenorphine and its 3-alkyl-ester prodrugs through human skin." *Pharm Res* **13**(10): 1519-23.

Swinyard, E. A. (1990). Local Anesthetics. *In* Remington's Pharmaceutical Sciences. Edited by A. R. Gennaro, Mack Publishing Company, Pennsylvania : 1048-56.

Tauber, U. and Rost, K. L. (1987). "Esterase activity of the skin including species variations." *Pharmacol Skin* **1**: 170-183.

Terndrup, T. E., Walls, H. C., Mariani, P. J., Gavula, D. P., Madden, C. M. and Cantor, R. M. (1992). "Plasma cocaine and tetracaine levels following application of topical anesthesia in children." *Ann Emerg Med* **21**(2): 162-6.

The Pharmaceutical Codex (1979). The Pharmaceutical Press, London : 26-7.

Thompson, C. T., LeBoit, P. E., Nederlof, P. M. and Gray, J. W. (1994). "Thick-section fluorescence *in situ* hybridization on formalin-fixed, paraffin-embedded archival tissue provides a histogenetic profile." *Am J Pathol* **144**(2): 237-43.

Thompson, S. and Slaga, T. J. (1976). "Mouse epidermal aryl hydrocarbon hydroxylase." *J Invest Dermatol* **66**: 108-111.

Udata, C., Tirucherai, G. and Mitra, A. K. (1999). "Synthesis, stereoselective enzymatic hydrolysis, and skin permeation of diastereomeric propranolol ester prodrugs." *J Pharm Sci* **88**(5): 544-50.

Valentino, R. J., Lockridge, O., Eckerson, H. W. and La Du, B. N. (1981). "Prediction of drug sensitivity inindividuals with atypical serum cholinesterase based on *in vitro* biochemical studies." *Biochemical Pharmacology* **30**(12): 1643-9.

van Pelt, F. N. A. M., Olde, M. Y. J. M., Blaauboer, B. J. and Weterings, P. J. J. M. (1990). "Immunohistochemical detection of cutochrome P-450 isoenzymes in cultured human epidermal cells." *J Histochem Cytochem* **38**: 1847-1851.

Vardaxis, N. J., Brans, T. A., Boon, M. E., Kreis, R. W. and Marres, L. M. (1997). "Confocal laser scanning microscopy of porcine skin: implications for human wound healing studies." *J Anat* **190**(Pt 4): 601-11.

Veiro, J. A. and Cummins, P. G. (1994). "Imaging of skin epidermis from various origins using confocal laser scanning microscopy." *Dermatology* **189**(1): 16-22.

Venkateshwaran, T. G. and Stewart, J. T. (1995). "HPLC determination of morphine-hydromorphone-bupivacaine and morphine-hydromorphone-tetracaine mixtures in 0.9% sodium chloride injection." *J Liq Chromatogr* **18**(3): 565-78.

Walker, C. H. and Mackness, M. I. (1983). "Esterases: Problems of identification and classification." *Biochemical Pharmacology* **32**: 3265-9.

Weller, R., Pattullo, S., Smith, L., Golden, M., Ormerod, A. and Benjamin, N. (1996). "Nitric oxide is generated on the skin surface by reduction of sweat nitrate." *J Invest Dermatol* **107**(3): 327-31.

Wester, R. C., Christoffel, J., Hartway, T., Poblete, N., Maibach, H. I. and Forsell, J. (1998). "Human cadaver skin viability for *in vitro* percutaneous absorption: storage and detrimental effects of heat-separation and freezing." *Pharm Res* **15**(1): 82-4.

Wester, R. C., Noonan, P. K., Smeach, S. and Kosobud, L. (1983). "Pharmacokinetics and bioavailability of intravenous and topical nitroglycerin in the rhesus monkey." *J Pharm Sci* **72**: 745-8.

Weterings, P. J. J. M., Vermorken, A. J. M. and Bloemendal, H. (1981). "A method for culturing human hair follicle cells." *Br J Dermatol* **104**: 1-5.

Wheater, P. R., Burkitt, H.G. and Daniels, V.G. (1982). Functional histology. A text and color atlas. Churchill Livingstone.

Wiebel, F. J. (1980). "Activation and inactivation of carcinogens by microsomal monooxygenases: modification by benzoflavones and polycyclic aromatic hydrocarbons." *Carcinog Compr Surv* **5**: 57-84.

Wiebel, F. J., Leutz, J. C. and Gelboin, H. V. (1975). "Aryl hydrocarbon (benzo(a)pyrene) hydroxylase: a mixed function oxygenase in mouse skin." *J Invest Dermatol* **64**: 184-189.

Windholz, M., Budavari, S., Blumetti, R. F. and Otterbein, E. S. (1983). The Merck Index. 10th ed. Merck & Co. Inc., N.J.

Wong, K. O., Tan, A. Y., Lim, B. G. and Wong, K. P. (1993). "Sulphate conjugation of minoxidil in rat skin." *Biochem Pharmacol* **45**(5): 1180-2.

Woolfson, A. D., McCafferty, D. F. and McGowan, K. E. (1990). "Metabolism of amethocaine by porcine and human skin extracts: influence on percutaneous anesthesia." *Int J Pharm* **62**: 9-14.

Yano, T., Kanetake, T., Saita, M. and Noda, K. (1991). "Effects of l-menthol and dl-camphor on the penetration and hydrolysis of methyl salicylate in hairless mouse skin." *J Pharmacobiodyn* **14**(12): 663-9.

Yokota, K., Matsue, H., Shibaki, A., Kawashima, T., Kobayashi, H. and Ohkawara, A. (1996). "Identification of mRNA-rich keratinocytes in the basal/suprabasal layers of psoriatic skin." *J Dermatol* **23**(12): 858-62.

Yoshimura, Y. and Mori, M. (1970). "Isoenzymes and histochemistry of non-specific esterases in normal and cancerous skin." *Histochemical Journal* **2**: 275-88.

Yu, C. D., Fox, J. L., Higuchi, W. I. and Ho, N. F. (1980). "Physical model evaluation of topical prodrug delivery-simultaneous transport and bioconversion of vidarabine-5'-valerate IV: distribution of esterase and deaminase enzymes in hairless mouse skin." *J Pharm Sci* **69**: 772-775.

Yu, C. D., Fox, J. L., Ho, N. F. and Higuchi, W. I. (1979). "Physical model evaluation of topical prodrug delivery-simultaneous transport and bioconversion of vidarabine-5'-valerate I: physical model development." *J Pharm Sci* **68**: 1341-1346.

Yu, R. C., Abrams, D. C., Alaibac, M. and Chu, A. C. (1994). "Morphological and quantitative analyses of normal epidermal Langerhans cells using confocal scanning laser microscopy." *Br J Dermatol* **131**(6): 843-8.

Zeiger, M. A. J., Tredget, E.E., and McGann, L.E. (1993). "A simple, effective system for assessing viability in split-thickness skin with the use of oxygen consumption." *J Burn Care Rehabil* **14**: 310-318.

APPENDIX A

STRUCTURE OF HUMAN SKIN

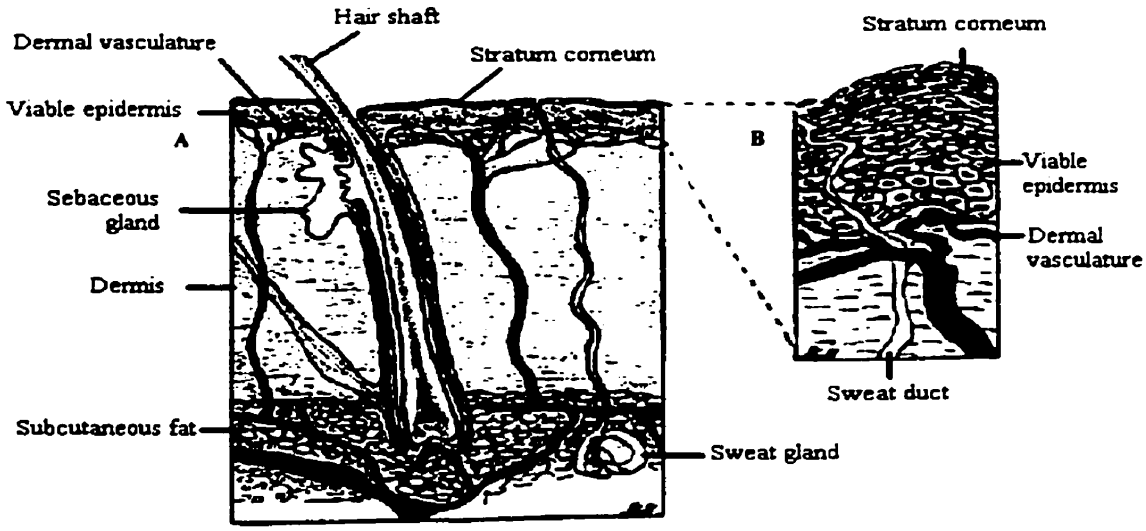

Cross-sectional structure of human skin; (A) full-thickness skin, (B) enlargement of the epidermis including the upper part of the dermis. The full-thickness skin consists of the epidermis, the dermis and skin appendages such as the eccrine sweat glands, apocrine glands and pilosebaceous units (hair follicles and sebaceous glands). The dermis supports extensive sensory nerve networks as well as the vasculature and lymphatics. (Modified from Flynn, 1996.)

APPENDIX B

COMPOSITION OF HEPES-BUFFERED HANK'S BALANCED SALT SOLUTION

NaCl	7000	mg/L
KCl	400	mg/L
$CaCl_2 \cdot 2H_2O$	185.5	mg/L
$MgSO_4 \cdot 7H_2O$	200	mg/L
Dextrose	1000	mg/L
$NaHCO_3$	350	mg/L
Na_2HPO_4	47.5	mg/L
KH_2PO_4	60	mg/L
Hepes	5957.5	mg/L

The buffer was adjusted to pH 7.4 with 10% w/v NaOH solution and filter sterilized. The osmolality was between 282 and 288 mOsm/kg H_2O. The buffer was stored at 4°C. Antibiotic antimycotic solution (100x) for tissue culture (product number A 9909, Sigma) was added in the ratio of 1 mL solution to 100 mL buffer before being used.